THE UNIVERSITY OF MANITOBA

ENERGY EXCHANGE AT THE SOIL SURFACE AND THE SOIL TEMPERATURE REGIME

by

REINDER DE JONG

A THESIS

SUBMITTED TO THE FACULTY OF GRADUATE STUDIES

IN PARTIAL FULFILLMENT OF THE REQUIREMENTS FOR THE DEGREE

DOCTOR OF PHILOSOPHY

DEPARTMENT OF SOIL SCIENCE

WINNIPEG, MANITOBA

SEPTEMBER, 1978

ENERGY EXCHANGE AT THE SOIL SURFACE AND THE SOIL TEMPERATURE REGIME

BY

REINDER DE JONG

A dissertation submitted to the Faculty of Graduate Studies of the University of Manitoba in partial fulfillment of the requirements of the degree of

DOCTOR OF PHILOSOPHY

© 1978

Permission has been granted to the LIBRARY OF THE UNIVERSITY OF MANITOBA to lend or sell copies of this dissertation, to the NATIONAL LIBRARY OF CANADA to microfilm this dissertation and to lend or sell copies of the film, and UNIVERSITY MICROFILMS to publish an abstract of this dissertation.

The author reserves other publication rights, and neither the dissertation nor extensive extracts from it may be printed or otherwise reproduced without the author's written permission.

THE UNIVERSITY OF MANITOBA LIBRARIES

ABSTRACT

ENERGY EXCHANGE AT THE SOIL SURFACE AND THE SOIL TEMPERATURE REGIME

Reinder de Jong, Ph.D.
University of Manitoba, 1978.

Supervisor:
Dr. C.F. Shaykewich

An analysis was made of the energy exchange at the soil-atmosphere interface and the resulting soil temperature regime underneath it, as affected by naturally occurring events.

In a field experiment various components of the radiation and energy balance were measured. Empirical and physically based models were used to predict the net radiation flux, the soil heat flux and potential evapotranspiration. The applicability of the simple heat conduction model in semi-infinite homogeneous media was studied using measured diurnal and annual soil temperature waves. A more comprehensive model, describing the simultaneous transfer of water and heat in the soil was developed and its output was compared with measured soil water content and soil temperature profiles.

The observed net radiation flux was positive during the summer, but negative in the winter because of the large reflectivity of the ground. The soil heat flux was only a small component of the energy balance, generally less than 10%, except during the winter when the soil heat flux was about 60% of the net radiation flux. The soil heat flux reversed in the early spring and again in the late summer, prior to a reversal of the net radiation flux. Large variations from one day to the next were noticed in the diurnal cycle of the net radiation flux and the soil heat flux.

The net radiation flux could be predicted with decreasing accuracy on a monthly, daily and hourly basis with either formulas based on physical considerations or the empirical relationship between the net and shortwave radiation fluxes. In 1974 a good correlation was found between the daily soil heat flux and the mean air temperature ($r^2 = 0.84$), but in 1975 the relationship was poor ($r^2 = 0.48$). The inclusion of other environmental variables in the relationship did not improve the predicted soil heat flux.

Fairly good agreement was found between the results of various potential evapotranspiration calculations and reported Class A pan measurements. Only the results of the Van Bavel and Penman equations were considerably higher than the reported measured values.

The simple heat conduction model was used successfully to estimate the thermal diffusivity from the annual soil temperature record. No such estimate could be obtained with this model from the diurnal soil temperature waves because of the non-homogeneous nature of the upper part of the soil profile.

The water-energy model predicted a total cumulative potential evapotranspiration of 500 mm and 283 mm actual evapotranspiration at the end of the 1975 growing season. The ratio of the cumulative potential to the cumulative actual evapotranspiration decreased sharply in May and June as a result of increasing soil temperatures, thereby enhancing actual evapotranspiration. The agreement between predicted soil water and soil temperature profiles as compared to the measured profiles was satisfactory. Convective heat transfer was only significant during days with heavy rainfall. Thermally induced water vapour flow and heat flow due to vapour movement were negligible under the experimental conditions studied.

ACKNOWLEDGEMENTS

The author would like to express his sincere appreciation to Dr. C.F. Shaykewich for his encouragement and support during this investigation and to Dr. C.M. Cho for his stimulating discussions and helpful suggestions. He is grateful to Dr. R.A. Hedlin and Dr. A.C. Trupp for serving on the graduate committee.

The author is greatly indebted to Dr. R. G. Hart, Director of the Whiteshell Nuclear Research Establishment for providing the accommodation and assistance to carry out the field study. The help with equipment and advice received from Mr. A. Reimer is much appreciated.

The efforts of Jim Green in the preparation of the data are appreciated.

Special thanks to the staff of the Agriculture Canada Research Station, Swift Current, Saskatchewan, for their assistance in preparation of this manuscript.

Financial support of the National Research Council, Canada and the Faculty of Graduate Studies of the University of Manitoba is gratefully acknowledged.

Finally, my appreciation to my wife, Willy, for the much needed help and understanding, without which the completion of this work would not have been possible.

TABLE OF CONTENTS

Page

LIST OF FIGURES

Page

LIST OF TABLES

FOREWORD

During the course of the investigation net radiation flux, soil heat flux and soil temperature data were collected on an hourly basis, except during the period from October 6, 1974 to April 26, 1975, when the data were recorded every two hours. This massive amount of data along with hourly precipitation, sunshine and windspeed data will not be reproduced in this manuscript, but are available from the author upon request. Also the data collected from the Colman soil moisture cells can be obtained from the author.

I. INTRODUCTION

The boundary between the atmosphere and the earth is one of the most interesting in nature. The soil surface, including its plant cover, plays a vital role in the heat and water budgets of the soil and the atmosphere, absorbing, reflecting and otherwise transforming the solar energy striking it.

The ultimate source of energy for the soil and the atmosphere above it is solar radiation. Depending upon the degree of cloudiness the amount of solar radiation reaching the surface of the earth varies between approximately 25 and 85% of the extraterrestrial radiation. During the summer about 25% of the solar radiation intercepted by the earth's surface is reflected back into the atmosphere, but during the winter, when the ground is snow covered, this could be as high as 80 to 90%.

The earth's surface emits longwave radiation towards the atmosphere. This thermal radiation from the earth is essentially black-body radiation at the temperature of the earth's surface. The atmosphere is relatively opaque to this thermal radiation, with water vapour, clouds and carbon dioxide being the principle absorbers. Observations and calculations have shown that this longwave radiation from the ground is the primary heat source for the atmosphere. The atmosphere re-emits this energy; some is sent back towards the ground and the rest is returned to space. The difference between the downward radiation flux (direct and diffuse solar radiation and longwave radiation) and the upward flux (reflected solar radiation, plus thermal radiation from the soil and vegetative cover) is known as the net radiation.

Part of the net radiation energy arriving at the soil surface is used to evaporate water, either directly from the soil or through the process of transpiration from plants. The term evapotranspiration is frequently used to describe the sum of these two effects. The amount of energy used in this process depends upon many factors, such as the availability of soil water and energy, as well as upon the ability of the atmosphere to remove the vapour.

During the summer and daylight hours the surface of the soil is heated by solar radiation to a temperature much higher than that of the air above or the soil below it; hence heat energy (not used in the evapotranspiration process) is conducted away from the surface into both the air and the deeper soil layers. Since air is a very poor conductor of heat, appreciable conduction occurs only with large temperature gradients in the very lower layer of air. Above this thin film of air, convective transfer mechanisms carry the heat to higher levels. The amount of energy penetrating into the soil will depend upon the thermal properties of the soil, as well as upon such factors as the plant cover, exposure, and slope.

The physical, chemical and biological process in the soil are all strongly influenced by temperature. The thermal pattern of the soil is thus one of the primary controls of the growth of plants. Soil temperature first affects the plant at the time of germination; later it strongly influences the growth of the plant root and therefore the development of the entire plant.

The root of the plant is exposed at any one time to a wide range of temperatures; there is no 'single soil temperature' which can be used to describe the plant's environment. It has also been shown (Walker 1970) that diurnal changes in soil temperature affect plant growth. Therefore it is not realistic to expect that plant growth models which use a weekly or a monthly average soil temperature can predict the behavior of the plant under constantly changing field conditions.

The primary objectives of the present study were to analyze the energy exchange at the soil-atmosphere interface and to study the soil temperature regime as affected by naturally occurring events. The various components of the radiation balance were analyzed and empirical and physically based models, to predict the net radiation flux, were evaluated. Potential evapotranspiration was calculated using existing formulas and the soil heat flux was related to soil and atmospheric parameters. The diurnal and annual cycles of soil temperatures have been studied and the applicability of a simple heat conduction model was investigated. A model to predict hourly soil temperature and soil water content changes throughout an entire growing season was developed and tested in a well instrumented field experiment.

The necessary data were collected at the Whiteshell Nuclear Research Establishment in Pinawa, which is situated in an ecological transition zone between boreal forest and prairie. A brief review of the weather experienced during the experimental period was presented.

II. LITERATURE REVIEW

A. RADIATION BALANCE.

1. Introduction.

Except for a small amount of heat from its inner core, all the energy received at the surface of the earth originates from the sun. Some of the solar radiation is reflected back to space. The earth reradiates some of the energy received from the sun. The quantity of radiant energy remaining at the earth's surface, the net radiation R_n, being the difference between the total upward and downward radiation fluxes, is the energy available to drive important processes like evaporation, heating the air and the soil, as well as other smaller energy consuming processes such as photosynthesis.

In the event that no direct measurements of R_n are available, which up to now has been the rule rather than the exception, R_n has to be derived from empirical formulas. These are based on physical considerations and need other meteorological data and locally adjusted constants.

From a practical point of view it is important that R_n be determined from relationships which are not location dependent, but more universally applicable and easier to use. Therefore empirical expressions based on the often noted high correlations between net- and shortwave radiation will be examined.

The radiation balance can be written as:

$$R_n = (1 - \alpha)\ R_s - R_{ln} \qquad (2.1)$$

where R_s is the incoming shortwave radiation flux also called global radiation or insolation, range 0.15 - 3.5μ. R_{ln} is the effective outgoing longwave (range 3.5 - 8.0μ) radiation flux and α is the surface reflection coefficient of shortwave radiation (also called albedo). According to this sequence the various terms will be discussed.

2. Shortwave radiation.

An empirical expression frequently used for the calculation of shortwave radiation flux (R_s) is the one proposed by Angstrom (1924):

$$R_s = R_s^c \, (a + b \, n/N) \tag{2.2}$$

where a and b are constants, n is the number of hours of bright sunshine in a daylength of N hours (the maximum n can reach on a clear day) and R_s^c is the solar radiation receipt on a horizontal surface at ground level on a clear day. The values of N and R_s^c are dependent upon the latitude and time of the year. The value of N can be found in the Smithsonian Meteorological Tables (1951) or by computation, e.g., Robertson and Russelo (1968).

Subsequent developments have shown that there are significant spatial and temporal variations in the magnitudes of the coefficients a and b. Black et al. (1954) obtained values of 'b' varying irregularly between 0.29 and 0.63 and values of 'a' varying irregularly between 0.19 and 0.40 among stations distributed over 50 degrees of latitude. In Canada, Mateer (1955) identified the values of 'a' and 'b' typical of the snow season, of the snow free season and of the transitional seasons. Driedger and Catchpole (1970) analyzing 18 years of Winnipeg data found that the seasonal regimes of 'a' and 'b' could be approximated by:

$$\begin{aligned} a &= 0.50187 - 0.0020752x + 0.00000483x^2 \\ b &= 0.35526 + 0.0032518x - 0.00000796x^2 \end{aligned} \tag{2.3}$$

where x is day of the year.

The major disadvantage of using R_s^c in equation (2.2) is that it can only be obtained by extrapolation from measured values of R_s, using methods similar to the one described by Sellers (1965). A modification of equation (2.2), first proposed by Kimball (1927) involves the replacement of R_s^c by R_s^{top}:

$$R_s = R_s^{top} \ (p + q \ n/N) \tag{2.4}$$

where R_s^{top} is the extra-terrestrial radiation flux at the top of the atmosphere. This parameter can be accurately computed by means of the following fundamental equation (for derivation see e.g. Kreith, 1973):

$$\begin{aligned} R_s^{top} &= I_o \cos Z/r^2 \\ &= I_o \ (\cos \delta \cos \phi \cos h + \sin \delta \sin \phi)/r^2 \end{aligned} \tag{2.5}$$

where I_o is the solar constant, r is the radius vector of the earth's orbit around the sun and Z is the solar zenith angle, a function of the angles of solar declination δ, latitude ϕ and solar hour angle h.

Linacre (1967) presented values for p and q in equation (2.4) from 39 different stations, with most values being near the means of 0.25 and 0.50 respectively. In Canada, Baier and Robertson (1965) found 'p' and 'q' to be 0.251 and 0.616 during the growing season. Generally it is found that the equations (2.2) and (2.4) are superior to those empirical formulas which contain values of fraction of sky covered by clouds instead of values of n/N (Scholte Ubing, 1961; Heldal, 1970).

3. Longwave radiation.

The effective longwave radiation flux is defined as the difference between the thermal radiation from the earth and the thermal radiation from the atmosphere. Empirical equations have been shown to be of sufficient accuracy to describe the intensity of the effective longwave radiation. One of the earliest and most widely used in Europe is a Brunt-type formula:

$$R_{1n} = \sigma T^4_k \ (a - b \sqrt{e}) \ [1 - d(1 - n/N)] \qquad (2.6)$$

where σ is the Stefan-Bolzmann constant, T_k is the Kelvin air temperature at screen height, e is the water vapour pressure, $(1 - n/N)$ is the fractional cloudiness and a, b and d are empirically determined constants. Brunt (1932) obtained values for 'a' and 'b' of 0.342 and 0.127 $\text{mbar}^{-\frac{1}{2}}$. Van Wijk and Scholte Ubing (1966) cite references in which the values for 'a' range from 0.34 to 0.62 and from 0.029 to 0.110 $\text{mbar}^{-\frac{1}{2}}$ for 'b'. The term d, which decreases when the clouds are higher and thinner has been taken either 0.10 (Penman, 1948), 0.20 (kramer, 1957), 0.24 (Impens, 1963) or 0.30 (Fitzpatrick and Stern, 1965).

More recently, the justification for using vapour pressure in equation (2.6) has been questioned by Swinbank (1963). Based on Swinbank's formulas, Linacre (1968) developed an expression for the effective longwave radiation flux which took the form:

$$R_{1n} = 32 \times 10^{-5} \ (1 + 4 \ n/N) \ (100 - T) \qquad (2.7)$$

In a re-evaluation of Swinbank's data, plus additional data from Phoenix and Alaska, Idso and Jackson (1969) concluded that the downward thermal radiation flux from a cloudless atmosphere could be described most accurately by:

$$R_1\downarrow = \sigma T^4_k \ [1 - 0.261 \exp \ (-7.77.10^{-4} \ (273 - T_k)^2)] \qquad (2.8)$$

Subsequent research by Idso (1972) has shown that equation (2.8) was equally applicable to cloudy conditions when used on a daily basis. Combining equation (2.8) with the outgoing longwave radiation from the earth, $R_l\uparrow = \sigma T_k^4$, one obtains:

$$R_{ln} = R_l\uparrow - R_l\downarrow$$

$$= \sigma T_k^4 \; [1 - (1 - 0.261 \exp\,(-7.77.10^{-4}\; (273 - T_k)^2))] \quad (2.9)$$

The above equations for effective longwave radiation flux are all subject to the assumption that the screen height air temperature and the surface temperature are equal, which is a good approximation only in the case of well watered crops. If the surface temperature exceeds the air temperature, R_{ln} increases at a rate roughly equal to 0.008 ly min^{-1} °C^{-1} (Linacre, 1968).

4. Reflected shortwave radiation.

Various authors have reported on the reflection coefficient of shortwave radiation, α, also called albedo. Monteith (1959) has shown from measurements over a variety of crops that, provided the ground surface is effectively shaded by plant material, α is close to 0.26. He quotes a considerable body of evidence in support of this value. More recently similar values have been reported for crops in Arizona (Fritschen, 1967) and Ontario (Davies and Buttimore, 1969). However lower values have been reported by Nkemdirim (1972a) in Alberta and McFadden and Ragotzkie (1967) for Central Canada. Since the latter study was based upon airborne measurements lower values (range 0.134 to 0.264 with a mean of 0.221) can be attributed in part to atmospheric attenuation of the reflected component.

The reflection coefficient of shortwave radiation is generally lower for bare soils than for vegetated soils. Piggin and Schwerdtfeger (1973) found that the albedo increased from 0.13 to 0.25 with increasing leaf area index. Similar results have been reported by Graham and King (1961). Stanhill (1970) noted the albedo was inversely related to the height of the vegetation canopy, presumably because of the greater opportunities for the reabsorption of reflected radiation within deep canopies. It has been long recognized that bare soil albedo is dependent upon the moisture status of the soil surface (Angstrom, 1925; Bowers and Hanks, 1965). Idso et al. (1975), investigating the possibility of using albedo measurements for the remote sensing of soil water content, reported a linear relationship between the water content of the uppermost layer of the soil and the albedo.

The variation of albedo values with solar elevation has been widely documented (Stanhill et al., 1966; Idso et al., 1969; Davies and Buttimore, 1969; Nkemdirim, 1972b). The rise in albedo values at low solar elevations is thought to be at least partly due to the lower level of multiple reflections within the plant canopy.

During the winter months when the ground is covered with freshly fallen snow the albedo might be as high as 0.95 (Sellers, 1965). Nkemdirim (1972a) reported a value of 0.42 on a day when 80% snow cover was observed. The snow depth was 4.5 cm and it had been lying on the ground for six days. Similar values for Central Canada were reported by McFadden and Ragotzkie (1967).

5. Net radiation.

If the reflection coefficient α is known, net radiation can be estimated using semi-empirical equations for shortwave and effective longwave radiation flux. Linacre (1968) developed a number of approximate expressions for R_n with decreasing accuracy but increasing simplicity of estimation, involving only the three terms n, N and R_s^{top}. However the incorporation of locally determined values of p and q in the Kimball equation (2.4) still seemed to be required.

An entirely empirical approach documented by many workers (e.g., Shaw, 1956; Stanhill et al., 1966; Davies, 1967; Fitzpatrick and Stern, 1970) is based on the correlation between net radiation and shortwave radiation flux:

$$R_n = a\,R_s - b \tag{2.10}$$

This regression equation can be computed either on an hourly, a daylight or on a 24-hour day basis, but little information is available on the effect of grouping the data.

Comparison of equation (2.1) and (2.10) shows that the slope 'a' mainly depends on the reflection coefficient α, and the intercept 'b' will be a function of the other terms in equations (2.6), (2.7), (2.8) or (2.9), i.e., of cloud cover and air temperature. Shaw (1956), for example, reports for clear days ($n/N > 0.75$) b = 0.06 and for overcast days ($n/N \leq 0.75$) b = 0.02 ly min^{-1}. The values for 'a' found by the latter author are 0.87 and 0.75 respectively. This means that data for clear days show a larger slope than those for overcast days, i.e., a larger proportion of incoming shortwave radiation is converted into net radiation. This led Linacre (1968) to suggest that clouds lower the net radiation intensity when it exceeds a critical value, but increase it when the intensity is lower.

Replacement of R_s by net shortwave radiation by using an expression such as:

$$R_n = a^1 (1 - \alpha) R_s - b^1 \qquad (2.11)$$

has not improved the regression model (Fritschen, 1967; Davies and Buttimor, 1969).

For clear days with a relatively constant incoming flux of thermal radiation, Monteith and Szeicz (1961) developed the expression:

$$R_n = \frac{(1 - \alpha)}{(1 + \beta)} R_s - b \qquad (2.12)$$

where the so-called heating coefficient β is defined as $-dR_{1n}/dR_n = (1 - a^1)/a^1$. The value of 'b' is equal to R_n when $R_s = 0$ and can be found by regression of R_n on $(1 - \alpha).R_s$. Equation (2.12) is useful for the routine estimation of R_n only if it is possible to assign a priori an appropriate value to β. However, this has met with little success, primarily because of the parameter's great variability with surface and atmospheric conditions (Idso, 1968; Idso et al., 1969; Arnfield, 1975). It is apparent from the literature that neither the inclusion of α nor β improves the regression of R_n upon R_s.

B. ENERGY BALANCE

1. Introduction.

Following the conservation of energy principle, the energy balance equation for a vegetated surface in the absence of advected energy may be written as:

$$R_n = H + LE + G + M \qquad (2.13)$$

where R_n is the net radiation flux, as discussed previously. H is the flux of sensible heat between the surface and the air, LE is the flux of latent heat to and from the surface through vaporization (evaporation) of water or condensation, G is the flux of heat into or out of the soil and M is the energy involved in a number of miscellaneous processes such as energy fixed in plants by photosynthesis, respiration and heat storage in the crop canopy. Since M is often small it can be neglected in energy balance studies (Yocum et al., 1964).

Once net radiation has been measured or calculated, the problem of estimating the various components of the energy balance reduces to estimating the different terms of the right hand side of equation (2.13).

2. Bowen ratio method.

Bowen (1926) recognized that the soil heat flux G constitutes only a small fraction of R_n when soil moisture is not limiting. He thus partitioned R_n between the H and LE terms.

The vertical flux of sensible heat was computed from the equation:

$$H = -\rho_a c^a K_h \frac{\partial T}{\partial z} \qquad (2.14)$$

where ρ_a is the density of air, c^a the specific heat of air at constant pressure, K_h the eddy diffusivity of heat and $\partial T/\partial z$ is the lapse of temperature with height z. The latent heat flux was written as:

$$LE = -\frac{\rho_a L\varepsilon}{P} K_v \frac{\partial e}{\partial z} \qquad (2.15)$$

where L is the latent heat of vaporization, ε the relative molecular weight of water with respect to air, P the barometric pressure, K_v the eddy diffusivity of water vapour and $\partial e/\partial z$ is the vertical water vapour pressure gradient. Bowen developed the relationship:

$$B = \frac{H}{LE} = \frac{Pc^a}{L\varepsilon}\left(\frac{K_h}{K_v}\right)\frac{\partial T/\partial z}{\partial e/\partial z} = \frac{Pc^a}{L\varepsilon}\frac{\partial T}{\partial e} \tag{2.16}$$

A simplifying assumption required to compute Bowen's ratio is

$$K_h = K_v \tag{2.17}$$

The validity of this assumption has been the object of much research in micrometeorology, e.g., Priestley and Swinbank (1947), Pasquill (1949), Rider and Robinson (1951) and Swinbank (1955). More recently, Swinbank and Dyer (1967), Dyer (1967) and Denmead and McIlroy (1970) have shown apparent identity between the turbulent transfer processes for heat and water vapour, under widely varying conditions of instability and of dryness of the evaporating surface.

The Bowen ratio has been shown to be accurate for many applications (Fritschen, 1965) and is widely used to calculate the latent heat flux:

$$LE = \frac{R_n - G}{1 + B} \tag{2.18}$$

A serious shortcoming of the Bowen ratio method is that equation (2.18) becomes indeterminate when the energy utilized in evapotranspiration, LE, is equal to the sensible heat supplied to the surface, H, (i.e., when B = -1). A modified Bowen ratio method such as suggested by Reimer and Desmarais (1973) overcomes this problem.

Ordinarily the measurements of the ratio of the temperature and vapour pressure gradients require elaborate instrumentation, and these data are not generally available. Therefore other methods have been devised to solve the energy budget equation.

3. Combination methods.

In the combination methods the energy balance and aerodynamic equations are combined to produce an equation that can be used to estimate potential evapotranspiration from measurements at a single height.

Penman's (1948) contribution was to derive an approximate expression for the Bowen ratio for a potential evaporating surface that could be computed from standard meteorological data. Penman's method makes use of the following aerodynamic equations:

$$H = \gamma L\ (T_o - T_a)\ f(u) \tag{2.19}$$

$$LE = L\ (e_o - e_a)\ f(u) \tag{2.20}$$

where $\gamma = \frac{c^a\ P}{L\varepsilon}$ is the psychrometric constant. These differ from (2.14) and (2.15) in that the turbulent transfer coefficient is replaced by a function of the horizontal windspeed f(u) and temperature and vapour pressure measurements are made at the surface (subscript o) and at screen level (subscript a). He then introduced the saturated vapour pressure at the surface (e^*_o) and at screen level (e^*_a) and the slope of the saturation vapour pressure curve at air temperature Δ (= de^*/dT). The slope should be evaluated at the mean of the surface and air temperatures, but the error arising from its evaluation at air temperature is slight (Van Bavel, 1966). It follows that

$$T_o - T_a = (\ e^*_o - e^*_a\ )\ /\ \Delta \tag{2.21}$$

and

$$H = \frac{\gamma}{\Delta}\ L\ (e^*_o - e^*_a)\ f(u) \tag{2.22}$$

Subtracting e_a from both e_o^* and e_a^* gives:

$$H = \frac{\gamma}{\Delta} L \left[(e_o^* - e_a) f(u) - (e_a^* - e_a) f(u) \right] \tag{2.23}$$

Since e_o should be saturated in the case of a freely evaporating surface equation (2.20) can be written as:

$$LE_{pot} = L (e_o^* - e_a) f(u) \tag{2.24}$$

where LE_{pot} is the potential latent heat flux. The symbol E_a is used to represent the second of the bracketed terms of equation (2.23), i.e.,

$$E_a = (e_a^* - e_a) f(u) \tag{2.25}$$

Upon combining equations (2.24) and (2.25) with equation (2.23) gives:

$$H = \frac{\gamma}{\Delta} (LE_{pot} - LE_a) \tag{2.26}$$

One is now ready to combine the aerodynamic equation (2.26) with the energy balance equation (2.13) to produce the combination equation:

$$R_n - \frac{\gamma}{\Delta} LE_{pot} + \frac{\gamma}{\Delta} LE_a - LE_{pot} - G = 0 \tag{2.27}$$

Solving the latter equation for the energy associated with potential evapotranspiration gives:

$$LE_{pot} = \frac{\frac{\Delta}{\gamma} (R_n - G) + LE_a}{\frac{\Delta}{\gamma} + 1} \tag{2.28}$$

$\frac{\Delta}{\gamma}$ can be regarded as a temperature dependent weighting factor which varies between 1.23 and 3.56 for temperatures ranging from 10°C to 30°C. These values in conjunction with (2.28) show that between about 55% and 78% of $(R_n - G)$ is incorporated in LE_{pot} compared with 45% to 22% in LE_a. This heavy dependence of LE_{pot} on $(R_n - G)$ prompted Penman to suggest that the aerodynamic term E_a need not to be accurately evaluated. He used this argument to defend his empirical formulation of f(u). Tanner and

Pelton (1960), however, showed that this term accounted for large discrepancies between measured and computed LE_{pot}. They replaced it with a function derived by Businger (1956) from the logarithmic form of the wind profile

$$f(u) = 1.2\ u_z\ [\ (1/k)\ \ln\ (z + z_o)/z_o]^{-2} \qquad (2.29)$$

where u_z is the horizontal windspeed at height z, k the Von Karman constant (= 0.4) and z_o the roughness length of the surface in question.

Building on Penman's earlier work, Van Bavel (1966) has developed a combination method for estimating potential evapotranspiration. His final equation has the same form as equation (2.28), except that the aerodynamic term E_a is replaced by:

$$B_v = \frac{\rho_a \varepsilon\ k^2}{P}\ \frac{u_a\ (e_a^* - e_a)}{[\ln\ (z_a\ /\ z_o)]^2} \qquad (2.30)$$

The model has been tested against measured evaporation from open water, wet bare soil, and well-watered alfalfa and showed good agreement between calculated and measured values. A wide range of climatic conditions was encompassed in the tests including advection of sensible heat to the evaporating surface.

Van Bavel's method requires no empirical constants and is not restricted to grass or any other specified set of surface conditions other than that water supply must be unrestricted. Another variation of equation (2.28), preferred by Slatyer and McIlroy (1961) and Monteith (1965) is given by:

$$LE = \frac{\Delta}{\Delta + \gamma}\ [(R_n - G) + \frac{\rho_a c^a}{\Delta}\ K\ ((e_a^* - e_a) - (e_o^* - e_o))] \qquad (2.31)$$

which assumes that the transport coefficients for heat and water vapour are equal ($K_h = K_v = K$). When the surface is wet, so that there is no saturation deficit, $(e_o^* - e_o) = 0$, the potential latent heat flux is given by:

$$LE_{pot} = \frac{\Delta}{\Delta + \gamma} (R_n - G) + \frac{\rho_a c^a}{\Delta} K (e_a^* - e_a) \tag{2.32}$$

Slatyer and McIlroy (1961) considered the special and apparently limited case when $(e_a^* - e_a) = (e_o^* - e_o)$, thereby eliminating the convective term. This reduces equation (2.31) to:

$$LE_{eq} = \frac{\Delta}{\Delta + \gamma} (R_n - G) \tag{2.33}$$

in which LE_{eq} is the equilibrium latent heat flux.

Interpretations of the physical meaning of (2.33) have varied. Monteith (1965) and Tanner and Fuchs (1968) have noted that it describes the evapotranspiration which would occur in a saturated atmosphere. This is the simplest case in which $(e_a^* - e_a)$ and $(e_o^* - e_o)$ are both equal to zero. Slatyer and McIlroy (1961) suggested that the wet bulb depressions would be equal when the surface and the overlying air had reached a state of mutual adjustment with regard to moisture. This would represent a lower limit to potential evapotranspiration.

Monteith (1965) anticipated that equation (2.33) would have limited application. However, Denmead and McIlroy (1970), Wilson and Rouse (1972) and Davies (1972) found that (2.33) gives a satisfactory approximation to evaporation from fairly dry surfaces. Hence its application is more general than anticipated originally.

Recently, Priestley and Taylor (1972) showed that LE_{pot} determined as the evaporation rate from saturated surfaces over a 24-hour period, is directly proportional to LE_{eq}:

$$LE_{pot} = a \frac{\Delta}{\Delta + \gamma} (R_n - G) \tag{2.34}$$

Several sets of data from diverse surfaces yielded 'a' values between 1.08 and 1.34, with an overall mean of 1.26. Similar values have been reported by Davies and Allen (1973).

Jury and Tanner (1975) found better agreement between measured and calculated results when equation (2.34) was extended to cover situations of advection assisted evaporation by changing 'a' from a constant to:

$$a^1 = 1.0 + (a - 1)\ (e^*_a - e_a)\ /\ (\overline{e^*_a - e_a}) \tag{2.35}$$

where $(\overline{e^*_a - e_a})$ is the long term mean saturation deficit.

4. Empirical methods.

A number of empirical or semi-empirical equations have been developed for estimating evapotranspiration. Thornthwaite (1948) describes the biological and physical importance of evapotranspiration in climatic determination. As a consequence of his efforts in studies of climatic classification systems he developed an equation for estimating potential evapotranspiration:

$$E_{pot} = c^1\ \overline{T}^{a^1} \tag{2.36}$$

in which $\overline{T}$ is the monthly mean temperature and c^1 and a^1 are parameters that vary from one place to another. Thornthwaite reasoned that the parameters c^1 and a^1 vary with another factor, one that is small in cool climates and large in hot ones. To account for this factor, he developed a monthly heat index from which c^1 and a^1 could be calculated. The monthly index was obtained from the equation:

$$i = \left(\frac{\overline{T}}{5}\right)^{1.514} \tag{2.37}$$

The summation of the twelve monthly index values gave an appropriate annual heat index I. The relation between a^1 and I was found to be closely approximated by the empirical equation:

$$a^1 = 6.75 \times 10^{-7} I^3 - 7.71 \times 10^{-5} I^2 + 1.79 \times 10^{-2} I + 0.49 \tag{2.38}$$

The coefficient c^1 in equation (2.36) is inversely related to I, so that the general equation for potential evaporation is:

$$E_{pot} = 1.6 \left(\frac{10\ \overline{T}}{I}\right)^{a^1} \tag{2.39}$$

in which a^1 must be calculated from equation (2.38).

Certain shortcomings are inherent in the Thornthwaite method. For example, evaporation lags the annual maximum heating during the late spring and is consequently out of phase in the fall as well. Furthermore application of the Thornthwaite concept to short-time periods leads to significant errors as a result of the often excessive variation in mean air temperature during these periods (Pelton et al., 1960).

Empirical equations, based on radiation methods for estimating potential evapotranspiration can be expected to resemble equation (2.13) or (2.28), but most take one of the following forms (Jensen, 1966)

$$LE = K_c\ \phi_1\ R_n \tag{2.40}$$

$$LE = K_c\ \phi_2\ R_s \tag{2.41}$$

in which K_c is a crop coefficient and ϕ_1 and ϕ_2 are net radiation and shortwave radiation coefficients. The products $\phi_1\ R_n$ and $\phi_2\ R_s$ generally represent potential evapotranspiration. When $K_c = 1.0$, equation (2.40) and (2.41) can be rearranged to assess the factors involved in the various coefficients. For example:

$$\phi_1 = 1.0 - \frac{H + G}{R_n} \tag{2.42}$$

$$\phi_2 = 1 - \alpha - \frac{R_{1n}}{R_s} - \frac{H + G}{R_s} \tag{2.43}$$

When considering daily totals the value of ϕ_1 will be approximately 1.0 when the algebraic sum of H and G ≃ 0. The value of ϕ_2 at this time will be $1 - \alpha - R_{1n}/R_s$ or about $0.75 - R_{1n}/R_s$ since the albedo is about 0.25 for most crops.

Makkink (1957) presented the following equation for estimating E_{pot} for grass over 10-day periods under the cool climatic conditions of the Netherlands:

$$E_g = 0.61 \frac{\Delta}{\Delta + \gamma} \quad \frac{R_s}{58.5} - 0.12 \tag{2.44}$$

where E_g is in mm day^{-1}, and R_s in cal cm^{-2} day^{-1}.

Turc (1961) simplified earlier versions of an equation for potential evapotranspiration for 10-day periods under the general climatic conditions of Western Europe.

Jensen and Haise (1963) evaluated the linear relationship between ϕ_2 and mean air temperature. From about 100 values for well-watered crops with full cover in the Western U.S.A. the constants for the following linear equation were $C_T = 0.025$ and $T_x = -3.0$

$$E_{pot} = C_T (T - T_x) R_s \tag{2.45}$$

where C_T is a temperature coefficient and T_x is the intercept of the temperature axis. These coefficients are considered as constants for an area. Jensen (1966) later defined C_T as:

$$C_T = \frac{1}{C_1 + C_2\ C_H} \tag{2.46}$$

and

$$C_H = \frac{50\ \text{mb}}{e_2 - e_1} \tag{2.47}$$

where e_2 and e_1 are the saturation vapour pressures at the mean maximum and mean minimum temperatures, respectively, for the warmest month of the year in the area, and $C_2 = 7.6°C$. Jensen et al. (1970) defined C_1 = 38 - (2°C x elevation in m/305) and $T_x = -2.5 - 0.14\ (e_2 - e_1)°C/mb$ - elevation in m/550.

Various empirical methods to estimate evapotranspiration are based on multiple correlation techniques. Baier and Robertson (1965) used simple meteorological observations and readily available astronomical data to predict daily latent evaporation from a bellani plate atmometer. They calculated multiple regression coefficients a_0 to a_6 which are used in the linear multiple regression equation:

$$Y = a_0 + a_1x_1 + a_2x_2 + a_3x_3 + a_4x_4 + a_5x_5 + a_6x_6 \tag{2.48}$$

where x_1 is the daily maximum air temperature (°F), x_2 the daily temperature range (°F), x_3 the solar radiation received at the top of the atmosphere (cal cm^{-2} day^{-1}), x_4 the solar radiation received at ground level (cal cm^{-2} day^{-1}), x_5 the total daily wind run (miles day^{-1}) and x_6 the daily vapour pressure deficit (mb). With all six variables involved, the correlation coefficient with latent evaporation was highly significant ($r = 0.84$). The reliability of the estimates could be further improved if daily values of estimated latent evaporation were accumulated.

In a later paper Baier (1971) suggested that latent evaporation could be converted to E_{pot} by applying a correction factor of 0.0094 cm cm^{-3}.

Christiansen (1968) and Christiansen and Hargreaves (1969) developed equations for estimating open-pan evaporation and potential evapotranspiration using radiation data and other climatic data. They also listed crop factors for converting pan evaporation to actual evapotranspiration. These crop factors are only applicable to the United States and to areas with similar climates.

5. Soil heat flux and environmental variables.

Using a number of simplifying assumptions, Van Wijk and De Vries (1963) showed in a theoretical development, that the soil heat flux is proportional to the temperature amplitude at the surface and the thermal properties of the soil. The amplitude of the surface temperature is generally unknown, but a number of publications deal with the empirical deduction of this quantity from observed air temperatures at screen height (Bonham and Fye, 1970; Stapleton et al., 1973; Hasfurther and Burmam, 1974). This approach has been used relatively successfully in predicting mean daily surface temperatures, but the prediction of hourly surface temperatures has been hampered because heat transfer in the air (equation 2.14) is proportional to the exchange coefficient for sensible heat K_h. It is not fully understood how this latter parameter varies with windspeed, surface roughness and thermal stratification (Stewart and Lemon, 1969).

The thermal properties of the soil depend mainly on the soil's mineral composition, its density and its moisture content. Idso et al. (1975) showed that the soil heat flux steadily increased from 'wet' to 'dry' conditions, whereas Fuchs and Hadas (1972) observed that the fraction of the net radiation dissipated as soil heat flux density was nearly identical for 'wet' and 'dry' soil. The apparent contradictory results were due to the fact that the latter authors worked with 'wet' conditions which were 50% drier than the 'wet' conditions reported by Idso et al. (1975).

The distribution of available radiation energy varies quite markedly with cloud conditions. Ho et al. (1968) showed that whereas on clear days the radiant energy is almost entirely converted into latent and sensible heat which is lost to the atmosphere, on overcast days a third of the available energy is stored in the soil.

Upon summarizing the literature one finds that there are numerous solutions for the energy balance equation. Most often the equation is solved for the latent heat flux, using either physical or empirical based relationships. It is apparent that the soil heat flux can be related empirically to a number of environmental variables, viz., net radiation, air temperature, windspeed, soil moisture conditions and canopy cover.

C. HEAT TRANSFER IN THE SOIL.

1. Heat transfer mechanisms.

Molecular conduction is the most important heat transfer mechanism operating in the soil. The flux of heat in a homogeneous medium is given by Fourier's law of heat conduction:

$$q^c = -\lambda \frac{\partial T}{\partial z} \tag{2.49}$$

where q^c is the heat flux, λ the thermal conductivity, T temperature and z depth. This force-flux relationship must be supplemented with the equation of continuity of energy in order to describe the heat transfer in the soil.

In addition three other heat transfer mechanisms are operating in the soil. The first of these is the movement of water through the soil; if water of one temperature flows through the soil at another, heat will be transported. This type of heat transfer, called convective heat transfer, can result from rain or irrigation water infiltrating the soil. Callendar (1895) discussed a rapid drop in temperature at the 20-cm depth in sandy soil due to the sudden release of a melting snow cover. More recently Sarson (1960) reported that thawing of a snow cover caused soil temperatures to fall 2.0°C at 120 cm and 4.7°C at 300 cm in a 48-hour period. Changes in soil temperatures following irrigation were reported by Wierenga et al. (1971). Although the effect of cold or warm irrigation water was of short duration, the addition of the water caused significant decreases in soil temperature by evaporative cooling for a relatively long period.

It has been observed by Smith (1943), Kersten (1949), Cary and Taylor (1962), and others, that when a soil sample of uniform moisture content is subjected to a temperature gradient, there is a flow of liquid water from the warmer to the colder region. Possible reasons why water flows in the liquid phase under the influence of a temperature gradient were suggested by Cary (1966). The amount of energy and mass transported in this manner is thought to be relatively small.

Another part of the moisture transfer is accomplished through the mechanism of vapour distillation from the warmer region with condensation in the colder soil. The amount of moisture transferred by this process is quite small, but the heat transfer could be considerable because of the very high value of the latent heat of vaporization of water. The problem of the transfer of moisture both in the liquid and the vapour form under the influence of temperature gradients has received much attention in the literature (De Vries, 1950, 1958a; Philip and De Vries, 1957; Woodside and Kuzmak, 1958; Taylor and Cavarza, 1954).

Heat can also be transferred from one soil particle to another by radiation. De Vries (1952) has concluded that this is a factor of negligible importance in the soil.

2. Fourier heat conduction equation.

The magnitude of the heat flux in a homogeneous soil is proportional to the temperature gradient and the thermal conductivity

$$q^c = - \lambda \frac{\partial T}{\partial z} \tag{2.49}$$

where the symbols were defined in the previous section. The negative sign was introduced because the heat flux is positive in the direction of falling temperatures and $\frac{\partial T}{\partial z}$ is negative. Equation (2.49) is known as the one-dimensional form of Fourier's law of heat conduction.

The principle of continuity of energy requires that the difference in heat flux into and out of an elementary soil element equals the rate of heat storage.

$$- \frac{\partial q^c}{\partial z} = C \frac{\partial T}{\partial t} \tag{2.50}$$

where C is the volumetric heat capacity of the soil and t is time. Applying equation (2.50) requires that no heat exchange in other than the vertical (z) direction and no heat generation takes place. Substitution of equation (2.49) into (2.50) gives:

$$C \frac{\partial T}{\partial t} = \frac{\partial}{\partial z} (\lambda \frac{\partial T}{\partial z}) \tag{2.51}$$

If we assume that λ is constant with depth, we obtain

$$\frac{\partial T}{\partial t} = \frac{\lambda}{C} \frac{\partial^2 T}{\partial z^2} = D \frac{\partial^2 T}{\partial z^2} \tag{2.52}$$

where D, the thermal diffusivity of the soil, determines the rate of temperature equalization. A large diffusivity causes rapid changes in soil temperature and a quick and deep penetration of the heat wave into the soil.

Equation (2.52) is not valid in the soil since the conductivity and heat capacity of the soil vary with depth and time and not all the heat transport is by conduction. However considerable insight into the nature of the flux of heat in the soil can be obtained by applying equation (2.52) and using certain assumptions which are not strictly valid in the soil. Two separate cases will be considered.

The first of these relates to the adjustment of the soil temperature profile to a sudden change in the temperature of the surface. Such a condition could arise when there is an invasion of the area by an air mass of temperature greatly different from that of the underlying soil. The other special situation relates to the propagation of the diurnal and annual temperature cycles produced by the solar radiation cycles.

The first of these useful relations may be obtained from equation (2.52), if we assume that the soil is homogeneous and a semi-infinite medium (that is, λ and C are constant with time and depth) and that the soil is isothermal at time $t = 0$. The temperature of the soil surface is then suddenly changed and kept at a constant temperature. The solution of equation (2.52) is sought with initial condition $T = T_o$ when $t = 0$ and $z > 0$ (z increases downwards) and the boundary condition $T = T_\infty$ at $z = 0$ and $t > 0$. It can be shown (Schneider, 1955) that the temperature of the soil at any depth z and time t is:

$$T = T_\infty + (T_o - T_\infty) \operatorname{erf} \left(\frac{z}{\sqrt{4Dt}}\right) \tag{2.54}$$

It follows from equation (2.54) that the time required for a given point to attain a given temperature varies inversely with the diffusivity.

The heat flux at any depth can be obtained from equation (2.49) by evaluating the temperature gradient or:

$$q^c = - \lambda \frac{\partial T}{\partial z}$$

$$= - \lambda \frac{T_o - T_\infty}{\sqrt{\pi D t}} \exp \left(\frac{-z^2}{4Dt}\right) \tag{2.55}$$

The second special case to be considered is the case of a homogeneous semi-infinite soil whose surface is heated in a periodic manner. This model corresponds to the daily and annual heating cycle experienced by the soil. The temperature at the soil surface can be expressed as:

$$T\ (0,t) = \overline{T} + A_o \sin \omega\ t \tag{2.56}$$

where $\overline{T}$ is the average temperature of the soil surface, A_o the amplitude of the surface temperature wave and ω the angular frequency. If it is further assumed that the wave is one of a series of similar waves so that transient effects are eliminated, the solution of equation (2.52) with the above boundary conditions is (Carslaw and Jaeger, 1959):

$$T\ (z,t) = \overline{T} + A_o \exp \left(- \frac{z}{d}\right) \sin \left(\omega t - \frac{z}{d}\right) \tag{2.57}$$

where $d = \sqrt{\frac{2D}{\omega}}$ is called the damping depth. This solution has been used by numerous workers to obtain values of the thermal diffusivity.

According to equation (2.57) the temperature amplitude decreases exponentially from the surface and the harmonic oscillation of the temperature wave travels downward. The value of D can be calculated as follows. Since the temperature amplitudes at z_1 and z_2 are $A_1 = A_o \exp (-z_1/d)$ and $A_2 = A_o \exp (-z_2/d)$ respectively, the value of D can be obtained by eliminating A_o thus

$$D = \frac{\omega}{2} \left(\frac{z_2 - z_1}{\ln A_1 - \ln A_2} \right)^2 \tag{2.58}$$

The diffusivity may also be computed from the lag in phase with depth. From equation (2.57) the time of maximum soil temperature at any depth occurs when $\sin(\omega t - z/d) = 1$ or $\omega t - z/d = \pi/2$. Solving for t, applying to two depths z_1 and z_2, and subtracting we get the phase equation $t_2 - t_1 = (z_2 - z_1)/\omega d$ or

$$D = \frac{1}{2\omega} \left(\frac{z_2 - z_1}{t_2 - t_1} \right)^2 \tag{2.59}$$

Both methods have been used by various investigators to estimate the thermal diffusivity of the soil. Good agreement between the two formulas (amplitude and phase) and with measured diffusivities have been found by some researchers (Fluker, 1958; Pearce and Gold, 1959; Wierenga et al., 1969) and poor agreement by others (Swinbank, 1948; Lettau, 1954; Rider, 1957). Carson (1963) has pointed out that those investigators who computed thermal diffusivities from the annual soil temperature record usually found realistic and consistent values, whereas those using the daily cycle (except Wieringa et al., 1969) did not. This would seem to indicate that nonconductive heat transfer mechanisms are quite large in the upper part of the soil profile, but that the averaging process over a year minimizes their importance.

De Vries (1958b) has shown that the heat flux at depth z, corresponding to the above mentioned initial and boundary conditions is:

$$q^c = -\lambda \frac{\partial T}{\partial z}$$

$$= A_o \sqrt{\lambda C \omega} \exp\left(-\frac{z}{d}\right) \sin\left(\omega t - \frac{z}{d} + \frac{\pi}{4}\right) \qquad (2.60)$$

It follows from equation (2.60) that the heat flux is also a harmonic function of time with a phase that is $\frac{1}{4}\pi$ advanced as compared with the temperature variation at the same depth. This corresponds to a time shift of 3 hours for the diurnal variation and 1½ month for the annual variation.

3. Convective heat transfer.

Soil water, under the influence of a potential gradient, moves from one location in the soil to another. If the water is in thermal equilibrium with its surroundings and the two locations are at a different temperature, conductive and convective heat transfer occurs. Wieringa (1968) reported that during infiltration heat transfer in the soil was mainly by mass movement (= convection) and that during the transitional stage, which involved rapid water distribution within the profile, heat transfer was by both mass movement and conduction. In the stage characterized by relatively slow water redistribution heat transfer was mainly by conduction.

The one-dimensional heat balance equation which describes the process of heat propagation in the soil by conduction and convection is (Stallman, 1963):

$$C \frac{\partial T}{\partial t} = \frac{\partial}{\partial z}\left(\lambda \frac{\partial T}{\partial z}\right) - c^w \frac{\partial (V^w T)}{\partial z} - c^v \frac{\partial (V^v T)}{\partial z} \qquad (2.61)$$

where C is the volumetric heat capacity of the soil, c the specific heat and V the moisture flux. The superscripts w and v denote liquid water and vapour respectively.

Assuming that the following conditions were satisfied:

1. The soil is saturated and there is no vapour flow.
2. The thermal characteristics are constant in space and time.
3. The fluid velocity is steady and uniform along the z axis.
4. The fluid is in thermal equilibrium with the surrounding soil.

Stallman (1965) was able to show that the solution of equation (2.61) with a sinusoidal surface temperature is:

$$T = \overline{T} + A_o \exp(-za) \sin(\omega t - zb) \tag{2.62}$$

where $a = [(K^2 + V^4/4)^{\frac{1}{2}} + V^2/2]^{\frac{1}{2}} - V$

$b = [(K^2 + V^4/4)^{\frac{1}{2}} - V^2/2]^{\frac{1}{2}}$

and $K = \dfrac{\omega}{2D}$

$V = \dfrac{V^w c^w}{2\lambda}$

Note that if $V^w = 0$, a and b reduce to $a = b = \sqrt{\dfrac{\omega}{2D}} = 1/d$ and equation (2.62) equals equation (2.57).

Equation (2.62) has been used by hydrologists to detect ground-water flow in saturated porous media by measuring temperature profiles (Cartright, 1970; Sorey, 1971). Its applicability to agricultural soils has been limited by the saturation and constant flow velocity assumption.

4. Combined transfer of heat and moisture.

Theories of combined heat and moisture transfer in soils have been developed along two different lines. One is based on classical fundamental relationships of soil physics and has been developed by Philip and De Vries (1957) and De Vries (1958). The second approach is based on the thermodynamics of irreversible process (Taylor and Cary, 1964; Cary, 1965).

The model of Philip and De Vries is based on the concept of liquid water flow under the influence of gravity, capillary and adsorption forces and on the concept of vapour movement by diffusion. They derived the following generalized transport equations for movement of liquid and vapour through a homogeneous porous medium under the combined influence of thermal and water content gradients:

$$V^w/\rho_w = - D_{\theta w} \frac{\partial \theta}{\partial z} - D_{Tw} \frac{\partial T}{\partial z} + K \tag{2.63}$$

$$V^v/\rho_w = - D_{\theta v} \frac{\partial \theta}{\partial z} - D_{Tv} \frac{\partial T}{\partial z} \tag{2.64}$$

where V^w and V^v are the liquid and vapour flux respectively, ρ_w is the density of water, $\partial\theta/\partial z$ is the water content gradient and $\partial T/\partial z$ is the temperature gradient. The terms $D_{\theta w}$, $D_{\theta v}$, D_{Tw} and D_{Tv} represent respectively the isothermal liquid and vapour diffusivity and the thermal liquid and vapour diffusivity. K is the hydraulic conductivity coefficient, which is dependent upon the physical properties of water and soil. The main assumptions in the derivation of equations (2.63) and (2.64) are:

1. The hydraulic conductivity, K, and the capillary potential, ψ, are assumed to be unique functions of the soil moisture content. This is not strictly true since these functions depend on the past history of wetting and drying which gives rise to hysteresis effects.

2. The capillary potential was thought to be proportional to the surface tension of the soil water.

3. The saturated vapour pressure is a function of temperature only and the relative humidity is a function of moisture content only.

Philip and De Vries considered two factors which may explain the differences in vapour fluxes found from measurements and those calculated with the molecular diffusion theory. The first one is that the macroscopic temperature gradient in the medium is generally exceeded by the microscopic temperature gradient across the air-filled pores. This will enhance the thermally induced vapour flux. The second reason is that vapour diffusion is aided by liquid islands which cause condensing on the upstream side and re-evaporation on the downstream side and therefore vapour diffusion is dependent on the total pore space. This holds for both the isothermally and thermally induced vapour flux.

The total moisture flux, V^m, was found by addition of equations (2.63) and (2.64):

$$V^m/\rho_w = - D_\theta \frac{\partial\theta}{\partial z} - D_T \frac{\partial T}{\partial z} + K \tag{2.65}$$

It should be noted that the two types of flow interact, so that strictly speaking they are not additive.

Application of the principle of mass conservation lead to:

$$\frac{\partial\theta}{\partial t} = - \frac{\partial V^w}{\partial z} - E \tag{2.66}$$

where the possibility of water transfer from the liquid to the vapour phase was recognized by the introduction of an evaporation rate, E, inside the pore system. Its value followed from the assumed vapour-liquid equilibrium condition. The final form of equation (2.66) became the general differential equation describing moisture movement under combined temperature and moisture gradients:

$$[1 + F_1 (\theta,T)] \frac{\partial\theta}{\partial t} + F_2 (\theta,T) \frac{\partial T}{\partial t} = \frac{\partial}{\partial z} (D_\theta \frac{\partial\theta}{\partial z})$$

$$+ \frac{\partial}{\partial z} (D_T \frac{\partial T}{\partial z}) - \frac{\partial K}{\partial z} \qquad (2.67)$$

where the functions F_1 and F_2, which express evaporation-condensation effects, are given in the original paper (De Vries, 1958a).

The concepts established by Philip and De Vries (1957) were extended by De Vries (1958a) to include in greater detail heat transfer by moisture movement. The heat flux, q^c, was expressed as:

$$q^c = - \lambda_x \frac{\partial T}{\partial z} + LV^v + c^v TV^v + c^w TV^w \qquad (2.68)$$

The first term on the right hand side represents the contribution of pure heat conduction; λ_x is the thermal conductivity of the porous medium in the hypothetical case where no moisture movement occurs. The second term represents the transfer of latent heat by vapour movement. The third and fourth terms represent the transfer of sensible heat in vapour and liquid form respectively. L is the heat of vaporization and c^w and c^v are the specific heat of water and vapour.

When the heat of wetting is neglected, De Vries used the principle of energy conservation to find:

$$[C + L\rho_w F_2 (\theta,T)] \frac{\partial T}{\partial t} + L\rho_w F_1 (\theta,T) \frac{\partial\theta}{\partial t} = \lambda_x \frac{\partial T}{\partial z}$$

$$+ L\rho_w \frac{\partial}{\partial z} (D_{T_v} \frac{\partial T}{\partial z}) + L\rho_w \frac{\partial}{\partial z} (D_{\theta_v} \frac{\partial\theta}{\partial z})$$

$$+ c^v \rho_w [D_{\theta_v} \frac{\partial\theta}{\partial z} + D_{T_v} \frac{\partial T}{\partial z}] \frac{\partial T}{\partial z}$$

$$+ c^w \rho_w [D_{\theta_w} \frac{\partial\theta}{\partial z} + D_{T_w} \frac{\partial T}{\partial z} - K] \frac{\partial T}{\partial z} \qquad (2.69)$$

The above analysis was subject to the assumption that all processes of heat transfer take place uniformly throughout the porous medium and that sources and sinks of heat (arising from evaporation-condensation) are distributed uniformly as well.

Equations (2.67) and (2.69) together govern the simultaneous moisture and heat fields in the soil.

Various attempts to test the theory as developed by Philip and De Vries have all met with the difficulty of determining the unknown parameters as functions of T and θ. In addition the effects to be measured are often very small and little is known about the influence of the simplifications that were introduced. In a number of cases the theory has been able to explain or predict the rate of moisture transfer under the influence of a temperature gradient (Rose, 1967; Cassel et al., 1969), but there are also instances in which no agreement between theory and experiment was obtained (Jury and Miller, 1974).

The thermodynamic theory starts from an expression for the production of entropy as caused by heat and moisture transfer (Taylor and Cary, 1960; Letey, 1968). The forces are the gradients of temperature and of the chemical potential of soil water at constant temperature. The latter is proportional to $(\partial\psi/\partial z)_T$ or $(\partial\theta/\partial z)_T$. Next phenomenological equations are obtained expressing the fluxes of moisture and heat as linear functions of $\partial\theta/\partial z$ and $\partial T/\partial z$. So obtained Joshua and DeJong (1973):

$$V^w = - L_{MM} \frac{v}{T} \frac{\Delta P}{\Delta x} - L_{MT} \frac{1}{T^2} \frac{\Delta T}{\Delta x} \tag{2.70}$$

$$q^c = - L_{TM} \frac{v}{T} \frac{\Delta P}{\Delta x} - L_{TT} \frac{1}{T^2} \frac{\Delta T}{\Delta x} \tag{2.71}$$

where v is the specific volume of soil water, P the soil water pressure, x the horizontal distance and L_{MM}, L_{MT}, L_{TT} and L_{TM} the phenomenological coefficients. The first term on the right hand side of equation (2.70) represents the flux that would move water under isothermal conditions, while the second represents the additional flux induced by a temperature gradient. The first term on the right of equation (2.71) represents the heat carried by the transfer of moisture and the second term accounts for heat flux due to molecular conduction along the thermal gradient through the soil. According to Onsager's theorem, and verified by Joshua and DeJong (1973) for a soil system, the cross-coupling coefficients L_{MT} and L_{TM} are equal.

Although the thermodynamic theory has the advantage of being quite general, it does not lead to expressions for the phenomenological coefficients, so that they must be determined or deduced from a physical model. It also obscures the actual processes involved like vapour diffusion and the interaction between heat transfer in the matrix and in the pore system.

The most obvious conclusion to be drawn is that the simultaneous flow of heat and moisture is an extremely complex matter. Although the suggested models may explain what is occurring in an experimental column of soil, their application to natural conditions with diurnal and annual temperature variations remains to be studied.

5. Thermal properties of soils.

As can be seen from equation (2.51) heat transfer in soil is governed by two independent thermal properties, the heat capacity and the thermal conductivity. These properties depend mainly on the mineral composition and the moisture content.

Thermal capacity.

For a non-homogeneous material such as soil, the heat capacity per unit volume of soil, C, equals the sum of the volumetric heat capacities of the different components. Denoting the volume fractions of the solid material, the organic matter, the water and the air as θ_s, θ_{om}, θ_w, and θ_a respectively, and the volumetric heat capacities of these components, as C_s, C_{om}, C_w and C_a, one can write:

$$C = \theta_s C_s + \theta_{om} C_{om} + \theta_w C_w + \theta_a C_a \qquad (2.72)$$

where each C-value is the product of the density ρ and the specific heat, c, of the component under consideration.

According to measurements by Kersten (1949) the specific heat of most soil minerals, c^s, varies linearly from 0.16 ± 0.001 cal g^{-1} °C^{-1} at -18°C to 0.19 ± 0.001 cal g^{-1} °C^{-1} at 60°C. Since the density of the minerals was about 2.7 g cm^{-3} an average value of C^s of about 0.46 cal cm^{-3} °C^{-1} holds for a mineral soil.

For organic materials ρ_{om} is as an average 1.3 g cm^{-3}, while for specific heat, c^{om}, an average value of 0.46 has been reported (De Vries, 1966, referring to measurements of Lang, Ulrich, Bracht and De Vries and De Wit).

The volumetric heat capacity of water is 1 cal cm^{-3} °C^{-1}. The contribution of air is usually neglected so that equation (2.72) becomes:

$$C = 0.46\theta_s + 0.60\theta_{om} + \theta_w \qquad (2.73)$$

Thermal conductivity.

An estimation of the thermal conductivity of the soil from its structure, in the same way as heat capacity, by considering the conduc tivity as a function of volume fractions and specific conductivities of the various components is difficult. De Vries (1952) has given a survey of the theoretical work and developed an approximate solution based on the theory of Burger (1915).

The model consists of a system made up of particles of one material immersed in a continuous medium of a second material. De Vries (1952) considered for dry soil air as the continuous medium. For moist soil he considered water as the continuous medium in which particles of air and solids were dispersed. The overall thermal conductivity of the soil could be expressed as:

$$\lambda = \frac{\sum_{i=0}^{n} \theta_i \ \lambda_i \ k_i}{\sum_{i=0}^{n} \theta_i \ k_i} \tag{2.74}$$

where n is the number of different kinds of particles contained in the continuous medium (all particles with approximately the same shape and conductivity were considered as of one type), θ_i is the volume fraction of the i^{th} kind of particles, λ_i is the thermal conductivity of the i^{th} kind of particles (subscript i=0 is the continuous medium) and k_i is the ratio of the average temperature gradient in the i^{th} kind of particles to the average temperature gradient in the continuous medium.

The value for k_i was estimated by De Vries (1952) from the following expression:

$$k_i = 1/3 \sum_{a,b,c} [1 + (\lambda_i/\lambda_o - 1) \ g_a]^{-1} \tag{2.75}$$

and

$$g_a + g_b + g_c = 1 \tag{2.76}$$

The values for g_a, g_b and g_c depend on the relative lengths of the major and minor axes of the dispersed particles. On a trial and error basis he was able to establish that $g_a = g_b = 0.125$ and $g_c = 0.750$, which corresponds to particles shaped like an ellipsoid of revolution. These values gave estimated thermal conductivities, using equation (2.74) that compared closely with measured values. Woodside and Cliffe (1959), Penner (1962, 1970) have also used equation (2.74) successfully to predict the conductivity of air-dry, water-saturated and frozen soils.

III. METHODS AND MATERIALS

A. General description of the experimental site.

The Whiteshell Nuclear Research Establishment (W.N.R.E.) is situated on the western edge of the Canadian Precambrian Shield (Lat. 50° 11' N, Long. 96° 03' W), at an elevation of 267 m. Boulder till deposits 3 to 6 m thick, resulting from Pleistocene glaciers and inundations from Glacial Lake Agassiz, overlie the granite bedrock. The general area is presently an ecotone with western, northern and southeastern vegetational elements present (Gill, 1960).

The experimental site was cleared from young aspen forest in 1956, planted in wheat the next four years and abandoned in 1960 after being sown with red clover. Natural succession has occurred since that time. A botanical survey carried out by Turner et al. (1972) revealed that the basal cover of the field varied between 18 and 36%. Grasses, primarily Kentucky blue grass (*Poa pratensis*) made up 62% of the basal cover, while forbs mainly clover (*Trifolium repens*) accounted for 35% of the basal cover.

B. Instrumentation.

In the spring of 1970 a micrometeorological energy budget study was initiated at W.N.R.E. Except for detailed soil temperature and soil water content measurements, most of the instrumentation at the experimental site has been in operation since 1970. The various components of the radiation and energy balance could not be measured, because of the lack of funds to purchase the necessary equipment. The data collected for this study cover the period from July 5, 1974 to September 30, 1975.

Net radiation flux.

Net radiation flux was measured with a Funk 250 junction thermopile (Funk, 1959), manufactured and calibrated by the Commonwealth Scientific and Industrial Research Organization (C.S.I.R.O.), Australia. It is constructed with polyethylene domes purged with dry nitrogen gas and a heating ring to prevent dew and frost formation at night. The instrument was fastened to a standpipe in the grass field at 150 cm above the ground.

The output signal of the instrument was fed into a small computer (PDP 8/S) which integrated the radiometer's output at 3600 points per hour using Central Standard Time (CST).

The sensitivity of the sensor used in this study ranged from 0.390 mV/mW cm^2 for longwave radiation to 0.396 mV/mW cm^2 for shortwave radiation. This small difference in sensitivity has been attributed (Collins and Kyle, 1966) to the lower spectral transmissivity of the polyethylene domes to longwave radiation. Data correction for this difference is difficult, if not impossible, and in any case, the error introduced is well within the overall experimental error of the instrument (Department of Transport, 1966). An average sensitivity of 0.393 mV/mW cm^2 has been used in this study.

The net radiometer's weak response to air temperature was compensated for by a correction of 0.1% per degree Celsius departure from the standard temperature of 20°C (Norris and Funk, 1961). For this purpose Stevenson screen daily maximum and minimum temperatures were used by applying a sinusoidal interpolation method to estimate hourly temperatures.

Sunshine.

A Campbell-Stokes sunshine recorder was installed on the top of a flat-roofed 5 m tall building near the experimental site. Hourly sunshine data were derived from this instrument. No corrections were made for the instrument's insensitivity to direct solar radiation of low intensities which occur when the solar elevation is less than 3°.

Air temperature.

Air temperatures were obtained from standard Meteorological Service of Canada maximum and minimum thermometers mounted in a Stevenson screen. Readings were taken twice a day at 8:30 a.m. and at 4:30 p.m. local time.

The Stevenson screen also contained a Lambrecht thermo- and hydrograph from which air temperatures and relative humidity data were extracted. Due to calibration problems the quality of the data from the latter instrument was questionable during the summer and fall of 1974.

Precipitation.

Precipitation was measured by means of a standard Meteorological Service of Canada rain gauge and snow gauge. Hourly precipitation was measured with a battery operated recording Fisher and Porter precipitation gauge. Errors in precipitation catch due to distorted air flow over the latter gauge were minimized by use of an Alter windshield consisting of free swinging, separated metal leaves suspended on rigid rods. The leaves were 1.3 cm above the level of the collecting orifice. The resolution of the gauge was 2.5 mm (0.1 inch).

Wind.

Windspeed was measured with a Bendix-Friez aerovane transmitter (model 120) mounted at the 7 m level of the meteorological tower (Reimer, 1966). The transmitter was connected by underground cable to a model 141-7 Aerovane Wind Recorder.

Soil heat flux.

In November 1972 two soil heat flux plates (Middleton and Company Pty. Ltd.) were installed in series at 2 cm below ground level. The average sensitivity of the two plates, as calibrated by the C.S.I.R.O., was 157.5 ± s.5 uV/mW cm^2. Drift of the calibration curve could not be checked after installation. The signal from the plates was amplified 20 times during the summer and 50 times during the winter before it was recorded on a Speedomax recorder. Amplifier drift, which was checked regularly, was found to be small.

Temperature.

Temperatures were measured using platinum resistance thermometers which were installed at 2 cm above ground level and at 10, 50, 100 and 200 cm below ground level in 1970. Additional probes were installed in June 1974 at the following depths: 1, 5, 15, 20, 30 and 75 cm. The soil temperature was therefore measured at ten levels, and air temperature at 2 cm above the ground, which was well within the plant canopy.

The resistance thermometers were installed very carefully: after a hole was dug, a wooden post was placed against a smoothly shaved side of the hole. The probes were inserted through holes drilled in the post at the desired depth levels. This ensured that the probes were kept at the correct vertical distance in the soil. The sensing head of the

THE UNIVERSITY OF MANITOBA LIBRARIES

probe protruded for about 20 cm from the post into the undisturbed soil. After the appropriate wire connections were made to a Speedomax temperature recorder, the hole was backfilled layer by layer with the original soil.

The data from the soil temperature and soil heat flux recorder, as well as the wind recorder, were transcribed for each hour of the day. This was done by recording ten-minute mean traces for the period five minutes before to five minutes after the hour. During the period from October 6, 1974 to April 26, 1975 the data were transcribed every second hour.

Soil moisture.

The moisture content of the soil profile was determined with Colman soil moisture cells (Soiltest Inc., model MC - 312). The cells were installed at eight depths, two cells per depth, giving a total of sixteen. The center of the cells were placed at 2, 5, 10, 20, 30, 50, 75 and 100 cm below the soil surface by pressing them into undisturbed soil from the edge of an auger hole. In refilling the auger hole care was taken to prevent it from becoming an abnormal water passage.

Readings were logged with a meter twice a day, except during weekends when no measurements were taken.

The relation between soil water content and tension was determined from undisturbed core samples (4.8 cm in diameter and 3.8 cm high) taken from a pit within the experimental area. Four core samples were taken from the following depths: 2, 10, 20, 30, 50 and 75 cm. The samples were saturated and using the pressure membrane apparatus, gravimetric water contents on the drying curve at pF values of 2.00, 2.48, 2.76, 3.35, 3.85 and 4.20 were determined. The same cores were used throughout the entire pF range. For each suction the mass of the sample plus the sample holder was determined at hydraulic equilibrium. At pF 4.20 the oven dry mass of the soil was determined and gravimetric water content was calculated at each suction.

The hydraulic conductivity was measured by the drying diffusivity method (Staple, 1965). Triplicate undisturbed soil cores from the 12 and 50 cm depths were taken. The cores, approximately 20 cm long, were carefully trimmed and shaved, so that they fitted snugly in the apparatus described by Shaykewich and Warkentin (1970). Subsequent phases of the procedure were similar to the ones described in detail by the above-mentioned authors.

Miscellaneous measurements.

Particle size analysis was conducted by the pipette method and organic matter was determined by the chromic acid oxidation method. Bulk densities were calculated from the mass of dry soil in the metal rings used in the water retention studies and the volume of the ring. Additional bulk densities were calculated from the undisturbed cores used in the experiment to determine hydraulic conductivities. Particle density was determined using a pycnometer with water as the displacement fluid.

Triplicate soil samples, including roots, were taken with a soil auger to a depth of 80 cm by 10-cm increments. The soil-root cores were placed in a 0.25 mm (60 mesh) sieve and washed with a strong jet of water (Williams and Baker, 1957). When all soil particles were washed through the sieve the roots were dried at 70°C, and by knowing the volume of the core (395.9 cm^3) root densities were determined.

C. Data Management.

The large number of data collected during the course of the experiment were stored on punched computer cards. The initial data handling and the subsequent calculations were all carried out on a high-speed computer.

Initial data handling involved conversion of the net radiometer's output of millivolts into ly min^{-1}. In this process, changes in the reference air temperature with time were taken into account. The output from the soil heat flux plates was in microvolts and had to be converted into mcal cm^{-2} min^{-1}, taking into account different summer and winter amplification of the signal. Readings from the Colman soil moisture cells were converted to resistance values. After a temperature correction, the resistance values were converted to gravimetric water contents, using the calibration curves* of the undisturbed soil of the experimental area.

Most of the micrometeorological and soil temperature data were collected on an hourly basis, except during the period October 6, 1974 to April 26, 1975 when net radiation flux, soil heat flux and soil temperature data were transcribed on a two-hourly basis. Average daily, weekly or monthly values were obtained by summation of the hourly data.

Air temperature and relative humidity data were obtained every two hours. In order to obtain hourly values either a linear interpolation technique or a sinusoidal interpolation method between maximum and minimum air temperatures was used.

---

*Unpublished data by A. Reimer, W.N.R.E.

D. Computational Procedures.

1. Radiation balance.

The net radiation flux could be computed through the use of equation (2.1). Various methods for calculating the shortwave radiation flux, the effective longwave radiation flux and albedo were selected.

Shortwave radiation.

The shortwave radiation flux was calculated by using an Angstrom (1924) and a Kimball (1927) type of equation. In the Angstrom equation:

$$R_s = R_s^c \,(a + b\ n/N) \qquad (3.1)$$

the solar radiation receipt at ground level on a clear day (R_s^c) was taken from Driedger (1969). The values a and b were thought to undergo seasonal changes such as proposed by Driedger and Catchpole (1970), i.e.,

$$a = 0.50187 - 0.0020752x + 0.00000483x^2 \qquad (3.2)$$

$$b = 0.35526 + 0.0032518x - 0.00000796x^2$$

where x was the day of the year. The resulting shortwave radiation flux was designated by RSDC.

In the Kimball equation

$$R_s = R_s^{top} \,(a + b\ n/N) \qquad (3.3)$$

the extra-terrestrial radiation flux at the top of the atmosphere (R_s^{top}) was computed from equation (2.5). By using a = 0.251 and b = 0.616 (Baier and Robertson, 1965) the calculated shortwave radiation flux was denoted by RSBR.

In order to obtain hourly shortwave radiation fluxes, R_s^c and R_s^{top} should be on an hourly basis. R_s^{top} was readily available on an hourly basis (see e.g., Robertson and Russelo, 1968), but this was not the case with R_s^c. Whenever needed the latter parameter was calculated on an hourly basis between sunrise and sunset using:

$$R_s^c \text{ (hourly)} = R_s^c \text{ (daily)} \times \frac{R_s^{top} \text{ (hourly)}}{R_s^{top} \text{ (daily)}} \qquad (3.4)$$

Effective longwave radiation.

The effective longwave radiation flux, R_{ln}, was calculated from formulas which employ air temperature and degree of cloudiness as only variables, i.e., equations (2.7) and (2.9). The Brunt-type formula (2.6) was not used because no reliable vapour pressures could be calculated during the first year of the study.

In the calculation of monthly and daily effective longwave radiation fluxes the temperature used is the mean temperature of the time period under consideration. It is also assumed that the ratio of n/N does not change during the night.

In the prediction of hourly effective longwave radiation flux Stevenson screen daily maximum and minimum temperatures were used by applying a sinusoidal interpolation method to estimate hourly temperatures. The maximum air temperature was assumed to occur at 3:00 p.m. Because no cloud conditions were measured at night the Linacre equation could not be used from sunset to sunrise. An attempt to relate hourly air temperatures and/or vapour pressures to effective longwave radiation at night was unsuccessful and hence no hourly night-time longwave radiation fluxes were calculated.

Albedo.

The albedo, α, was assumed to be either 0.22 after Nkemdirim (1972a) or 0.26 after Monteith (1959) in the months May to November. During the remainder of the year the albedo was 0.42. An exponential increase in α with the zenith angle Z in degrees:

$$\alpha = 0.0453 \exp (0.027 Z) \tag{3.5}$$

was assumed in the hourly prediction of the net radiation flux. This relationship is similar to the ones presented by Nkemdirim (1972b).

No attempt was made to find a daily or hourly value for the albedo during the winter months, because it changes very rapidly with the degree and depth of snow cover.

2. Energy balance.

Various methods of estimating potential evapotranspiration were selected. They represented combination theory and various methods based primarily on solar radiation, temperature and miscellaneous parameters. The length of period for which the methods are applicable should be dependent upon the data from which the various empirical coefficients were derived because the relationships might not be valid for shorter time periods. In this study all methods were applied to a daily period. Monthly evapotranspiration rates were obtained by adding daily rates, except in the Thornthwaite's method were E_{pot} was obtained from monthly data.

Climatic parameters.

Methods of estimating or calculating evapotranspiration require the computation of parameters such as vapour pressure, the psychrometer constant, etc., from climatic data. Computation of these climatic parameters was oriented toward digital computer data processing.

The Von Karman's constant (k) was used as a universal constant in turbulent flow. Its value has been determined to be near 0.4 with a range of 0.36 to 0.43; k was assumed to be 0.41 for these calculations.

The ratio of molecular weights, water vapour to air (ε) was used as 0.622. The specific heat of air at constant pressure (c^a) varies slightly with atmospheric pressure and humidity with extreme values ranging from 0.239 to 0.241 for conditions reasonable of plant growth. A constant value of 0.240 was used in the calculations.

The latent heat of vaporization (L, cal g^{-1}) is virtually unchanged by atmospheric pressure but does change with temperature. L was estimated as follows: (Brown and Van Haveren, 1972)

$$L = 597.67 - 0.58\ T \qquad (3.6)$$

where T is the average of the daily maximum and minimum air temperature.

The Smithsonian Meteorological Tables (1951) provide approximations of atmospheric pressure (P, mbar) and density (ρ_a, g cm^{-3}) which are sufficiently accurate for evapotranspiration estimates (Jensen, 1973). The following linear relationships were used to estimate atmospheric pressure and density.

$$P = 1013 - 0.1055\ ELV \qquad (3.7)$$

$$\rho_a = 0.00123 - 0.000034\ ELV/1000 \qquad (3.8)$$

where ELV is the elevation (m) of the location.

An empirical expression (Tetens, 1930) for saturation vapour pressure (e^*, mbar) as a function of temperature was used to convert relative humidity data to vapour pressures, where necessary and to provide values for Δ (mbar $°C^{-1}$) from the derivative of the expression:

$$e^* = 6.107 \exp\left(\frac{17.27\ T}{T + 237.3}\right) \qquad (3.9)$$

$$\Delta = \frac{25028}{(T + 237.3)^2} \exp\left(\frac{17.27\ T}{T + 237.3}\right) \qquad (3.10)$$

The roughness parameter z_o was calculated after Tanner and Pelton (1960) according to:

$$z_o = (ht^{0.964}) / 7.638 \tag{3.11}$$

where the height of the vegetation (ht) was estimated to be 40 cm.

The available windspeed was obtained at an elevation above the ground surface other than the elevations specified for E_{pot} formulas. According to Jensen (1973) the variation of windspeed with elevation near the ground surface can be adequately represented by:

$$u_z = u_z^1 \left(\frac{z}{z^1} \right)^b \tag{3.12}$$

where u_z^1 is the measured windspeed at z^1 (7 m above the ground) and u_z is the extrapolated windspeed at 2 m (z). The value of b was assumed to be 0.2 for this investigation which approximates a logarithmic profile over a crop like grass.

Potential evapotranspiration.

Potential evapotranspiration was calculated using the energy balance equation and combination theory:

$$E_{pot} = \frac{1}{L} \left(\frac{\frac{\Delta}{\gamma} (R_n - G) + LE_a}{\frac{\Delta}{\gamma} + 1} \right) \tag{3.13}$$

where R_n was the measured daily net radiation flux (ly day^{-1}) and G the measured daily soil heat flux (ly day^{-1}), and E_{pot} the potential daily evaporation (cm day^{-1}). The aerodynamic term E_a was calculated as proposed by Tanner and Pelton (1960):

$$E_a = 1.2\, u_z^* \,[1/k \ln(z + z_o)/z_o]^{-2}\, (e_a^* - e_a) \times 2.4 \tag{3.14}$$

where u_z^* is the extrapolated windspeed in miles per hour and 2.4 a conversion factor from mm hr^{-1} to cm day^{-1}. The aerodynamic term was also computed using Van Bavel's theory (1966):

$$E_a = B_v = \frac{\rho_a \varepsilon k^2}{P} \; \frac{u_z\,(e_a^* - e_a)}{[\ln\,(z/z_o)]^2} \times 10^5 \tag{3.15}$$

where 10^5 is the conversion from km to cm.

The Priestley and Taylor method (1972) was employed as a third method to compute potential evapotranspiration from combination theory:

$$E_{pot} = \frac{1}{L} \times a \times \frac{\Delta}{\Delta + \gamma}\,(R_n - G) \tag{3.16}$$

where the constant 'a' was assumed to be 1.26.

The Thornthwaite method (1948) for calculating evapotranspiration requires only temperature data:

$$E_{pot} = 1.6\, \left(\frac{10\,\overline{T}}{I}\right)^{a'} \tag{3.17}$$

where E_{pot} is in cm $month^{-1}$. The monthly heat index was obtained from:

$$i = \left(\frac{\overline{T}}{5}\right)^{1.514} \tag{3.18}$$

and upon summation of the twelve monthly index values an appropriate annual heat index I was found. The relation between a' and I was approximated by the empirical equation

$$a' = 6.75 \times 10^{-7}\, I^3 - 7.71 \times 10^{-5} I^2 + 1.79 \times 10^{-2} I + 0.49 \tag{3.19}$$

Makkink's (2.44) and Jensen and Haise's equation (2.45) were selected as empirical formulas which use shortwave radiation and air temperature as only variables to compute E_{pot}. In Jensen's equation C_T was computed as:

$$C_T = \frac{1}{C_1 + C_2\ C_H} \tag{3.20}$$

where

$$C_H = \frac{50 \text{ mb}}{e_2^* - e_1^*} \tag{3.21}$$

where e_2^* and e_1^* are the saturation vapour pressures at the mean maximum and mean minimum temperatures, respectively for the warmest month (July) of the year, and $C_2 = 7.6°C$. Jensen et al. (1970) defined $C_1 = 38 - (2°C \times ELV/305)$ and $T_x = -2.5 - 0.14\ (e_2^* - e_1^*)°C/mb - ELV/550$. The shortwave radiation flux R_s (in ly day^{-1}) was calculated as RSBR and RSDC in both Jensen's and Makkink's formula.

Baier and Robertson's (1965) linear multiple regression equation:

$$E_{pot} = (a_o + a_1x_1 + a_2x_2 + a_3x_3 + a_4x_4 + a_5x_5) \times 0.0094 \tag{3.22}$$

was used to calculate potential evapotranspiration (in cm day^{-1}) as well. In the above equation x_1 was the daily maximum air temperature (°F), x_2 the daily temperature range (°F), x_3 the solar radiation received at the top of the atmosphere (ly day^{-1}), x_4 the solar radiation received at ground level, calculated as RSBR (ly day^{-1}) and x_5 the total daily wind run (miles day^{-1}). The regression coefficients a_o to a_5 were respectively -78.68, 8.97×10^{-1}, 3.40×10^{-1}, 1.66×10^{-3}, 6.13×10^{-2} and 1.18×10^{-1}.

Similar to Baier and Robertson's equation a linear regression equation was developed from data gathered at Carberry,* which is approxi-

*Personal communication, Dr. C.F. Shaykewich mately 250 km southwest of the experimental site at W.N.R.E. The same meteorological variables x_1 to x_5 were used but different regression coefficients were obtained: $a_o = -35.97$, $a_1 = 8.97 \times 10^{-1}$, $a_2 - 7.938 \times 10^{-1}$, $a_3 = 1.337 \times 10^{-3}$, $a_4 = 7.443 \times 10^{-2}$ and $a_5 = 7.984 \times 10^{-2}$. Both the original Baier and Robertson formula as well as the one which used the 'Carberry' coefficients were employed to predict potential evapotranspiration.

3. Soil heat transfer

Fourier analysis.

The diurnal soil temperature waves at various depths were subjected to a Fourier harmonic analysis. Expressing the temperatures at each depth as a sum of cosine and sine components and taking 24 temperatures at equidistant, fixed intervals of one hour, the following equation can be evolved (e.g., Whittaker and Robinson, 1958):

$$T = a_o + a_1 \cos \omega t + a_2 \cos 2\omega t + \ldots. + a_{12} \cos 12\omega t$$

$$+ b_1 \sin \omega t + b_2 \sin 2\omega t + \ldots. + b_{11} \sin 11\omega t \qquad (3.23)$$

where a_o was the mean temperature (°C), a_k and b_k the amplitudes (°C) of the cosine and sine waves respectively, ω the radial frequency (7.27×10^{-5} sec^{-1} for the diurnal cycle) and t time (sec). Using the property that in one period equal absolute values of cos $k\omega t$ and sin $k\omega t$ occur, the 24 unknown coefficients a_k and b_k could be determined by applying schemes of successive sums and differences of the 24 temperature values.

Instead of representing the temperature as a dual coordinate wave (equation 3.23) a more convenient expression in the form of a single sine wave can be found. For that purpose the following auxiliary relationship was introduced:

$$a_k \cos k\omega t + b_k \sin k\omega t = (a_k^2 + b_k^2)^{\frac{1}{2}} \left[\frac{a_k}{(a_k^2 + b_k^2)^{\frac{1}{2}}} \cos k\omega t + \frac{b_k}{(a_k^2 + b_k^2)^{\frac{1}{2}}} \sin k\omega t\right] \quad (3.24)$$

where k is the wave number of the harmonics.

Denoting the phase angle of the single sine wave as ϕ_k (radians) it was calculated from:

$$A_k = (a_k^2 + b_k^2)^{\frac{1}{2}} \quad (3.25)$$

$$\phi_k = \arcsin \frac{a_k}{A_k} \quad (3.26)$$

$$\phi_k = \arccos \frac{b_k}{A_k} \quad (3.27)$$

where A_k is the amplitude of the single sine wave. Substitution of equations 3.25, 3.26 and 3.27 yielded the following expression:

$$T = a_o + \sum_{k=1}^{11} A_k \sin (k\omega t + \phi_k) + a_{12} \cos 12\omega t \quad (3.28)$$

This form of the Fourier equation is better for meteorological data, since the amplitude of each harmonic can easily be computed. The maximum value of any harmonic is reached when $(k\omega t + \phi_k) = \pi/2$. Further details of the computational procedures may be found in Whittaker and Robinson (1958).

Thermal properties.

Conductive heat transfer is largely governed by the heat capacity and the thermal conductivity of the soil. The heat capacity per unit volume of soil was found by adding the heat capacities of the different soil constituents in one cm^3. Assuming that the volumetric heat capacities of soil minerals, organic matter and water were 0.46, 0.60 and 1.00 cal cm^{-3} $°C^{-1}$, respectively, the heat capacity of the bulk soil (cal cm^{-3} $°C^{-1}$) equalled:

$$C = 0.46\ \theta_m + 0.60\ \theta_{om} + \theta_w \tag{3.29}$$

where θ_m, θ_{om} and θ_w denote the volume fractions of soil minerals, organic matter and water, respectively.

The thermal conductivity of the soil was calculated using De Vries' model (equation 2.74). For dry soil ($\theta_w \leq 0.05$) air was considered as the continuous medium. For moist soil ($\theta_w > 0.05$) water was considered as the continuous medium, in which ellipsoids of air, solid minerals and organic matter were dispersed. Hence the thermal conductivity was calculated from the equation:

$$\lambda = \frac{\theta_w \lambda_w + \theta_m \lambda_m k_m + \theta_{om} \lambda_{om} k_{om} + \theta_a \lambda_a k_a}{\theta_w + \theta_m k_m + \theta_{om} k_{om} + \theta_a k_a} \tag{3.30}$$

where θ is the volume fraction with the subscripts w, m, om and a referring to water, soil minerals, organic matter and air respectively, and where

$$k_m = 1/3 \left[\frac{2}{1 + (\frac{\lambda_m}{\lambda_w} - 1)\ g_m} + \frac{1}{1 + \frac{\lambda_m}{\lambda_w} - 1)(1 - 2g_m)}\right]$$

$$k_{om} = 1/3 \left[\frac{2}{1 + (\frac{\lambda_{om}}{\lambda_w} - 1)\ g_{om}} + \frac{1}{1 + (\frac{\lambda_{om}}{\lambda_w} - 1)(1 - 2g_{om})}\right]$$

$$k_a = 1/3 \left[\frac{2}{1 + (\frac{\lambda_a}{\lambda_w} - 1)\ g_a} + \frac{1}{1 + (\frac{\lambda_a}{\lambda_w} - 1)(1 - 2g_a)}\right] \tag{3.31}$$

with g a factor depending on the shape of the ellipsoid.

In accordance with De Vries (1963) the conductivities of soil minerals, organic matter and air were taken as 7.0, 0.6 and 0.0615 mcal

cm^{-1} sec^{-1} $°C^{-1}$ respectively. The thermal conductivity of water was taken as 1.42 mcal cm^{-1} sec^{-1} $°C^{-1}$. The shape factor g_a of the air filled pores was determined according to De Vries (1963), assuming that the air in the soil pores was saturated with water vapour, whereas g_m and g_{om} were taken to be 0.144 and 0.5 respectively.

The rate of temperature equalization in the soil is determined by the thermal diffusivity, D (cm^2 sec^{-1}), being the ratio of the thermal conductivity and the volumetric heat capacity of the soil. D was calculated by using equation (3.29) and (3.30).

The thermal diffusivity of the soil was also determined from amplitude and phase relationships. If the assumption of a homogeneous soil with constant diffusivity and a sinusoidal temperature wave at the surface are valid, plotting the logarithm of the amplitude versus soil depth and plotting of the time of the maximum soil temperature versus soil depth should yield straight lines for the annual or diurnal heating cycle, according to:

$$D = \frac{\omega}{2} \left(\frac{z_2 - z_1}{\ln A_1/A_2} \right)^2 \qquad (3.32)$$

$$D = \frac{1}{2\omega} \left(\frac{z_2 - z_1}{\Delta t} \right)^2 \qquad (3.33)$$

where ω is the radial frequency (1.99×10^{-7} sec^{-1} for the annual variation and 7.27×10^{-5} sec^{-1} for the diurnal variation), z the soil depth (cm), A the amplitude of the temperature wave (°C) and Δt the time lag (sec).

E. Model Development.

The purpose of the modelling effort was to understand the specifics of simultaneous heat and water flow through a field soil. The model was designed to simulate the temperature and water regime of the soil profile as a function of time. Since water was affecting the thermal properties of the soil and acting as one of energy transporting media, the development of the model was handled in two parts. The first part was the development of a 'water model' to describe soil water flow subject to natural precipitation, root extraction and transpiration by plants, evaporation of water directly from the soil and drainage. The second part was the development of an 'energy model' to predict the soil temperature regime. The energy model was built upon the water model as a foundation, although certain interactions between water and soil temperature were also considered. The water model and the energy model are described separately in the following.

1. Water model.

The movement of water was treated using the bookkeeping approach as proposed by Baier and Robertson (1966). The soil profile was divided into nine zones of varying thickness (see Table 1). It was assumed in the model that the water infiltrating in the soil recharged the water content in the top zone to its field capacity value (pF = 2.7) and that the remaining water infiltrated into the next zone and so forth, until either all infiltration water was used up, or all zones were brought to field capacity.

During the spring of 1975 it was noticed that the lower soil zones did not drain to field capacity, but remained near saturation for a considerable period of time (from the beginning of May till the end of July). It was therefore decided that once all the soil zones had reached their respective field capacities, any additional infiltration water would

Table 1. Spacial division of the water-energy model and some characteristics of the soil zones.

Soil zone depth cm	Grid point depth cm	Saturation % by vol.	Field capacity % by vol.	Permanent wilting point % by vol.	Rooting density (10^{-3} g cm^{-3})
0 - 3.0	1	44.8	42.4	24.1	2.50
3.0 - 7.5	5	48.3	44.3	24.4	2.45
7.5 - 12.5	10	53.0	42.7	23.2	2.07
12.5 - 17.5	15	52.5	42.2	23.2	1.84
17.5 - 25.0	20	53.2	42.3	23.6	1.21
25.0 - 40.0	30	46.1	39.3	24.6	0.71
40.0 - 62.5	50	46.1	42.9	26.7	0.61
62.5 - 87.5	75	45.8	43.1	28.5	0.25
87.5 - 112.5	100	45.8	43.1	28.5	0.10

drain into the lowest zone until it reached its saturation value. Any remaining water would fill up the second lowest zone and so forth until either all water was allocated or all zones were brought to saturation. Any surplus of water after all the zones were saturated was designated as runoff. The only loss of water from a zone was through root extraction and water vapour transport, including evaporation from the upper soil zone. Liquid water movement due to thermal gradients was not included in the model.

Boundary conditions.

The chosen boundary conditions approximated those existing in the field. The basal boundary condition was an impermeable layer, which restricted downward water movement as described above.

Two upper boundary conditions were employed at the soil surface to simulate infiltration and evaporation. To determine the appropriate condition daily climatic parameters like maximum and minimum air temperature, accumulated windspeed, net radiation, relative humidity and hourly precipitation data were required input data for the solution of the model.

The hourly precipitation data, collected from the Fisher and Porter precipitation gauge, were used to calculate infiltration rates, assuming an even rainfall intensity during the hour that the data were collected. Foliar interception was assumed to be negligible and no surface runoff occurred, except when the entire soil profile was saturated, as was described above.

Daily potential evapotranspiration was calculated according to Baier and Robertson's formula (equation 3.22). The partitioning of evaporation and transpiration was done rather crudely: potential evaporation was assumed to be 10% of the potential evapotranspiration after

King and Hanks (1973).

The actual evaporation, which caused water loss from the upper soil zone only, was thought to be limited by the amount of available water according to:

$$\left.\begin{array}{ll} AE = PE \times (0.10 \exp (3.00 \times AVH_2O)) & \text{if } AVH_2O < 0.79 \\ AE = PE & \text{if } 0.79 \leq AVH_2O \leq 1.00 \end{array}\right\} \quad (3.34)$$

where AE is the actual evaporation (cm day^{-1}), PE the potential evaporation (cm day^{-1}) and AVH_2O the fraction of available water in the upper soil zone. Equation (3.34) was derived after a model presented by Holmes and Robertson (1963) for a clay soil.

Actual evaporation was assumed to occur between 08:00 and 20:00 hours, and was normally distributed during that time, peaking at 14:00 hours.

Root extraction.

Attempts to describe the water regime in the soil-water-plant system have been divided into two types depending on whether or not individual roots were modelled. If the roots were modelled, the approach has been termed "microscopic" and the water flow equation is written in cylindrical coordinates and solved between the root surface and some radius from that surface (Gardner, 1960; Feddes and Rijtema, 1972).

The second approach to modelling the soil water under a growing crop ignores water flow to individual roots. In the "macroscopic" techniques the overall root system is assumed to extract water from each differential volume of the root zone at a given rate (Ogata et al. 1960; Molz and Remson, 1970). The moisture removing roots may then be represented as an extraction (negative source) term in the water balance equation.

In order to postulate a realistic model for a negative source term, account must be taken of the variation in rooting density with depth, the relative difficulty of extracting water from a given volume of soil and the effect of soil temperature on water uptake by plant roots. The potential amount of water taken up by the roots, from each soil zone (PRU_i, cm day^{-1}) was calculated according to:

$$PRU_i = \frac{\dfrac{RD_i}{\sum\limits_{i=1}^{n} RD_i} \times THICKN_i \times PT}{\left[\sum\limits_{i=1}^{n} \left(\dfrac{RD_i}{\sum\limits_{i=1}^{n} RD_i} \times THICKN_i \times PT\right)\right] / PT} \qquad (3.35)$$

where the subscript i refers to the soil zone under consideration, and RD is the rooting density (g cm^{-3}), THICKN the thickness of the soil zone (cm) and PT the potential transpiration rate (cm day^{-1}), assumed to be 90% of the potential evapotranspiration rate. It should be noted that PRU_i is defined so that

$$\sum_{i=1}^{n} PRU_i = PT \qquad (3.36)$$

An extraction term model such as described by equation (3.35) might give reasonable qualitative results for higher water contents, but undoubtedly would fail at lower water contents. One reason for this is that as the upper layers of the soil dry, more of the transpiration requirement comes from deeper roots in the wetter soil (Van Bavel et al. 1968). In order to describe this effect equation (3.35) was modified in the same way as potential evaporation was changed to actual evaporation, by taking into account the amount of available water.

Optimum root temperatures for many temperate grasses are about 20 - 25°C according to Hughes (1965). A decrease in root zone temperature has resulted in decreased water uptake (Nielsen et al. 1961; Cox and Boersma, 1967). The effect of soil temperature on water uptake by plant roots was accounted for by using a normal curve, which had a relative maximum value of 1.0 at 20°C.

The actual water uptake from each soil zone (ARU_i cm day^{-1}) equalled the potential uptake, but modified according to the relative difficulty of extracting water and the prevailing temperature in the soil zone under consideration:

$$ARU_i = PRU_i \times (0.10 \exp (3.00 \times AVH_2O_i)) \times \exp \left(- \frac{(T_i - 20)^2}{10^2} \right) \quad (3.37)$$

where subscript i refers to the soil zone under consideration and T is the soil temperature (°C). The other symbols were explained before. When the fraction of available water exceeded 0.79, it was set equal to 0.79, i.e., water uptake by plant roots was only limited by temperature conditions. A second restriction placed upon equation (3.37) was that no water uptake took place when the temperature was 2°C or lower.

Vapour flow.

Although the flow of water vapour in the soil is generally thought to be small in comparison with the liquid water flow, it is accompanied principally by a transfer of latent heat which influences the temperature regime in the soil. The general molecular diffusion equation describing the flow of water vapour can be written as:

$$V^v = - D_a \frac{\partial C}{\partial z} \quad (3.38)$$

where V^v is the water vapour flux (g cm^{-2} sec^{-1}), D_a the molecular diffusion coefficient of water vapour in air ($cm^2\ sec^{-1}$) and $\frac{\partial C}{\partial z}$ the water vapour concentration gradient ($g\ cm^{-3}/cm$). Under equal conditions of vapour gradient and temperature gradient, the water vapour flow in the soil is less than in air because of the available cross-sectional area and increased pathlength; hence instead of D_a a reduced diffusion coefficient ($\overline{D}_a$) has to be used. Penman (1940) and Blake and Page (1948) found from diffusion experiments that the empirical equation

$$\overline{D}_a = 0.66\ \theta_a D_a \tag{3.39}$$

where θ_a is the air filled porosity ($cm^3\ cm^{-3}$) fitted with a large range of θ_a values. Hence diffusion of water vapour in the soil profile can be described by:

$$V^v = -0.66\ \theta_a D_a\ (\varepsilon \frac{\rho_a}{P})\ \frac{\partial e}{\partial z} \tag{3.40}$$

where ε is the ratio of the molecular weight of water vapour to air, ρ_a the density of air ($g\ cm^{-3}$) and P the atmospheric pressure (mbar). The value of D_a was found from Krischer and Rohnalter (1940):

$$D_a = 4.42 \times 10^{-4}\ T_k^{2.3}/0.75\ P \tag{3.41}$$

and upon substituting the appropriate values for P and ρ_a (see equations 3.7 and 3.8) this lead to:

$$V^v = -3.425 \times 10^{-13}\ \theta_a\ T_K^{2.3}\ \frac{\partial e}{\partial z} \tag{3.42}$$

where e is the vapour pressure (mbar).

Except at very low water contents the water vapour pressure in soils is very close to the saturation water vapour pressure e^*, e.g., at pF = 4.2 and T = 20°C, $e/e^* = 0.989$, so that equation (3.42) becomes:

$$V^V = -3.425 \times 10^{-13} \; \theta_a \; T_K^{2.3} \frac{\partial e^*}{\partial z} \tag{3.43}$$

Since the saturation vapour pressure is temperature dependent only, it can be seen that the water vapour flux is only dependent upon temperature as well, provided the pF of the soil is less than 4.2.

The relatively much lower thermal conductivity of air causes temperature changes in the soil pores, where vapour diffusion takes place, to lag behind those of the soil matrix. This results in pronounced temperature gradients across narrow air spaces. The low thermal conductivity of air is the main factor causing the ratio of temperature gradient in the air filled pores to that of the bulk soil to be as large as 6.02 (Woodside and Kuzmak, 1958). Philip and De Vries (1957) presented vapour flux enhancement factors ranging from 1.4 to 3.0. For the prevailing porosities and water contents in this study the enhancement factor was about 1.75 from table 2 of Philip and De Vries, so that the final equation describing water vapour flow became:

$$V^V = -5.994 \times 10^{-13} \; \theta_a \; T_K^{2.3} \frac{\partial e^*}{\partial z} \tag{3.44}$$

2. Energy model.

Existing, computer operational, soil heat transfer models are primarily based on Fourier's molecular heat conduction law. However under field conditions where wetting and drying of the soil profile are regular reoccurring phenomena, water transfer cannot be ignored. In the following a soil energy model will be described which includes molecular heat conduction, transfer of sensible heat in the liquid and vapour form and transfer of latent heat by vapour diffusion.

Conductive heat flow.

Conductive heat flow in the soil is governed by Fourier's law of heat conduction:

$$q^c = -\lambda \frac{\partial T}{\partial z} \tag{3.45}$$

where q^c is the conductive heat flux (cal cm^{-2} sec^{-1}), λ the thermal conductivity (cal cm^{-1} sec^{-1} °C^{-1}) and $\partial T/\partial z$ the temperature gradient (°C/cm).

In the numerical approach equation (3.45) was discretized in the following way. Let a coordinate net or grid be drawn over a scale diagram of the temperature field under consideration, as shown in Figure 1. In this grid the index along the time abscissa is denoted j. The space interval chosen was not uniform, but taken according to the depths of the water content and temperature measurements (see Table 1). Within each zone the soil was assumed to be homogeneous, and therefore each grid point had its own corresponding thermal conductivity and heat capacity. These thermal properties were computed according to equations (3.29) and (3.30) with changes in soil composition with depth (see Table 11) and changes in water content with time taken into account.

The net conductive heat flux to zone 'i' during the time interval 'j + 1' ($q^{nc}_{i,j+1}$, cal cm^{-2} sec^{-1}) is the difference between the conductive heat flux into and out of the zone:

$$q^{nc}_{i,j+1} = q^{c}_{i,j+1} - q^{c}_{i+1,j+1} \tag{3.46}$$

and was approximated by:

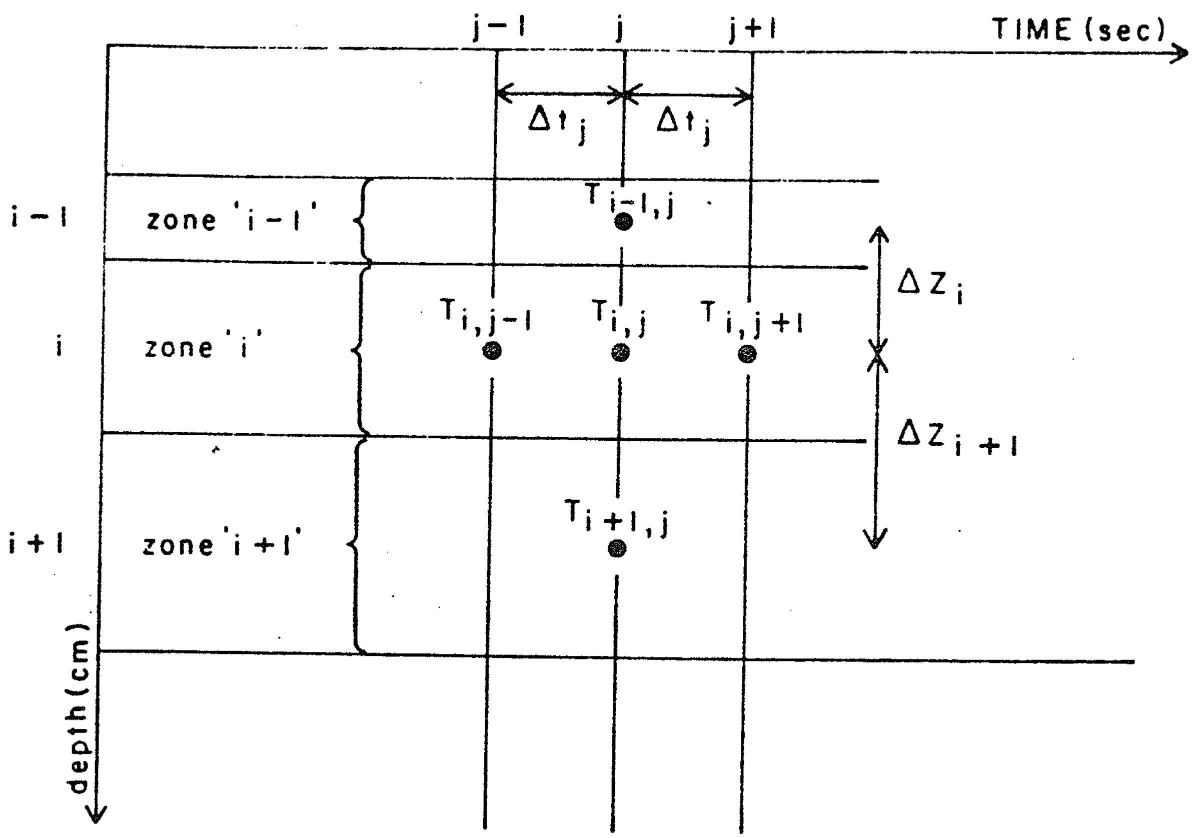

Figure 1. Grid of rectangular mesh with time arms of equal and space arms of unequal lengths.

$$q^{nc}_{i,j+1} = (-\overline{\lambda_{i,j}} \frac{T_{i,j} - T_{i-1,j}}{\Delta z_i}) - (-\overline{\lambda_{i+1,j}} \frac{T_{i+1,j} - T_{i,j}}{\Delta z_{i+1}}) \quad (3.47)$$

where $\overline{\lambda_{i,j}}$ and $\overline{\lambda_{i+1,j}}$ are the geometric mean thermal conductivities of grid points 'i-1' and 'i', and of grid points 'i' and 'i+1' respectively. Δz_i is the distance between the centres of the 'i-1' and 'i' zone, and Δz_{i+1} is the distance between the centres of zone 'i' and 'i+1' (see Figure 1).

Convective heat flow.

The transport of heat in soils is complicated by the fact that temperature gradients cause water movement, so that the water will tend to redistribute ifself when the temperature field changes. The water movement in its turn under the influence of both thermal and non-thermal gradients, gives rise to the transport of sensible and latent heat, which influences the temperature distribution.

Sensible heat transfer in the liquid phase.

The rate at which heat is transferred in the liquid water phase (q^w, cal cm^{-2} sec^{-1}) is given by:

$$q^w = V^w \int_o^{T^{Kw}} c^w \; dT \quad (3.48)$$

where V^w is the liquid water flux (g cm^{-2} sec^{-1}), T^{Kw} the temperature of the water (°K) and c^w the specific heat of the water (cal g^{-1} °C^{-1}).

The liquid water flux consisted only of infiltration and drainage of water from one soil zone to the one underneath it, as was described in the water model. Assuming that within each soil zone the soil temperature (T^K) and the temperature of the water (T^{Kw}) were in thermal equilibrium the convective heat transfer in the liquid phase from zone 'i-1' to zone 'i' was described by:

$$q^{w}_{i,j+1} = V^{w}_{i,j+1} \int_{o}^{T^{K}_{i-1,j}} c^{w} \, dT \qquad (3.49)$$

where $T^{K}_{i-1,j}$ is the temperature (°K) of the liquid water flux $V^{w}_{i,j+1}$ between zone 'i-1' and 'i'. Similarly the flux $q^{w}_{i+1,j+1}$, of heat contained within the moving liquid from zone 'i' to zone 'i+1' was described by:

$$q^{w}_{i+1,j+1} = V^{w}_{i+1,j+1} \int_{o}^{T^{K}_{i,j}} c^{w} \, dT \qquad (3.50)$$

The net gain or loss of heat contained in the water entering soil zone 'i' was the difference between the flux into and out of the zone:

$$\begin{aligned} q^{nw}_{i,j+1} &= q^{w}_{i,j+1} - q^{w}_{i+1,j+1} \\ &= V^{w}_{i,j+1} \int_{o}^{T^{K}_{i-1,j}} c^{w} \, dT - V^{w}_{i+1,j+1} \int_{o}^{T^{K}_{i,j}} c^{w} \, dT \qquad (3.51) \end{aligned}$$

In order to solve equation (3.51), the integral of c^{w} dT evaluated between o°K and $T^{K}_{i-1,j}$ and between o°K and $T^{K}_{i,j}$ was calculated as follows:

$$\int_{o}^{T^{K}_{i-1,j}} c^{w} \, dT = \int_{o}^{273} c^{w} \, dT + \int_{273}^{T^{K}_{i-1,j}} c^{w} \, dT \qquad (3.52)$$

The first term on the right hand side of equation (3.52) is a constant, K^{w}. Assuming that at temperatures above 273°K (=0°C) the specific heat of water, c^{w}, is independent of temperature, equation (3.52) transformed into:

$$\int_{o}^{T^{K}_{i-1,j}} c^{w} \, dT = K^{w} + c^{w} \, T^{K}_{i-1,j} \qquad (3.53)$$

Similarly the second term on the right hand side of equation (3.51) transformed into:

$$\int_{o}^{T^K_{i,j}} c^w \, dT = K^w + c^w \, T^K_{i,j} \tag{3.54}$$

Substituting equations (3.53) and (3.54) into equation (3.51) yielded

$$q^{nw}_{i,j+1} = V^w_{i,j+1} \, (K^w + c^w \, T^K_{i-1,j}) - V^w_{i+1,j+1} \, (K^w + c^w \, T^K_{i,j}) \tag{3.55}$$

To the author's knowledge the numerical value of K^w is unknown; hence in order to solve the sensible heat transfer rate in the liquid phase (i.e., equation 3.55) it must be assumed that the difference between $V^w_{i,j+1} \, K^w$ and $V^w_{i+1,j} \, K^w$ is small, and negligible error is introduced by equating these two terms. By doing so equation (3.55) reduced to:

$$q^{nw}_{i,j+1} = c^w \, (V^w_{i,j+1} \, T^K_{i-1,j} - V^w_{i+1,j+1} \, T^K_{i,j}) \tag{3.56}$$

Sensible and latent heat transfer in the vapour phase.

The transport of water vapour in the soil is accompanied by sensible and latent heat transfer according to:

$$q^v = V^v \int_{o}^{T^{Kv}} c^v \, dT + V^v L \tag{3.57}$$

where V^v is the water vapour flux (g cm^{-2} sec^{-1}), T^{Kv} the temperature of the water vapour (°K), c^v the specific heat of the water vapour (cal g^{-1} °C^{-1}), and L the latent heat of vaporization at 273°K calculated from equation (3.6). In contrast to the liquid water flux which was only in the downward direction, the vapour flux as described in equation (3.44) was dependent upon the temperature gradient, and hence could be directed upward or downward.

The numerical approximation of the vapour flux (equation 3.44) between soil zone 'i-1' and 'i' ($V^v_{i,j+1}$, g cm^{-2} sec^{-1}) in conjunction with the grid system, as shown in Figure 1, was written as:

$$V^v_{i,j+1} = 5.994 \times 10^{-13}\ \overline{\theta_{ai,j}}\ (\overline{T^K_{i,j}})^{2.3}\ \frac{e^*_{i-1,j} - e^*_{i,j}}{\Delta z_i} \tag{3.58}$$

where $\overline{\theta_{ai,j}}$ is the average air filled porosity of soil zone 'i-1' and 'i', $\overline{T^K_{i,j}}$ is the average soil temperature of the same zones and e^* the saturated vapour pressure, calculated according to equation (3.9). Similarly the rate at which water vapour was moving from zone 'i' to soil zone 'i+1' was given by:

$$V^v_{i+1,j+1} = 5.994 \times 10^{-13}\ \overline{\theta_{ai+1,j}}\ (\overline{T^K_{i+1,j}})^{2.3}\ \frac{e^*_{i,j} - e^*_{i+1,j}}{\Delta z_{i+1}} \tag{3.59}$$

Assuming thermal equilibrium within each soil zone, the net heat transfer in the vapour phase was:

$$q^{nv}_{i,j+1} = q^v_{i,j+1} - q^v_{i+1,j+1}$$

which could be approximated by:

$$q^{nv}_{i,j+1} = V^v_{i,j+1}\ [\int_0^{T^K_{i-1,j}} c^v\, dT + L] - V^v_{i+1,j+1}[\int_0^{T^K_{i,j}} c^v\, dT + L] \tag{3.60}$$

where L is the latent heat of the water vapour flux.

Evaluating the integrals $\int_0^{T^K_{i-1,j}} c^v\, dT$ and $\int_0^{T^K_{i,j}} c^v\, dT$ in a similar manner as was done for the sensible heat flux in the liquid phase, and by assuming that negligible error was introduced by equating the terms $V^v_{i,j+1}\ K^v$ and $V^v_{i+1,j+1}\ K^v$, where K^v is defined as $\int_0^{273} c^v\, dT$, equation (3.60) could be evaluated according to:

$$q^{nv}_{i,j+1} = V^{v}_{i,j+1} \, (c^{v} \, T^{K}_{i-1,j} + L) - V^{v}_{i+1,j} \, (c^{v} \, T^{K}_{i,j} + L) \qquad (3.61)$$

Energy conservation equation.

The rate at which heat is either gained by or lost from the soil zone under consideration is defined as the sum of the three heat transfer components, i.e., 1) heat conduction, 2) heat convection due to liquid water transport and 3) heat transfer due to water vapour transport as defined by equations (3.45), (3.48) and (3.57) respectively.

For problems involving the simultaneous transfer of heat and mass with phase changes associated with soil water evaporation and condensation, the equation expressing the conservation of energy for the system may be written as:

$$\frac{\partial Q}{\partial t} = \frac{1}{\mathrm{THICKN}} \, (q^{nc} + q^{nw} + q^{nv}) \qquad (3.62)$$

where THICKN is the thickness of the soil (cm) and Q the heat content of the soil (cal cm^{-3}) defined as:

$$Q = \int_{o}^{T^{K}} C \, dT \qquad (3.63)$$

where C is the volumetric heat capacity of the soil (cal cm^{-3} °C^{-1}). Equation (3.63) can be expanded as follows:

$$Q = \int_{o}^{T^{K}} C \, dT = \int_{o}^{273} C \, dT + \int_{273}^{T^{K}} C \, dT \qquad (3.64)$$

For a given water content, the first term on the right hand side of equation (3.64) is a constant, K^{s}. Assuming that at temperatures above 273 °K the heat capacity of the soil is independent of temperature, equation (3.64) became:

$$Q = K^s + CT^K \tag{3.65}$$

The numerical approximation of the energy balance equation (3.62) can be written as:

$$\frac{Q_{i,j+1} - Q_{i,j}}{\Delta t_j} = \frac{1}{THICKN_i} (q^{nc}_{i,j+1} + q^{nw}_{i,j+1} + q^{nv}_{i,j+1}) \tag{3.66}$$

and substituting equation (3.65) for Q into equation (3.66) yields:

$$K^s_{i,j+1} + C_{i,j+1} T^K_{i,j+1} - K^s_{i,j} - C_{i,j} T^K_{i,j} = \frac{\Delta t_j}{THICKN_i}$$

$$(q^{nc}_{i,j+1} + q^{nw}_{i,j+1} + q^{nv}_{i,j+1}) \tag{3.67}$$

Equation (3.67) could only be solved when it was assumed that $K^s_{i,j+1} = K^s_{i,j}$, that is the heat content of the soil in the temperature range between 0 and 273°K does not change, despite changes in water content during the time interval Δt_j. Because the time interval Δt_j is small, only small changes in water content occur and the error introduced by equating $K^s_{i,j+1}$ and $K^s_{i+1,j+1}$ was thought to be small. Neglecting $K^s_{i,j+1}$ and $K^s_{i,j}$ and rearranging equation (3.67) yielded:

$$T^K_{i,j+1} = [\frac{\Delta t_j}{THICKN_i} (q^{nc}_{i,j+1} + q^{nw}_{i,j+1} + q^{nv}_{i,j+1}) + C_{i,j}\ T^K_{i,j}]/C_{i,j+1} \tag{3.68}$$

where the volumetric heat capacity, C, was calculated from equation (3.29) which ignored the contribution of air and water vapour to the heat capacity of the soil.

The boundary conditions used in conjunction with (3.68) were the hourly measured temperature values from 1 and 100 cm depths. It was assumed that the temperature distribution at these depths showed a linear change with time in between full hours, when no actual temperatures were read. The initial conditions were the measured water content and temperature profiles on May 1, 1975. Using a time interval Δt_j of 300 seconds and.the above mentioned boundary and initial conditions, the soil temperature regime could be calculated.

A FORTRAN computer program was written to perform all the necessary calculations in the soil water and temperature simulation model. Program documentation is given in Appendix C.

IV. RESULTS AND DISCUSSION

A. Introduction.

Before the analysis of the W.N.R.E. net radiation, soil heat flux and soil temperature data is presented, it might be well to review the weather experienced during the time interval of the experiment and compare this period with the climatic averages over a longer period of time. Such a comparison is necessary since in a short record, a few periods of abnormally hot or cold weather, or of excessively wet or dry intervals can help to explain unexpected soil heat flux and soil temperature patterns.

The daily maximum, minimum and mean air temperature, precipitation, windspeed, as well as the duration of bright sunshine at W.N.R.E. for each day during the fifteen months study period are given in Appendix B. Monthly averages and totals are included in this table. The corresponding monthly long term averages at Winnipeg International Airport are listed also. This airport is about 130 km southwest of W.N.R.E. and hence one must be careful in making a direct comparison between the two locations.

During the experimental period there were six months, namely August and September of 1974 and 1975, March 1975 and April 1975 in which the monthly mean temperature at W.N.R.E. was at least 2°C lower than the corresponding long term average in Winnipeg. Only two months, December 1974 and January 1975 had a mean temperature of 2°C or more above the Winnipeg mean. This departure of about 2°C from the monthly mean temperature is generally not considered abnormal.

January and February 1975 were the coldest months with a mean temperature of -16.1°C. The coldest day was February 8 when the mean daily temperature was -29.2°C and an extreme minimum of -38.3°C was recorded on January 16.

In both years, July was the warmest month with a mean monthly temperature of 20.9°C, which is 1.2°C more than the long term mean in Winnipeg. Maximum temperatures of 32.2°C in 1974 were recorded on July 6 and 7. In 1975 a maximum temperature of 35°C was observed on July 30.

In July 1974 and 1975 and in October 1974 at least 20 mm less precipitation was recorded at W.N.R.E. than the comparable long term average in Winnipeg. Excessively wet months were August 1974 and 1975 and June 1975. The maximum rainfall of 7.34 cm on a single day was recorded on June 22, 1975.

B. Radiation Balance.

1. Measured results.

The daily and monthly average net radiation flux, calculated from a 24 hour day, is presented in Table 2. These data were derived from hourly values.

The maximum monthly net radiation flux occurring in July 1975 was around 0.23 ly min^{-1}. During the winter, when the ground was snow covered, a large proportion of the short-wave radiation was reflected. As a result the net radiation flux was negative, which means that radiation energy was lost from the soil-atmosphere interface.

It is apparent from Table 2 that considerable variation in the daily net radiation flux can occur from one day to the next. As an example one might consider June 22, 1975 which was a completely

Table 2. Average daily and monthly net radiation flux in 1974 (ly min^{-1})

Date	July	Aug.	Sept.	Oct.	Nov.	Dec.
1		0.171	0.109	0.047	0.004	-0.015
2		0.206	0.156	0.070	0.015	-0.021
3		0.220	0.184	0.032	0.004	-0.014
4		0.195	0.167	0.008	0.010	0.001
5	0.266	0.193	0.110	0.067	0.035	0.000
6	0.249	0.228	0.096	0.045	0.028	-0.005
7	0.156	0.224	0.071	0.032	0.000	-0.037
8	0.152	0.214	0.136	0.035	-0.005	-0.023
9	0.244	0.126	0.147	0.081	-0.015	-0.015
10	0.258	0.148	0.029	0.075	-0.004	-0.035
11	0.263	0.045	0.057	-0.009	0.008	-0.010
12	0.288	0.138	0.070	0.052	0.002	-0.042
13	0.214	0.155	0.150	0.052	0.011	-0.030
14	0.197	0.063	0.080	0.015	-0.017	-0.003
15	0.254	0.135	0.133	0.015	-0.024	0.001
16	0.140	0.218	0.084	0.031	-0.020	-0.007
17	0.240	0.127	0.144	0.021	-0.048	-0.025
18	0.265	0.203	0.108	0.042	-0.034	0.000
19	0.243	0.174	0.067	0.056	-0.004	0.000
20	0.259	0.029	0.095	0.029	-0.008	-0.013
21	0.269	0.060	0.085	0.032	-0.006	-0.005
22	0.240	0.099	0.111	0.022	-0.004	-0.010
23	0.205	0.154	0.074	0.028	-0.014	-0.009
24	0.177	0.118	0.037	0.001	-0.024	-0.038
25	0.241	0.134	0.071	0.014	-0.012	-0.040
26	0.226	0.147	0.133	0.021	-0.005	-0.031
27	0.214	0.127	0.089	0.026	-0.004	-0.052
28	0.054	0.035	0.119	0.039	-0.002	-0.056
29	0.155	0.187	0.021	0.025	-0.015	-0.063
30	0.139	0.087	0.047	0.030	-0.023	-0.052
31	0.207	0.124		-0.027		-0.027
Mean	0.215	0.145	0.099	0.032	-0.006	-0.022

Table 2. (cont.) Average daily and monthly net radiation flux in 1975 (ly min^{-1})

Date	Jan.	Feb.	Mar.	Apr.	May	June	July	Aug.	Sept.
1	-0.033	-0.029	-0.006	-0.010	0.101	0.262	0.213	0.113	0.149
2	-0.017	-0.019	-0.025	-0.012	0.122	0.203	0.311	0.147	0.107
3	-0.001	0.012	-0.018	-0.009	0.116	0.239	0.289	0.189	0.130
4	0.001	0.015	0.007	0.011	0.135	0.055	0.289	0.214	0.143
5	0.003	0.023	-0.011	0.030	0.187	0.105	0.290	0.238	0.085
6	-0.006	0.002	-0.014	0.031	0.220	0.101	0.294	0.242	0.055
7	0.001	-0.023	-0.034	0.025	0.225	0.277	0.237	0.124	0.131
8	0.000	-0.020	0.004	0.012	0.210	0.201	0.161	0.189	0.178
9	0.004	-0.003	-0.025	0.039	0.216	0.077	0.247	0.203	0.159
10	0.002	-0.012	-0.011	0.045	0.186	0.043	0.270	0.224	0.044
11	0.003	-0.005	-0.015	0.062	0.222	0.185	0.257	0.251	0.099
12	-0.017	-0.039	-0.013	0.074	0.238	0.275	0.177	0.176	0.061
13	-0.019	0.003	-0.024	0.097	0.143	0.187	0.215	0.225	0.099
14	-0.028	-0.015	-0.025	0.118	0.152	0.167	0.282	0.079	0.152
15	-0.021	0.006	-0.022	0.076	0.244	0.266	0.282	0.234	0.057
16	-0.017	-0.021	-0.008	0.083	0.216	0.212	0.173	0.198	0.151
17	-0.023	-0.019	0.014	0.057	0.214	0.280	0.199	0.205	0.143
18	-0.010	-0.030	0.025	0.068	0.236	0.247	0.188	0.157	0.043
19	-0.039	-0.027	-0.012	0.039	0.229	0.212	0.151	0.151	0.070
20	0.017	-0.046	0.008	0.141	0.099	0.237	0.166	0.076	0.066
21	-0.050	-0.028	0.015	0.222	0.202	0.249	0.250	0.105	0.093
22	-0.016	-0.014	-0.003	0.157	0.213	0.028	0.091	0.167	0.063
23	0.009	-0.021	-0.015	0.146	0.116	0.262	0.182	0.195	0.126
24	0.004	-0.012	0.010	0.111	0.259	0.207	0.245	0.108	0.118
25	0.002	-0.022	-0.017	0.154	0.221	0.263	0.242	0.134	0.111
26	-0.028	-0.010	0.001	0.019	0.208	0.205	0.254	0.140	0.108
27	-0.038	-0.033	0.007	0.062	0.147	0.328	0.219	0.067	0.100
28	-0.023	-0.039	0.010	0.152	0.211	0.149	0.237	0.195	0.069
29	-0.038		-0.025	0.154	0.178	0.166	0.205	0.099	0.038
30	-0.033		-0.014	0.061	0.102	0.283	0.256	0.187	0.094
31	-0.038		-0.006		0.196		0.142	0.090	
Mean	-0.015	-0.015	-0.008	0.074	0.186	0.199	0.226	0.165	0.101

overcast day ($n/N = 0.0$) with an average flux of 0.028 ly min^{-1}. In contrast the next day, June 23, was sunny ($n/N = 0.85$) and the average flux was 0.262 ly min^{-1}. Undoubtedly the soil heat flux and surface soil temperatures will be influenced by these large variations in net radiation flux.

The maximum observed daily net radiation flux (0.328 ly min^{-1}) occurred on June 27, 1975; the minimum was observed on December 29, 1974 (-0.063 ly min^{-1}).

The diurnal variation in net radiation flux on June 22 and 23, 1975 is presented in Figure 2. On June 22 there was almost no noticeable diurnal variation: the range was only 0.119 ly min^{-1}. June 23 on the other hand showed a typical net radiation pattern. During the night, radiation energy was lost from the surface, but shortly after sunrise the radiation flux increased rapidly. A maximum flux of 0.903 ly min^{-1} was reached at noon, after which it started to decrease again.

2. Results of the analyses and discussion.

The shortwave radiation flux calculated with the Angstrom equation (RSDC) or with the Kimball equation (RSBR) was dependent upon time of the year and the degree of cloudiness. Figure 3 illustrates that at W.N.R.E. the shortwave radiation flux during cloudless days ($n/N = 1.0$) varied between 0.106 and 0.612 ly min^{-1} on December 22 and June 21 respectively, using RSBR. During overcast days the yearly variation was very much dampened: the total range was only 0.146 ly min^{-1} as compared to a range of 0.506 ly min^{-1} for the cloudless days.

The difference between RSDC and RSBR is depicted in Figure 4. RSDC was smaller than RSBR during the entire year when $n/N \geq 0.6$. Under

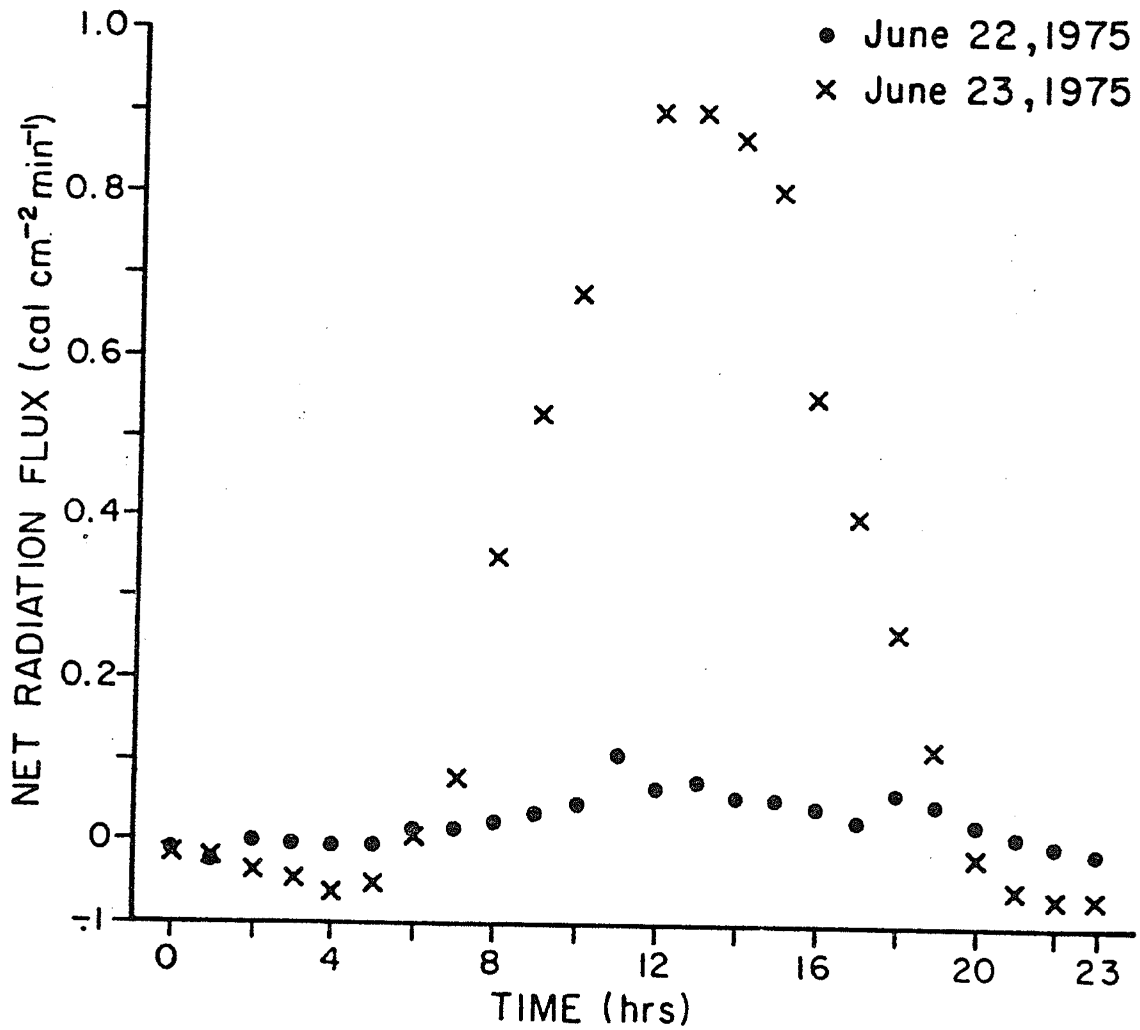

Figure 2. Diurnal variation in net radiation flux.

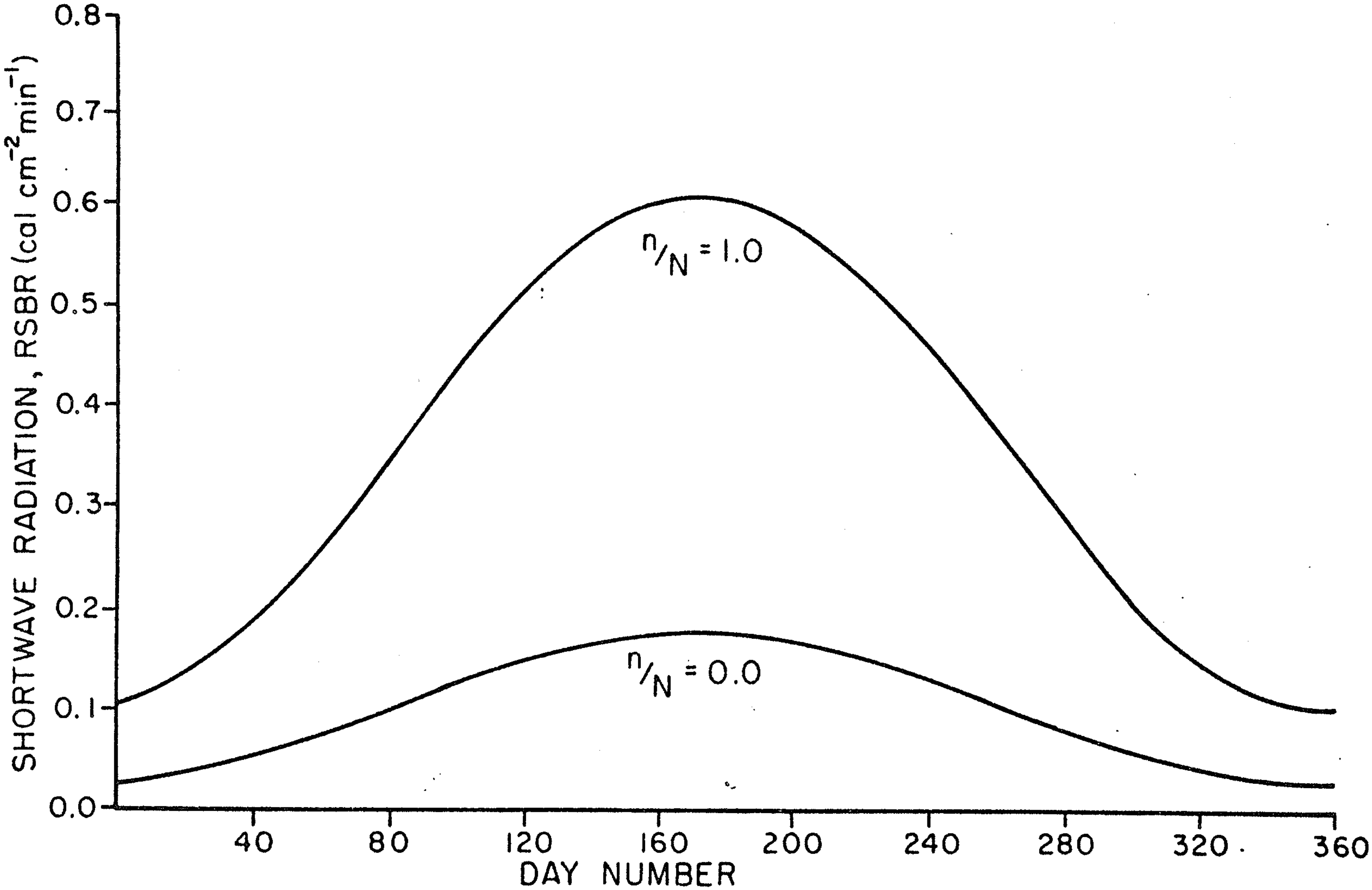

Figure 3. Annual change in shortwave radiation for cloudless (n/N = 1.0) and overcast (n/N = 0.0) sky conditions.

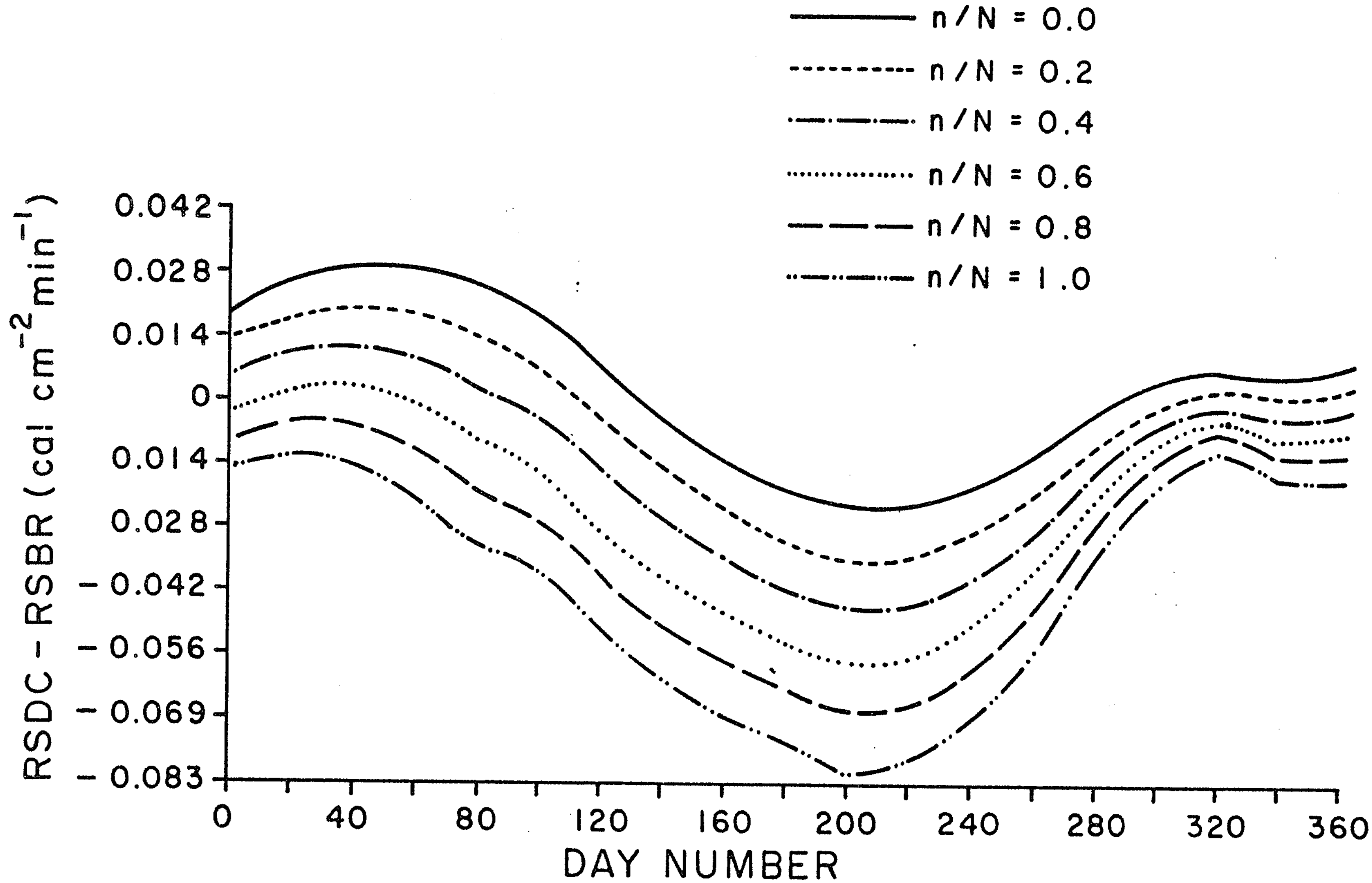

Figure 4. The difference in shortwave radiation flux as calculated with the Driedger-Catchpole equation (RSDC) and the Baier-Robertson equation (RSBR).

more cloudy conditions ($n/N < 0.6$) RSDC was larger during the winter but again smaller in the summer months. Because this study was primarily directed towards the summer months it is worth noting that the maximum difference between RSDC and RSBR was 14% on day number 204, which is July 23.

Figure 5 shows that Linacre's equation (2.7) for the effective longwave radiation flux, RLNLI, increased linearly with decreasing air temperatures. The Idso-Jackson formula (2.9), designated as RLNIJ, showed a curvilinear increase with decreasing temperatures, but when the temperature fell below 9°C RLNIJ decreased with decreasing temperatures.

The curves in Figure 5 were calculated for cloudless conditions. For less sunny conditions the difference between the Linacre and the Idso-Jackson formula is displayed in Figure 6 as a function of temperature and various degrees of cloudiness. Except for very sunny conditions ($n/N > 0.9$) RLNIJ was larger than RLNLI. The differences were small when n/N was 0.8 or 0.9, especially in the temperature range from 5 to 30°C. The deviations became larger under either sunnier or cloudier conditions.

The results of a linear regression analysis of monthly mean radiation data for $R_n = a + b\ X$ are given in Table 4. X which is either the predicted net- or shortwave radiation flux was derived from formulas summarized in Table 3. Mean monthly temperatures and cloud data (n/N) were used to calculate monthly mean short- and effective longwave radiation fluxes.

All combinations yielded intercepts which were significantly different from zero at the 5% probability level. Two combinations, line 1 and 5 had a slope which was significantly different from one.

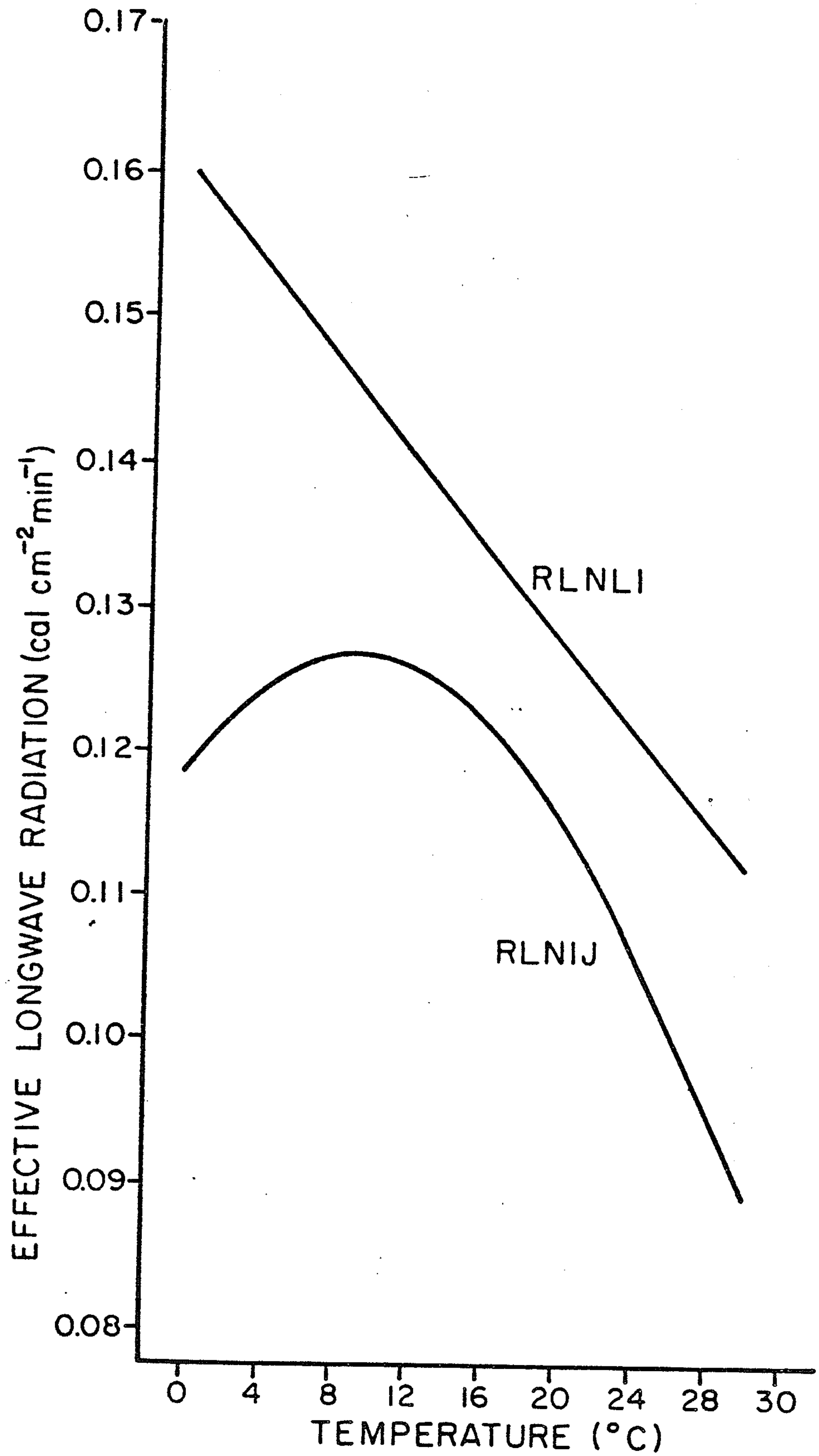

Figure 5. The change in effective longwave radiation as a function of temperature under cloudless sky conditions.

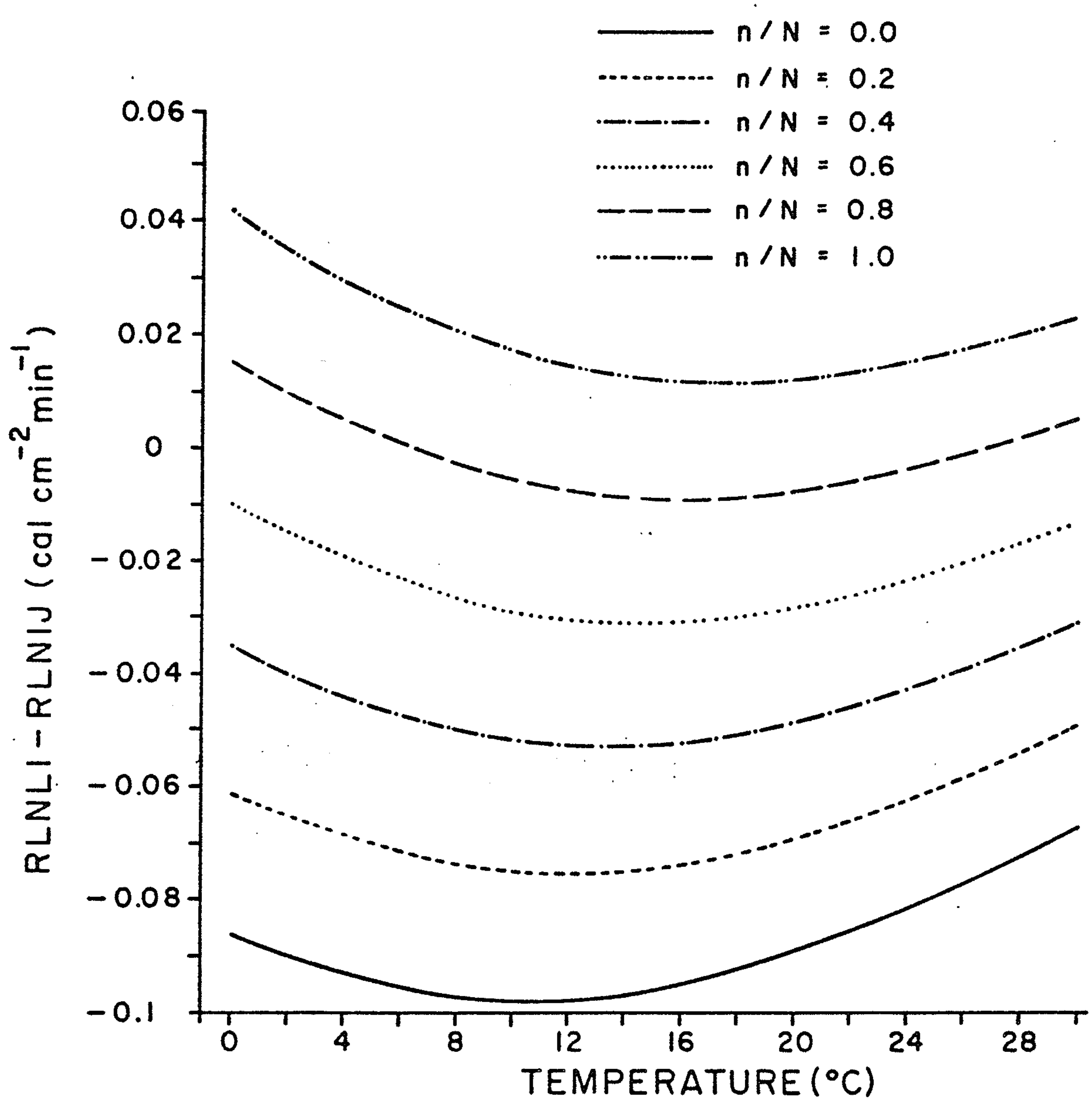

Figure 6. The difference in RLNLI and RLNIJ as a function of temperature for various cloud conditions.

Table 3. Summary of the equations used in the prediction of the net radiation flux Supplement to Tables 4, 5, 6, 7.

Equation No.	
1	$R_n = (1 - \alpha)\ R_s - R_{ln}$
2	$\alpha = 0.22$ (during the summer)
3	$\alpha = 0.26$ (during the summer)
4	$\alpha = 0.42$ (during the winter)
5	$\alpha = 0.0453 \exp(0.027\ Z)$ (for hourly data)
6	$R_s = RSBR = R_s^{top}\ (p + q\ n/N)$ where $p = 0.251$ and $q = 0.616$
7	$R_s = RSDC = R_s^{c}\ (a + b\ n/N)$ where $\begin{cases} a = 0.50187 - 0.0020752x + 0.00000483x^2 \\ b = 0.35526 + 0.0032518x - 0.00000796x^2 \end{cases}$
8	$R_{ln} = RLNLI = 32 \times 10^{-5}\ (1 + 4\ n/N) \times (100 - T)$
9	$R_{ln} = RLNIJ = \sigma T_k^4\ [\ 1 - (1 - 0.261 \exp(-7.77 \times 10^{-4}\ (273 - T_k)^2))]$

Table 4. Results of linear regression analysis of monthly mean radiation data for $Y = a + bX$. Period of measurement July 1974-October 1975 (15 data points)

Line	Y Measured	X	Derivation of X with[1]	Intercept a ly min^{-1}	Slope b	r^2	S_{yx} ly min^{-1}
1	R_n	R_n	1,2,4,6,8	0.013*	0.838**	0.984	0.012
2	R_n	R_n	1,2,4,6,9	0.030*	0.898	0.913	0.028
3	R_n	R_n	1,2,4,7,8	0.015*	1.004	0.968	0.017
4	R_n	R_n	1,2,4,7,9	0.038*	1.055	0.851	0.037
5	R_n	R_n	1,3,4,6,8	0.015*	0.891**	0.981	0.013
6	R_n	R_n	1,3,4,6,9	0.034*	0.953	0.900	0.030
7	R_n	R_n	1,3,4,7,8	0.018*	1.066	0.961	0.019
8	R_n	R_n	1,3,4,7,9	0.043*	1.111	0.826	0.040
9	R_n	R_s	6	-0.073	0.677	0.908	0.029
10	R_n	R_s	7	-0.080	0.775	0.824	0.040

[1]equation numbers refer to Table 3 only.

*significantly different from 0 at the 5% probability level.

**significantly different from 1 at the 5% probability level.

The equations which used RSDC (lines 3, 4, 7 and 8) had more slope than the equations which used RSBR. This might be explained by the fact that all months had cloud conditions such that $0.3 < n/N < 0.7$. According to Figure 4 this meant that RSDC was smaller than RSBR, except in January, February and March. Therefore the predicted net radiation flux would be smaller when RSDC was employed in the calculations, rather than RSBR. Upon plotting measured net radiation flux versus predicted net radiation flux a steeper line would result when RSDC was used in the calculations.

It should also be noticed that the slopes of the equations using RSDC were closer to 1.0, compared to the equations where RSBR was used, except in line 8, Table 4. On this basis one might conclude that the relationships used to calculate R_n in lines 3, 4 and 7 are superior to those in lines 1, 2 and 5.

The intercepts of the equations which used RLNLI (lines 1, 3, 5 and 7, Table 4) for effective longwave radiation were lower than the comparable ones which used RLNIJ (lines 2, 4, 6 and 8, Table 4). Figure 6 showed that at above freezing temperatures RLNLI was smaller than RLNIJ for almost all cloud conditions, except very sunny ones ($n/N \geq 0.9$) which were not encountered on a monthly basis in this study. Only in January and February very low mean temperatures were recorded and as a consequence RLNLI was larger than RLNIJ during those two months only. Hence a larger predicted net radiation flux was calculated when RLNLI was used rather than RLNIJ. When the measured and predicted net radiation fluxes were compared the intercept would be less if one used RLNLI, assuming that the albedo and the shortwave radiation flux were equal.

The standard error from the regression line, S_{yx}, was considerably lower when RLNLI was used in calculating the net radiation flux. The average standard error of lines 1, 3, 5 and 7, Table 4, was 0.015 ly min^{-1}, which was approximately between 7 and 15% of the net radiation flux received in the months May to October. The random errors in measuring R_n as quoted by Linacre (1968), were of the same order of magnitude. Even measurements of two net radiometers exposed side by side above pasture land, as reported by Holmes and Watson (1967) showed differences of 10%.

Using a summer albedo of 0.22 (lines 1-4, Table 4) rather than 0.26 (lines 5-8, Table 4) produced a smaller standard error from the regression line. This was true for all tested combinations.

The results of a linear regression analysis of net radiation flux upon shortwave radiation flux are also listed in Table 4, lines 9 and 10. The correlation coefficients, r, exceeded 0.95 and 0.90 for line 9 and 10 respectively and the standard errors from the regression line ranged from 0.029 to 0.040 ly min^{-1}. These results compared well with those found by other authors (Fritschen, 1967; Fitzpatrick and Stern, 1973). However, upon plotting the relationship between net- and shortwave radiation flux a distinct seasonal loop was found (Figure 7). For instance, the net radiation flux in fall was some 0.06 to 0.10 ly min^{-1} larger than in spring, even though the shortwave radiation intensities were about the same. The high albedo of the snowcover was largely responsible for the low radiation efficiency in spring.

Due to the seasonal loop exhibited in the relationship between net- and shortwave radiation flux, preference should be given to lines 1-8, Table 4 for the prediction of monthly mean net radiation fluxes. Because

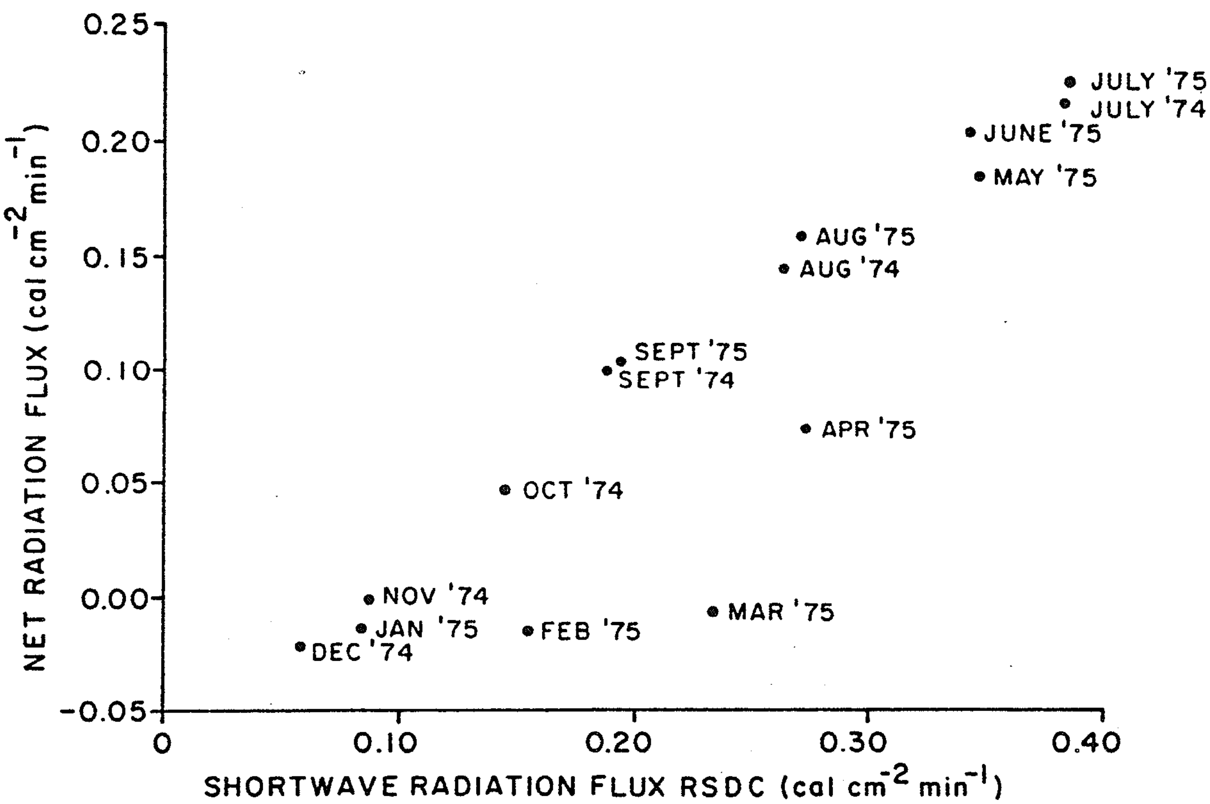

Figure 7. Seasonal change in net and shortwave radiation flux.

summer albedos of 0.26 gave higher standard errors than comparable equations which used an albedo of 0.22, lines 5-8 were also eliminated. It then appeared that line 3 would give the most accurate predicted monthly net radiation flux.

Table 5 displays the results of the linear regression analysis of daily mean measured net radiation values upon the daily predicted net radiation fluxes. In lines 1-4 all days during the measurement period were included in the regression analysis. In the remainder of the table the days were separated into cloudy ones ($n/N < 0.66$) and sunny ones ($n/N > 0.66$).

As with the monthly mean data, it was again observed that the equations which use RSDC to calculate the shortwave radiation flux (lines 3, 4, 7, 8, 11 and 12) had more slope and were generally closer to 1.0 than the comparable ones which used RSBR. The explanation of this feature was discussed previously.

Also the effect of using RLNIJ or RLNLI as effective longwave radiation flux showed similar features as discussed previously. However it is interesting to note that during sunny days ($n/N > 0.66$) when RLNLI was used (lines 5 and 7, Table 5) the intercept was larger than when the same equations were used for cloudy days ($n/N < 0.66$) (lines 9 and 11, Table 5). This might be explained by the fact that under cloudy conditions the effective longwave radiation flux, as calculated with Linacre's equation was reduced. On the other hand the Idso-Jackson formula was independent of cloud conditions expressed as n/N. The lower intercepts on sunny days when RLNIJ was used (lines 6 and 8, Table 5) as compared to the ones found during cloudy days (lines 10 and 12, Table 5) are thought to be caused by decreased temperatures under more

Table 5. Results of linear regression analysis of daily mean radiation data for $R_n = a + b\ X$, where X is the predicted net radiation flux. Period of measurement July 5-October 31, 1974 and May 1-September 30, 1975.

Line	Derivation of X with[1]	n/N	Number of data	Intercept a ly min^{-1}	Slope b	r^2	S_{yx} ly min^{-1}
1	1,2,6,8		272	0.011	0.847**	0.892	0.044
2	1,2,6,9		272	0.069*	0.651**	0.857	0.046
3	1,2,7,8		272	0.014	1.012	0.883	0.050
4	1,2,7,9		272	0.079*	0.753**	0.856	0.049
5	1,2,6,8	>0.66	105	0.015	0.816**	0.913	0.048
6	1,2,6,9	>0.66	105	0.024	0.797**	0.889	0.054
7	1,2,7,8	>0.66	105	0.028*	0.944	0.909	0.053
8	1,2,7,9	>0.66	105	0.037*	0.918**	0.881	0.060
9	1,2,6,8	<0.66	167	0.002	0.926**	0.818	0.027
10	1,2,6,9	<0.66	167	0.072*	0.728**	0.821	0.027
11	1,2,7,8	<0.66	167	0.005*	1.091**	0.800	0.029
12	1,2,7,9	<0.66	167	0.083	0.842**	0.823	0.027

[1]equation numbers refer to Table 3 only.

*significantly different from 0 at the 5% probability level.

**significantly different from 1 at the 5% probability level.

overcast sky conditions. As was shown in Figure 5 RLNIJ increased with decreasing temperatures till 9°C. During the period of measurement July 5-October 31, 1974 and May 1-September 30, 1975, there were relatively few days when the temperature dropped below 9°C on cloudy days and hence increased cloudiness resulted indirectly in a larger effective longwave radiation flux, when calculated by the Idso-Jackson formula.

Separating the data into sunny and cloudy days reduced the standard error for the cloudy days only. This could be expected because average net radiation flux was also lower during cloudy days. The average standard error when all data were included in the analysis was 0.047 ly min^{-1}.

The relationship between net- and shortwave radiation flux is shown in Table 6 for daily mean data. Upon comparing this relationship with equation (2.1), it was inferred that the factor 'a' depends particularly on the degree to which the sky is overcast. This is confirmed in Table 6: cloudy days (lines 5, 6, 11 and 12) had a considerably lower intercept than comparable sunny ones. The b values which depend upon albedo show that the data for clear days had a larger slope, i.e., a lower albedo than those for overcast days in the summer, but the reverse was true for the winter data.

Relatively few expressions are known for varying cloud conditions. Davies and Buttimor (1969) developed the relation: $R_n = 0.556\ R_s - 0.023$, which had a standard error of 0.027 ly min^{-1}. The slope of this line is practically the same as found for the experimental field (lines 1 and 2, Table 6), but the intercepts of the two lines with the ordinate differ. This might be partly due to differences in calculation procedures, because the last mentioned authors extrapolated the intercept which was obtained

Table 6. The relationship between daily net- and shortwave radiation flux expressed as $R_n = a + b\ R_s$.

Line	Derivation of R_s with[1]	Period	n/N	Number of data	Intercept a ly min^{-1}	Slope b	r^2	S_{yx} ly min^{-1}
1	6	S		272	-0.014	0.522	0.854	0.044
2	7	U		272	-0.017	0.606	0.851	0.046
3	6	M	>0.66	105	-0.084	0.651	0.888	0.049
4	7	M	>0.66	105	-0.086	0.753	0.877	0.055
5	6	E	<0.66	167	-0.022	0.588	0.824	0.027
6	7	R	<0.66	167	-0.025	0.682	0.825	0.027
7	6	W		181	-0.024	0.188	0.184	0.069
8	7	I		181	-0.030	0.266	0.211	0.071
9	6	N	>0.66	59	-0.076	0.309	0.426	0.084
10	7	T	>0.66	59	-0.075	0.327	0.410	0.089
11	6	E	<0.66	122	-0.027	0.335	0.382	0.071
12	7	R	<0.66	122	-0.034	0.369	0.394	0.073

[1]equation numbers refer to Table 3 only.

on a minute basis, to a daytime basis by multiplying the intercept with an approximate 11-hour average, the period that the R_n values were positive.

The correlation coefficients for the winter data were very low, ranging from 0.42 to 0.65. This must be ascribed to a highly variable albedo during the period when the ground was partly snow covered.

An attempt was made to predict hourly net radiation fluxes and compare the values with the measured fluxes. Only daylight values (from sunrise to sunset) were used in this analysis. The results in Table 7 show that little success was obtained if the physically based equations were used: the slopes and intercepts were significantly different from one and zero, respectively. Part of this failure must be ascribed to the fact that for all days the same equation for albedo was used, viz. equation 5, Table 3. However Piggin and Schwerdtfeger (1973) showed that under overcast conditions the albedo varied little with solar elevation.

Lines 5 and 6, Table 7, give the results of the correlation between measured net radiation flux and shortwave radiation flux for the summer of 1974. Using this 1974 relationship, net radiation was predicted in 1975 and compared with the measured values (line 7 and 8). Using statistical analysis it was found that the intercept a and the slope b were not significantly different from zero and one. The standard error from the regression line, S_{yx}, was 0.110 and 0.109 ly min^{-1} respectively for line 7 and 8, not much larger than found in line 5 and 6.

Upon summarizing this last section it can be said that the net radiation flux can be predicted on a monthly, daily and hourly basis with

Table 7. Linear regression analysis of daylight (sunrise to sunset) hourly radiation data for Y = a + b X.

Line	Y measured	X	Derivation of X with[1]	Period of measurement	Intercept a ly min^{-1}	Slope b	r^2	S_{yx} ly min^{-1}
1	R_n	R_n	1,5,6,8	July 5 - Oct. 5, 1974	0.042*	0.913**	0.868	0.089
2	R_n	R_n	1,5,7,8	July 5 - Oct. 5, 1974	0.037*	0.814**	0.868	0.089
3	R_n	R_n	1,5,6,8	May 1 - Sept. 30, 1975	0.047*	0.923**	0.864	0.097
4	R_n	R_n	1,5,7,8	May 1 - Sept. 30, 1975	0.039*	0.825**	0.864	0.097
5	R_n	R_s	6	July 5 - Oct. 5, 1974	-0.027	0.688	0.836	0.099
6	R_n	R_s	7	July 5 - Oct. 5, 1974	-0.030	0.621	0.834	0.099
7	R_n	R_n	line 5	May 1 - Sept. 30, 1975	0.003	1.021	0.824	0.110
8	R_n	R_n	line 6	May 1 - Sept. 30, 1975	0.002	1.026	0.828	0.109

[1]equation numbers refer to Table 3 only.

*significantly different from 0 at the 5% probability level.

**significantly different from 1 at the 5% probability level.

decreasing accuracy using either formulas based on physical considerations or the empirical relationship between net- and shortwave radiation flux. It is suggested that the net radiation flux in most localities in southern Manitoba could be calculated in a similar way as described in this study, if air temperatures and hours of bright sunshine measurements are available.

C. Energy Balance.

1. Soil heat flux data.

The average daily and monthly soil heat flux data are presented in Table 8. These data were derived from hourly values as measured with the soil heat flux plates.

The maximum monthly soil heat flux occurring in July 1974 was 14.2 mcal cm^{-2} min^{-1}. During the fall and winter a negative soil heat flux was observed, which meant that energy was leaving the soil. The minimum monthly soil heat flux was observed during the early part of the winter (November and December), prior to any significant snowfall which has an insulating effect.

On December 7, 1974, when the mean daily air temperature dropped by more than 13°C over the previous day mean temperature of -2.5°C a minimum daily soil heat flux of -30.0 mcal cm^{-2} $min^{-1}$was observed. The total snowfall from the middle of November till that date was 7.4 cm. In contrast on January 11, 1975 when an additional 25.1 cm snow had fallen the soil heat flux was "only" -11.7 mcal cm^{-2} min^{-1} while the mean daily temperature had dropped by almost 20°C over the previous day mean of -2.8°C. Although total snowfall is not necessarily a good indicator of the depth of the snowpack since part of the snow might

Table 8. Average daily and monthly soil heat flux in 1974 (mcal cm^{-2} min^{-1})

Date	July	Aug	Sept	Oct	Nov	Dec
1		10.0	-11.2	-21.1	-13.9	-16.8
2		03.6	-03.6	-12.5	-14.5	-09.4
3		09.8	07.1	-00.1	-16.2	-15.1
4		16.3	04.5	-06.4	-12.3	-06.4
5	19.8	17.0	10.8	-05.5	-11.8	-04.9
6	26.4	22.8	10.9	-18.4	-04.5	-03.1
7	18.1	23.5	04.2	-12.7	-00.8	-30.0
8	16.8	20.8	-09.4	02.0	01.2	-29.9
9	19.4	14.8	-01.1	11.2	-11.4	-11.8
10	25.7	07.8	-08.7	05.5	-19.3	-03.0
11	27.1	-09.9	-07.4	-10.9	-13.4	-10.9
12	15.9	09.9	-11.5	-12.4	-14.2	-27.7
13	08.6	08.6	-02.5	02.3	-16.6	-25.8
14	07.2	-00.1	-02.4	-10.9	-13.4	-10.1
15	14.2	00.9	05.1	-14.9	-12.3	-02.3
16	14.3	09.3	16.2	-03.7	-09.3	-10.9
17	19.5	00.3	01.4	-10.6	-08.9	-12.7
18	21.3	03.2	05.6	-07.0	-12.9	-08.5
19	17.8	11.6	-12.0	-11.5	-08.5	-06.5
20	22.3	-03.8	-16.6	-07.7	-11.0	-06.6
21	14.8	-03.8	-21.0	00.9	-11.2	-08.5
22	06.1	-06.9	-13.7	-10.8		-10.2
23	15.7	03.1	04.8	-02.4		-04.1
24	10.3	07.4	-01.7	-06.6		-07.6
25	19.6	13.1	-07.2	-09.6		-09.1
26	01.2	-02.6	07.4	-01.1		-02.6
27	10.1	-05.5	-14.3	-01.6		-04.1
28	-00.9	-14.5	-11.9	-02.2		-02.3
29	00.3	03.1	-15.8	-00.3	-11.3	-07.8
30	04.1	-08.9	-17.5	09.9	-20.3	-09.6
31	06.4	-06.4		-11.2		-07.7
Mean	14.2	05.0	-03.7	-05.8	-11.6	-10.5

Table 8 (continued). Average daily and monthly soil heat flux in 1975 (mcal cm^{-2} min^{-1})

Date	Jan	Feb	Mar	Apr	May	June	July	Aug	Sept
1	-10.2	-08.5	-06.8	-05.8	14.2	05.4	02.2	06.5	-15.0
2	-06.6	-09.0	-06.5	-05.6	15.6	03.6	04.8	-05.8	-19.0
3	-04.7	-09.1	-06.8	-05.8	20.0	06.8	04.6	-02.5	-08.6
4	-06.1	-06.9	-07.9	-05.6	15.7	-00.0	11.8	-05.8	04.4
5	-05.0	-05.7	-06.0	-03.7	14.2	-01.4	11.8	-04.7	-04.8
6	-06.6	-07.0	-03.6	-02.4	14.8		09.0	03.9	-10.4
7	-05.9	-07.4	-03.3	-00.9	15.2		02.1	12.4	-05.3
8	-05.8	-08.6		01.0	10.1		-08.7	00.6	-13.2
9	-05.3	-10.5		06.6	01.7	09.8	-07.3	-01.1	02.5
10	-02.1	-11.0	-10.1	06.1	14.3	06.8	-03.7	02.1	-03.9
11	-11.7	-10.7	-10.0	04.0	04.2	11.2	-01.9	03.5	-20.7
12	-23.7	-09.0	-08.3	03.7	00.5	15.8	06.0	01.4	-23.4
13	-24.0	-09.7	-07.7	03.1	19.5	07.5	16.1	01.1	-22.6
14	-23.4	-10.0	-07.5	03.2	00.3	-03.3	13.7	-08.3	06.8
15	-16.9	-08.0	-05.3	03.8	-17.9	02.8	20.1	-08.2	-01.6
16	-22.4	-06.4	-03.0	20.2	20.8	05.2	18.6	-07.8	-02.0
17	-17.5	-05.7	01.9	25.5	25.1	07.9	14.1	-10.8	13.9
18	-09.1	-04.6	04.6	19.7	15.8	08.8	05.5	-11.6	04.4
19	-16.6	-04.7	04.3	02.0	23.2	14.6	00.9	-11.7	-04.3
20	-12.1	-04.2	03.9	07.4	00.5	22.6	-01.3	-11.0	-17.1
21	-08.2	-03.3	03.6	08.0	-01.5	18.3	08.8	00.0	-11.1
22	-12.7	-01.9	02.6	32.3	-03.1	01.5	-02.0	-04.4	-01.0
23	-08.2	-02.5	02.5	22.3	20.7	16.1	04.1	12.3	-09.8
24	-05.8	-05.2	-08.9	28.2	206.	13.1	00.3	08.8	-07.9
25	-03.0	-03.1	-10.9	20.1	19.4	22.8	08.6	-06.9	-03.1
26	-02.7	-02.6	-14.5	08.9	02.2	12.2	07.6	-13.2	-03.7
27	-03.8	-03.8	-08.7	22.0	-06.8	04.0	06.2	-13.3	-03.5
28	-05.2	-05.8	-05.2	24.3	00.7	05.3	13.9	04.9	-01.4
29	-06.0			09.5	-08.5	09.0	19.1	03.2	-03.6
30	-06.5			05.1	-01.7	12.2	19.1	08.8	-23.2
31	-08.0		-05.1		01.2		13.8	06.6	
Mean	-09.9	-06.6	-04.5	08.6	08.7	08.8	07.0	-01.6	-06.9

have drifted away, the above example does illustrate the insulating properties of snow.

In the second half of March 1975 the soil heat flux was reversed for a week, that is heat was flowing into the soil. The onset of this period coincided with precipitation in the form of rain and above freezing daily mean air temperatures.

Assuming that the rain had the same temperature as the air, the infiltration water was carrying heat into the soil by convection. A further analysis of the moving heat source theory will be given in another section.

In the second half of April 1975 when the mean daily temperature was about 5°C large quantities of heat flowed into the soil and on April 22 a high of 32.3 mcal cm^{-2} min^{-1} was reached.

A comparison between the monthly soil heat and net radiation flux is given in Figure 8. During the growing season the soil heat flux was only a small component of the energy balance (generally less than 10%), but during the winter the soil heat flux was about 60% of the net radiation flux. During the fall of 1974 and 1975 the soil heat flux was reversed prior to a reversal of the net radiation flux. Consequently more energy was available for the latent and sensible heat flux.

In November 1974 both the soil heat and the net radiation flux were negative, but the magnitude of the former was almost twice the latter. This meant that the total amount of available energy at the soil-atmosphere interface (0.056 ly min^{-1}) came entirely from the soil.

The diurnal variation in soil heat flux changed considerably from one day to the next as is exemplified in Figure 9. On June 22, 1975, which was a completely overcast day, the soil heat flux varied between

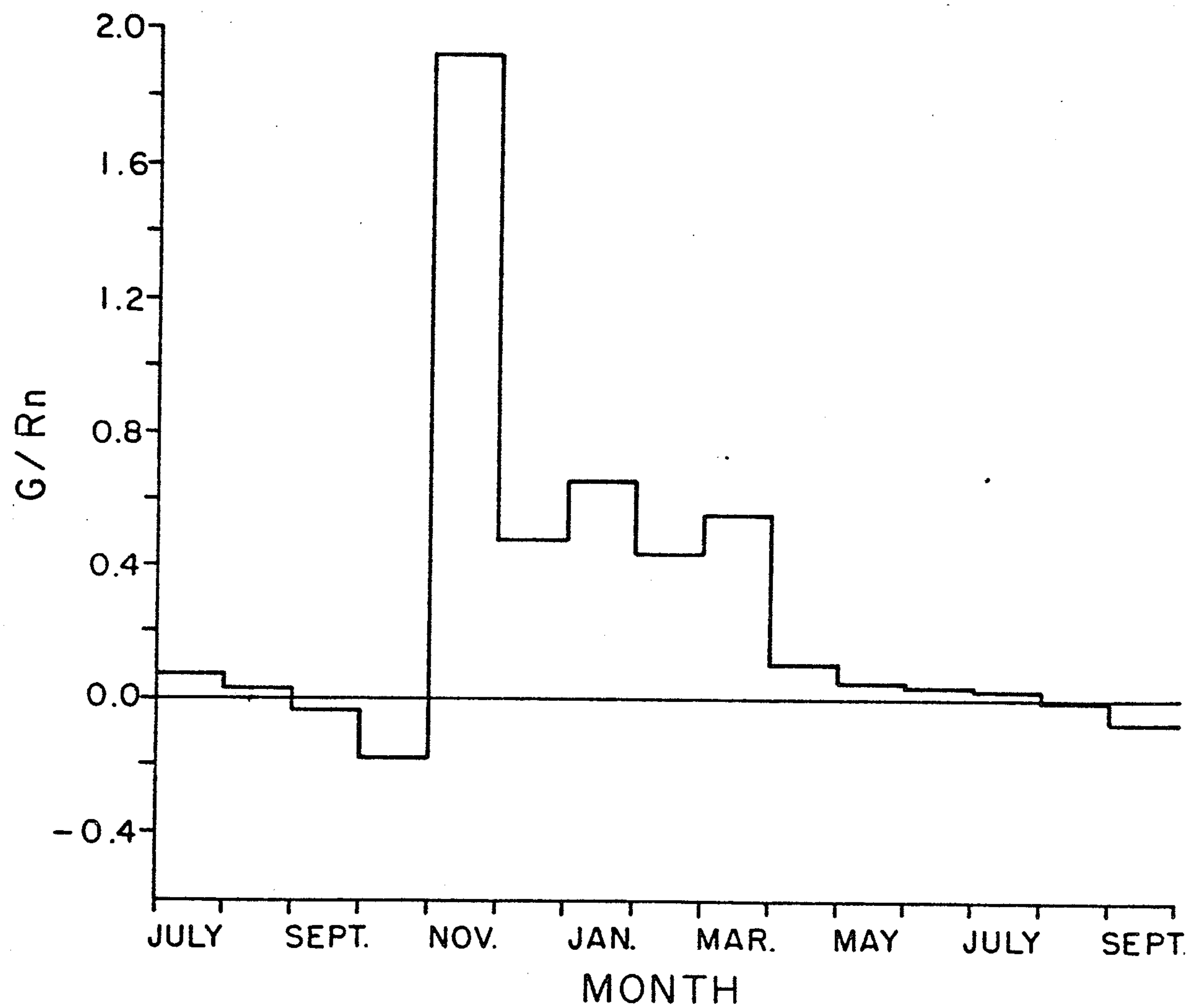

Figure 8. The ratio soil heat flux/net radiation flux during the course of the investigation.

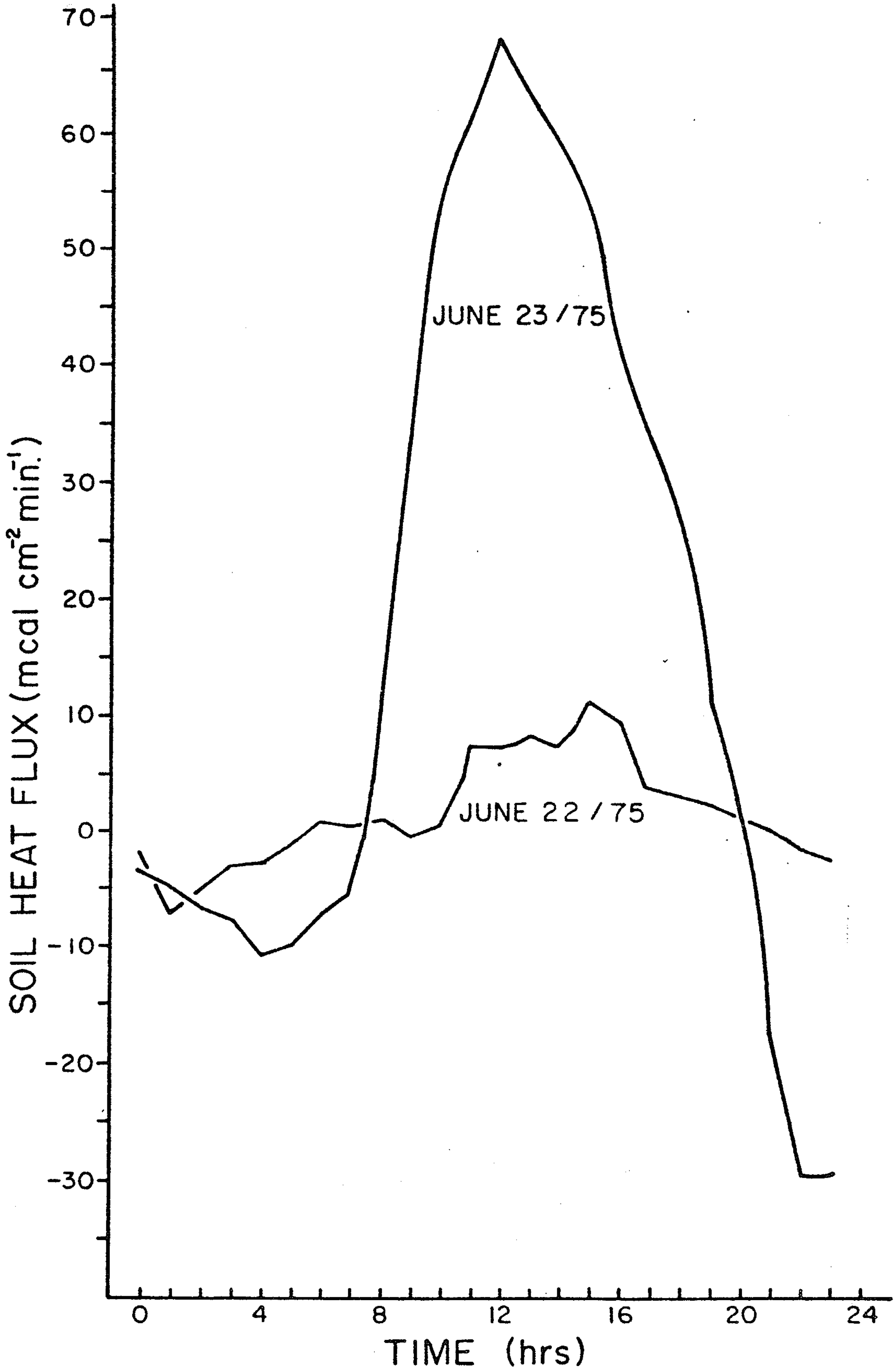

Figure 9. Diurnal variation in the soil heat flux.

-7.773 and 10.92 mcal cm^{-2} min^{-1}, with a daily average of 1.5 mcal cm^{-2} min^{-1}. However the next day June 23, which was sunny ($n/N = 0.85$), a maximum soil heat flux of 67.89 mcal cm^{-2} min^{-1} was reached by 12:00 noon. By the end of the day heat was leaving the soil at a rate of 29.57 mcal cm^{-2} min^{-1}. The average daily rate was calculated to be 16.1 mcal cm^{-2} min^{-1}.

2. Potential evapotranspiration.

The results of the potential evapotranspiration calculations are shown in Table 9. In the Makkink and Jensen - Haise equation the shortwave radiation flux was calculated either as RSBR (columns 1 and 3, Table 9) or as RSDC (columns 2 and 4, Table 9). In each of the investigated months the equation which used RSDC rather than RSBR resulted in a lower potential evapotranspiration rate. This was to be expected since during the growing season RSDC was smaller than RSBR as was shown in Figure 4.

The results of the Baier-Robertson equation agreed within a satisfactory degree of variation with the 'Carberry' formula which used the same meteorological variables but different regression coefficients. The potential evapotranspiration rates as calculated with the Baier-Robertson equation were higher in the summer but lower in the spring and fall as compared to the results obtained with the 'Carberry' formula.

The Thornthwaite approximations underestimated the evapotranspiration rates as compared to the other methods. Similar results have been reported in the literature (Pelton and Korven, 1969; Taylor and Ashcroft, 1972). The reasons for the failure of this method were discussed by Pelton et al. (1960). Reimer and Desmarais (1973) found the Thornthwaite method to underestimate in spring and overestimate in fall at W.N.R.E., whereas over the whole growing season these errors tended to cancel.

Table 9. Comparison of Potential Evapotranspiration Equations (cm $month^{-1}$)

	Method												
	Makkink		Jensen-Haise		Baier Robertson	'Carberry'	Thornthwaite	Priestley Taylor	Van Bavel	Penman	Class A Pan		
											Winnipeg	Bissett	Indian Bay
	1	2	3	4	5	6	7	8	9	10	11	12	13
July 74	12.46	10.72	13.88	11.98	14.25	12.55	10.62	11.86	18.69	18.40	20.85	14.40	15.85
Aug 74	9.01	7.62	9.09	7.74	9.22	8.62	8.06	8.64	14.15	13.92	13.46	9.68	9.02
Sept 74	4.96	4.26	4.05	3.51	2.84	4.74	4.53	5.17	8.74	8.59	8.46	4.57	7.09
May 75	9.57	8.72	8.27	7.54	9.39	11.14	5.75	9.82	16.28	16.01	16.26	--	12.29
June 75	9.88	8.76	9.98	8.87	10.21	9.94	8.11	10.33	15.18	15.00	14.74	11.58	11.71
July 75	14.19	12.22	15.75	13.62	15.28	13.54	10.62	14.74	19.57	19.31	18.32	15.62	15.72
Aug 75	9.21	7.80	9.20	7.84	9.39	8.72	8.26	10.25	14.10	13.91	--	9.30	9.73
Sept 75	5.38	4.61	4.64	4.03	4.50	5.52	5.34	5.69	9.85	9.68	8.08	5.41	5.72

Note: In column 1, 3, 5 and 6 the shortwave radiation flux was calculated according to the Baier-Robertson equation (equation 6, Table 3) and in columns 2 and 4 according to the Driedger-Catchpole equation (equation 7, Table 3).

Of the three combination methods the Priestley and Taylor equation yielded considerably lower potential evapotranspiration rates than the Van Bavel or Penman equation. The results from the latter two equations were comparable, that is they agreed within 2%.

Unfortunately no direct measurements of potential evapotranspiration rates were made at the experimental site of W.N.R.E. However, meteorological stations at Winnipeg International Airport, Bissett (95 km north of W.N.R.E.) and Indian Bay (95 km southeast of W.N.R.E.) reported class A pan measurements from which total estimated lake evaporation was published monthly (Environment Canada, 1974 and 1975). The Winnipeg data are considerably larger than those of Bissett or Indian Bay, reflecting the effects of stronger surface winds in a grassland region, as compared to a forested region. Since W.N.R.E. is located in the same transitional zone between grassland and boreal forest as Bissett and Indian Bay, it is desirable to compare potential evapotranspiration rates among these three locations.

There was generally fairly good agreement between the Bissett and Indian Bay data and those reported in columns 1-8 in Table 9. The physically based equations of Van Bavel and Penman (columns 9 and 10, respectively) overestimated the potential evapotranspiration rates. Similar results were found by Reimer and Desmarais (1973) who contributed the overestimation to the implied surface saturation assumption.

A number of problems evolved during the computation of the potential evapotranspiration rates:

1. In 1974 the relative humidity measurements were not very accurate due to calibration problems with the hydrograph. This measurement error would affect all E_{pot} equations

which employ a vapour pressure deficit term $(e^* - e)$.

2. Because of the nonlinear e^* vs. T relationship, vapour pressure deficits calculated using average temperatures may not be representative of the average daily deficit.
3. The windspeed was extrapolated from a height of 7 m to 2 m using an approximate logarithmic profile. The effect of atmospheric stability on the wind profile was not taken into consideration.
4. The roughness parameter z_o was estimated from the height of the vegetation which was assumed to be 40 cm throughout the entire growing season.
5. Many of the potential evapotranspiration equations used locally adjusted constants which may or may not be applicable at W.N.R.E.

3. Soil heat flux and environmental factors.

The relationship between soil heat flux and environmental variables was investigated using multiple regression analysis. The following variables were considered on a daily basis: mean air temperature, °C (TMEN), maximum air temperature, °C (TMAX), total wind run, km day^{-1} at 2 m height (WIND), net radiation flux, mcal cm^{-2} min^{-1} (RNET), vapour pressure deficit mbar (VAPD) and soil moisture content at 2 cm depth, gg^{-1} (SOILM). The results of the analysis for the period of July 5, 1974 to September 30, 1974 are shown in Table 10.

Table 10. Multiple correlation and regression coefficients of environmental factors on the daily soil heat flux.

Environmental factors	Regression coefficient	Constant	R^2	S_{yx} (mcal cm^{-2} min^{-1})
TMEN	2.05	-43.22	0.88	4.22
WIND	-2.82×10^{-2}			
SOILM	5.42×10^{-1}			
RNET	1.90×10^{-2}			

When the daily mean air temperature was the only variable involved the correlation coefficient (R^2) was 0.84 and the standard deviation from the regression line (S_{yx}) was 4.65 mcal cm^{-2} min^{-1}:

Soil heat flux = -22.18 + 1.81 TMEN

The inclusion of wind, soil moisture content and net radiation flux improved the correlation only slightly (Table 10). No improvement was obtained when the variables maximum air temperature and vapour pressure deficit were included in the analysis.

Using the regression coefficients found in the 1974 season, the daily soil heat flux was calculated for the 1975 season (May 1-September 30) and compared with the measured data. It was found that the calculated values were on the average twice as large as the measured ones. Part of the discrepancy could be due to the fact that there was more lush plant growth in 1975, thereby shading the ground more effectively. The installation of the soil temperature sensors in 1974 also caused a certain degree of trampling of the grass in the neighbourhood of the soil heat flux plates. A possible drift in the calibration curve of the plates could also have caused the observed anomaly.

When separate regression coefficients for the 1975 season were calculated with the above mentioned variables, the correlation coefficient remained low (0.48) and the standard deviation large (12.75 mcal cm^{-2} min^{-1}). It is possible that under a tall, lush grass canopy a lag effect might be operating; the inclusion of previous day or days environmental factors might have improved the regression equation.

For individual days a good correlation between the hourly soil heat flux and the hourly net radiation flux was obtained in many instances. A typical example is given in Figure 10 where the correlation coefficient r was 0.97 and the standard error from the regression line was 7.99 mcal cm^{-2} min^{-1}. Approximately 8% of the net radiation was dissipated as soil heat flux, which compared well with the data reported by Monteith (1958) for wheat, potatoes and short grass.

There was no increase in the slope of the regression line going from high to low soil moisture conditions, as was reported by Idso et al. (1975). Under the experimental conditions at W.N.R.E. the soil heat flux remained a fairly constant proportion of the net radiation flux. Apparently when soil moisture became a limiting factor in evaporation, the excess energy was used in heating the air rather than heating the soil.

D. Soil temperature regime and heat transfer.

During the course of the investigation soil temperature data were collected on an hourly basis, except during the period from October 6, 1974 to April 26, 1975, when the data were recorded every two hours. This massive amount of soil temperature data along with hourly precipitation, sunshine and windspeed data will not be reproduced in this manuscript, but are available from the author upon request. Also the data

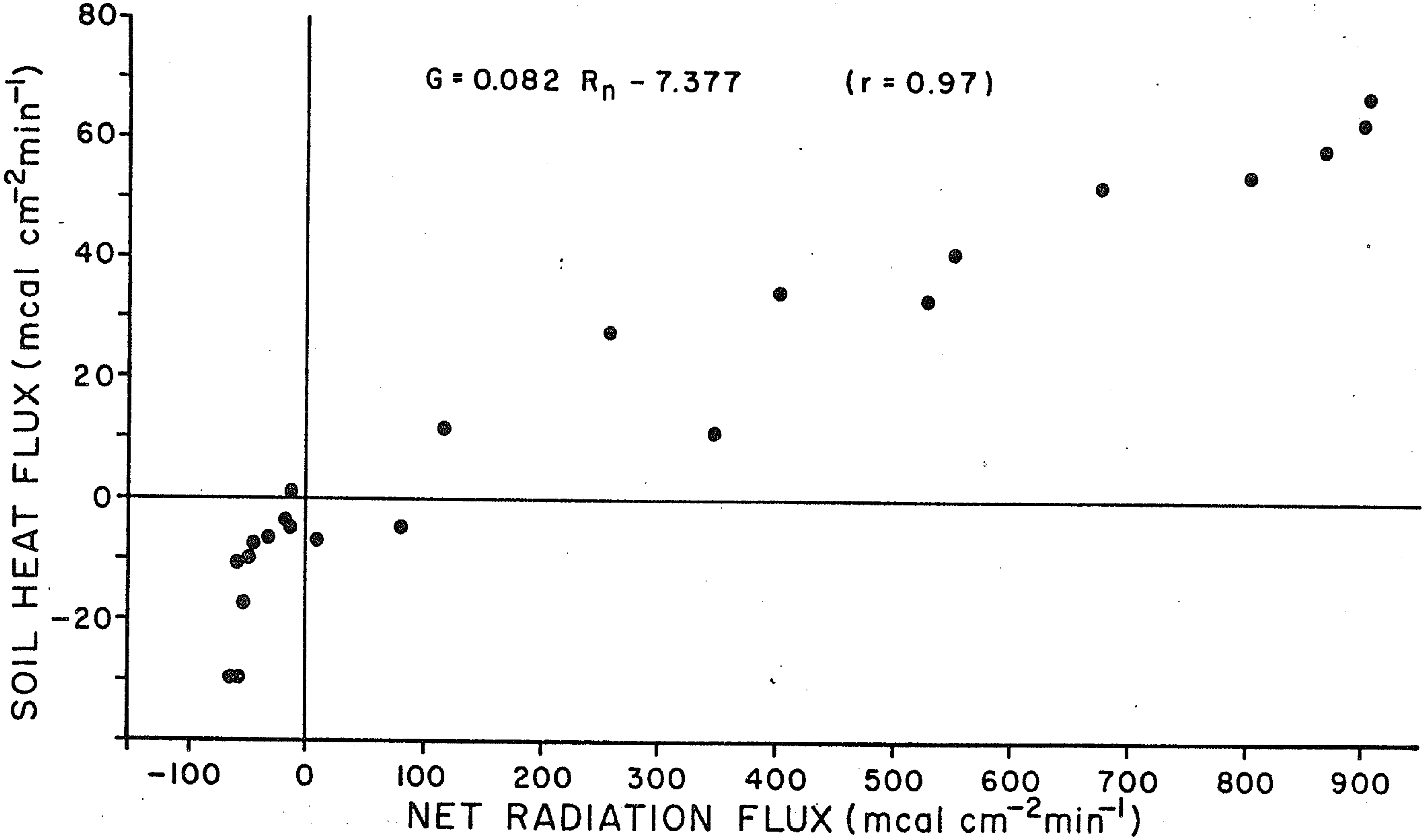

Figure 10. Relationship between soil heat flux and net radiation flux on June 23, 1975.

collected from the Colman soil moisture cells can be obtained from the author.

1. Thermal properties.

The thermal properties of soil profiles are dependent upon porosity, moisture content, organic matter content and chemical composition of the solid fraction. Table 11 presents particle size distribution, organic matter content and bulk density versus soil depth at the experimental site. The soil was classified as a Whitemouth clay (Smith et al. 1967).

The volumetric heat capacity of the soil, as calculated according to equation (3.29) is shown in Figure 11 for three depths; the 2 and 10 cm depths were representative for the 0-20 cm layer, while the 30 cm depth was representative for the layers below 20 cm. The organic matter content of the two upper levels were very similar and the differences in volumetric heat capacities at the same water contents must be ascribed to the larger volume fraction of the solid material (x_m in equation 3.29) at the 2 cm level. Although at the 30 cm level the volume fraction of the solids was larger than at the 2 cm level, the organic matter content was considerably lower (1.6%), and therefore the heat capacity was also lower.

The thermal conductivity was calculated according to the De Vries method (equation 3.30). The results are shown in Figure 12. Due to the high organic matter content in the upper part of the soil profile a lower thermal conductivity was calculated for a given water content, as compared to the lower profile depths. Since the total porosity at the 10 cm level was about 10% larger than at the 2 cm level, which meant that at any given water content more air was present, a lower

Table 11. Particle size distribution, organic matter content and bulk density of Whitemouth clay at various depths.

Depth cm	Sand %	Silt %	Clay %	Organic matter %	Bulk density g cm^{-3}
0 - 2.5	19.0	38.6	42.4	15.1	1.03
2.5 - 7.5	20.0	29.5	50.4	12.1	1.11
7.5 - 12.5	23.4	27.2	49.4	15.5	1.22
12.5 - 17.5	25.7	20.4	53.9	8.2	1.23
17.5 - 22.5	25.4	26.5	48.1	3.4	1.26
27.5 - 32.5	18.1	18.2	63.7	1.6	1.45
47.5 - 52.5	37.2	21.5	41.3	1.3	1.45
72.5 - 77.5	14.3	19.3	66.4	1.2	1.44
97.5 - 102.5	10.6	33.8	55.5	0.4	1.44

Table 12. Monthly average volumetric water contents (%)

Depth cm	May	June	July*	Aug*	Sept*	Oct
2	40.8	40.7	33.0	37.1	40.5	41.1
5	43.8	43.9	31.4	36.5	42.4	42.2
10	48.4	47.9	31.9	36.3	44.7	45.8
20	52.5	52.2	35.0	34.6	45.2	46.2
30	45.8	45.8	38.1	37.9	39.5	41.0
50	45.9	45.8	40.0	37.5	38.8	39.3
75	45.7	45.7	44.9	39.3	37.5	37.5
100	45.7	45.7	45.6	44.9	44.2	44.7

*Average of 1974 and 1975.

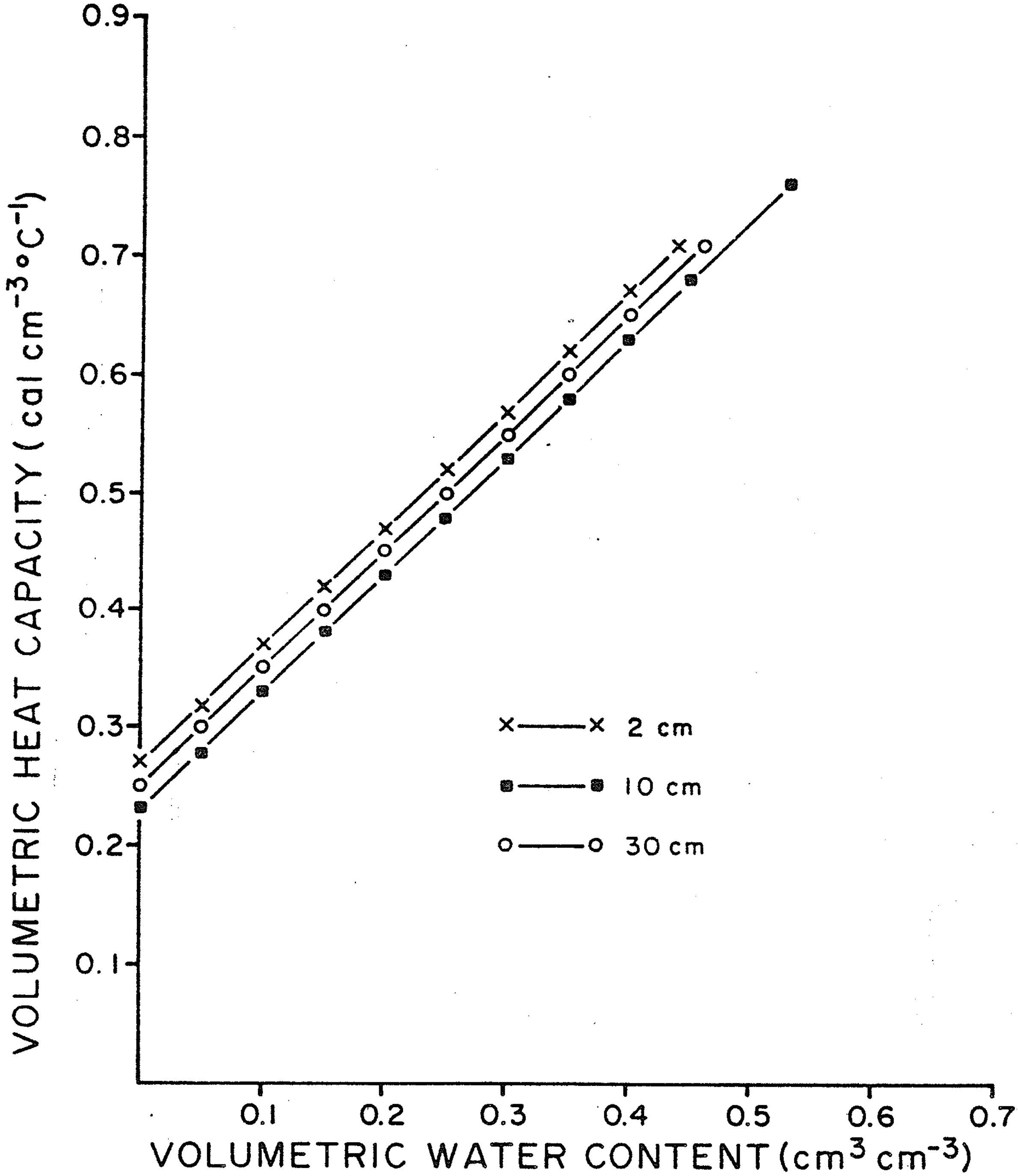

Figure 11. Dependence of heat capacity on volumetric water content for three depths.

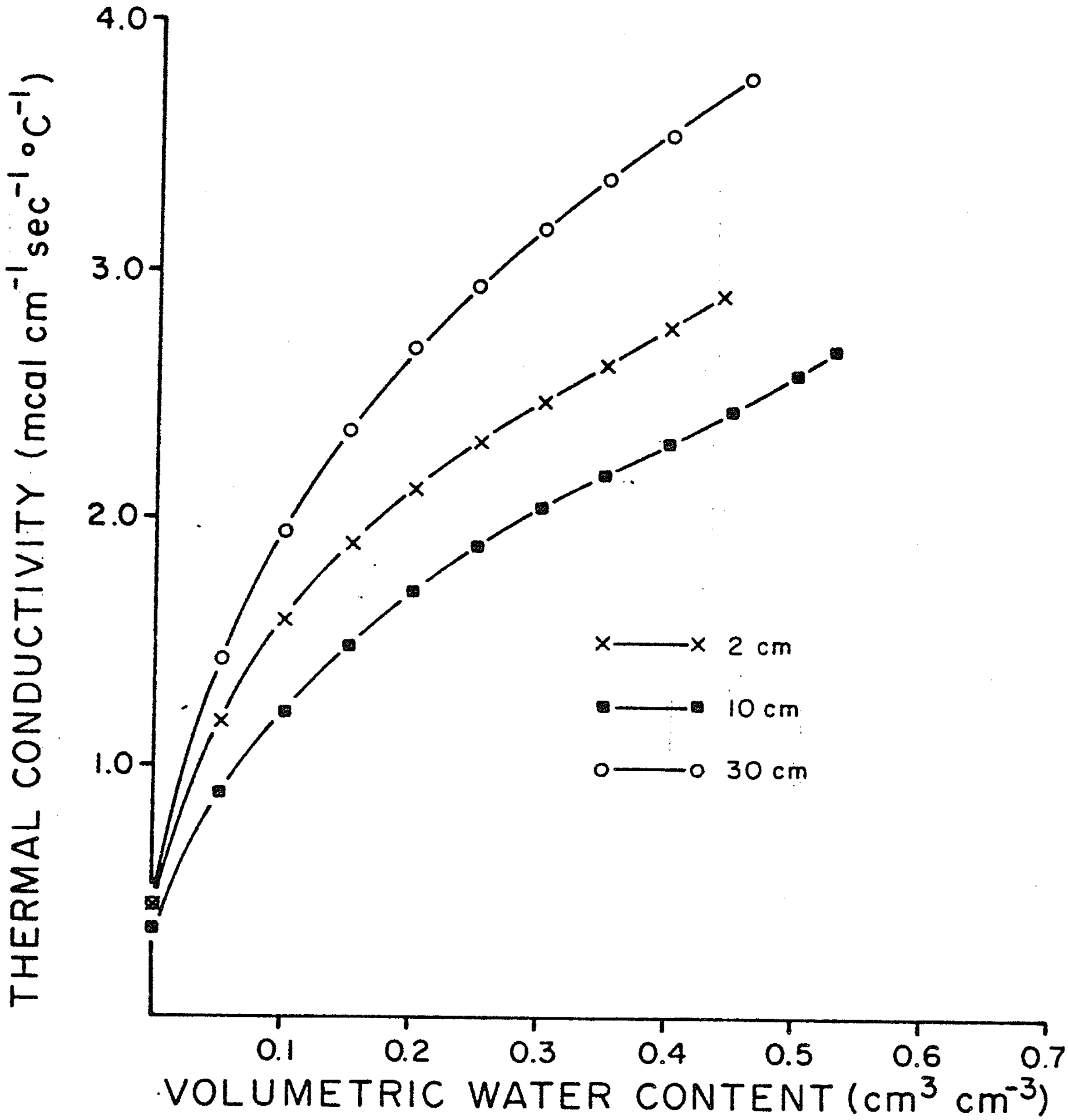

Figure 12. Variation of the thermal conductivity with water content for three depths.

thermal conductivity was calculated for the 10 cm level.

An attempt was made to calculate thermal conductivity values from the measured soil heat flux plate data and measured soil temperatures at the 1 and 5 cm depth, assuming that a linear temperature profile existed between these depths. In almost each instant the thermal conductivity was calculated to be less than 1.0 mcal cm^{-1} sec^{-1} $°C^{-1}$, which was unrealistic for the water contents observed in the soil. It is thought that because the soil heat flux plates and the soil temperature sensors were not installed during the same year (see methods and materials), the heat flux plates were under more vegetative cover than the soil temperature sensors both in 1974 and 1975. This would give an increased soil heat flux at the temperature measurement site, as compared to measured heat flux data, about 150 cm removed from the temperature site. Drift of the calibration curve could be also partly responsible for the calculated discrepancy.

The rate of temperature equalization in the soil is determined by the thermal diffusivity $D = \lambda/C$. A large diffusivity causes rapid changes in temperature and a quick and deep penetration of the heat wave into the soil. An example of the thermal diffusivities of the investigated clay soil in relation to water content and soil depth is shown in Figure 13. The shape of all three curves was very similar, but considerable differences of magnitude are to be observed. The maximum values of D occurred roughly at 20% volumetric water content.

2. Annual soil temperature data and analysis.

The average monthly soil temperature data for five selected depths are presented in Figure 14. The data are based on one year's result, except for July, August and September when two years data were averaged.

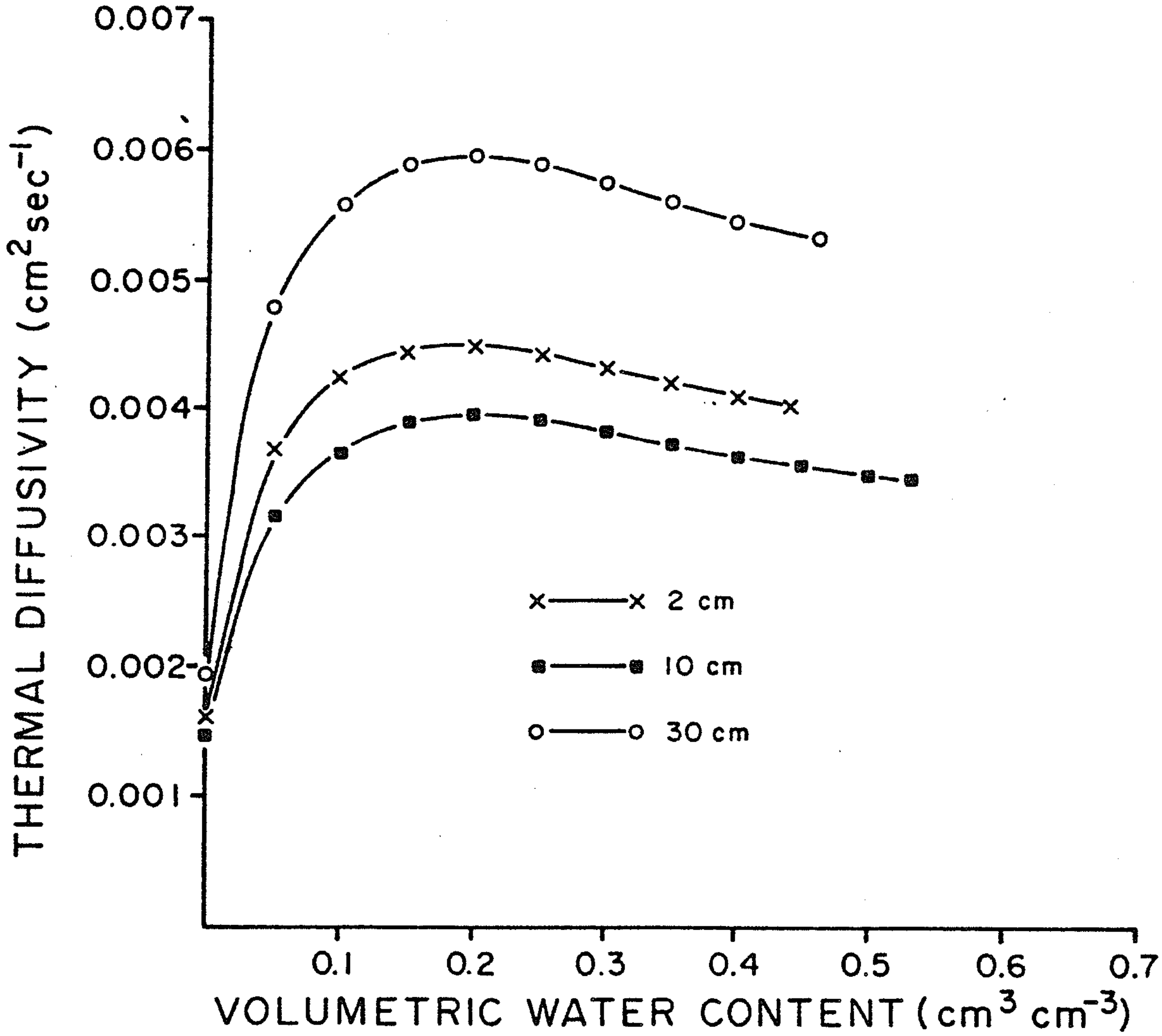

Figure 13. Thermal diffusivity versus volumetric water content, as derived from Figures 11 and 12.

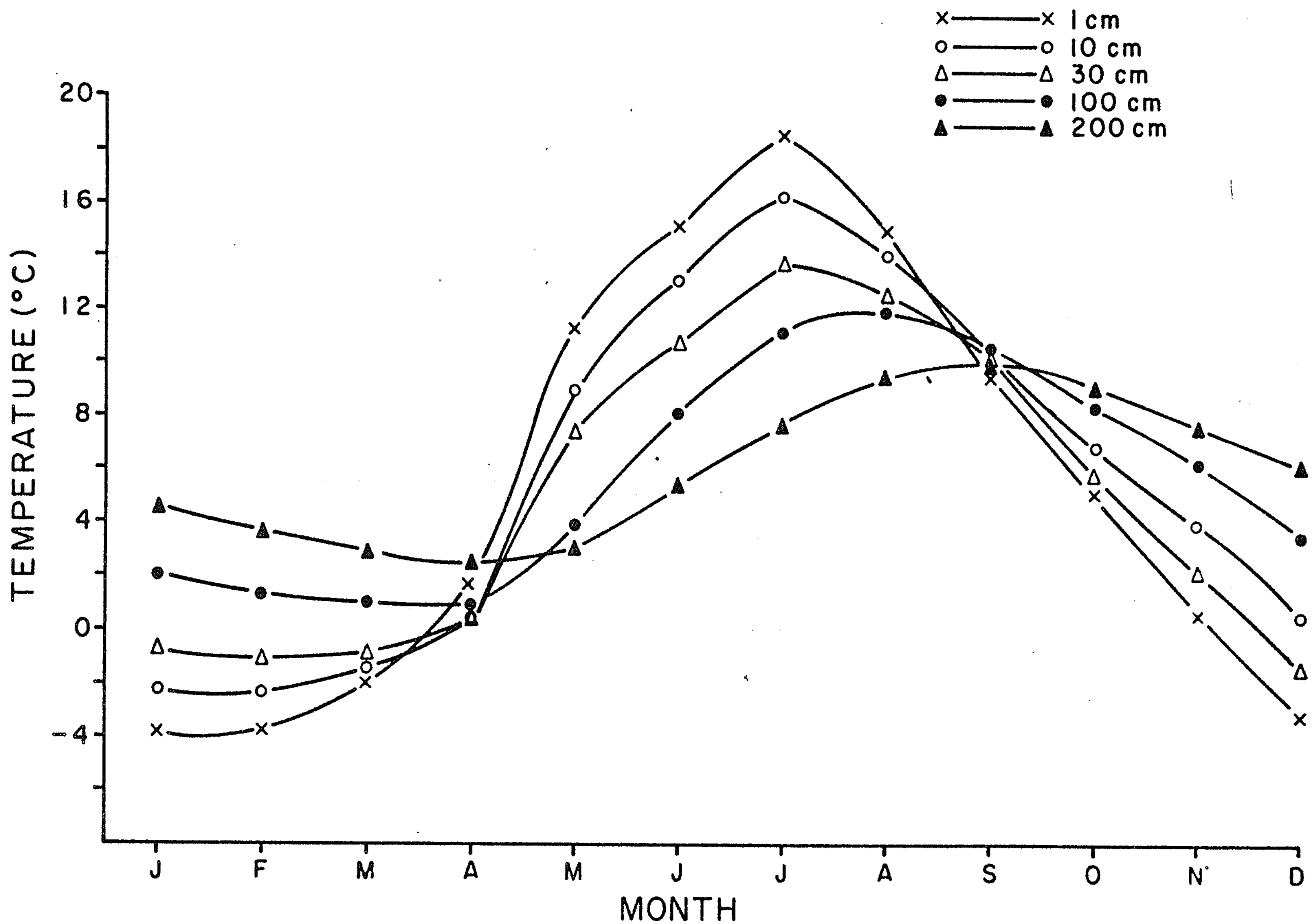

Figure 14. Annual progression of soil temperatures.

The mean annual temperature increased slowly from 5.4°C at the 1 cm depth to 6.0°C at the 200 cm depth. Using linear regression analysis it was found that the mean annual temperature gradient for the upper 200 cm of soil was 0.0035 °C/cm, which is about ten times the mean geothermal gradient over a depth of 33 m (Geiger, 1965).

The amplitude of various temperature waves, calculated as the difference between the maximum and the mean annual temperature, decreased steadily from 13.2°C at 1 cm to 4.0° at 200 cm. Near the soil surface to a depth of 30 cm the maximum temperatures occurred in July, while the minimum temperatures were observed in January (1 cm depth) and February (10 and 30 cm depth). At the lower depths a phase shift was apparent, e.g., temperature at 200 cm reached a maximum in September and a minimum in April.

The theory of heat conduction in semi-infinite homogeneous media predicts that the logarithm of the temperature amplitude should decrease linearly and that the lag of extreme values should increase linearly with increasing depths. Using the data presented in Figure 14 and additional data from the 5 and 15 cm temperature waves, the logarithm of the annual amplitude and the time of occurrence of the annual maximum temperature were plotted versus soil depth in Figure 15. The graph shows that, except for the top 20 cm, there was a distinct linear relationship, and the diffusivities computed by using equation (3.32) and (3.33) were consistent, 0.0052 cm^2 sec^{-1} and 0.0053 cm^2 sec^{-1} respectively. These values are in excellent agreement with the computed thermal diffusivity for the 30 cm depth in Figure 13, assuming a yearly average volumetric water content of 40 to 45%. This latter assumption is not unrealistic, as can be seen from Table 12, where the monthly average volumetric water contents are presented. The

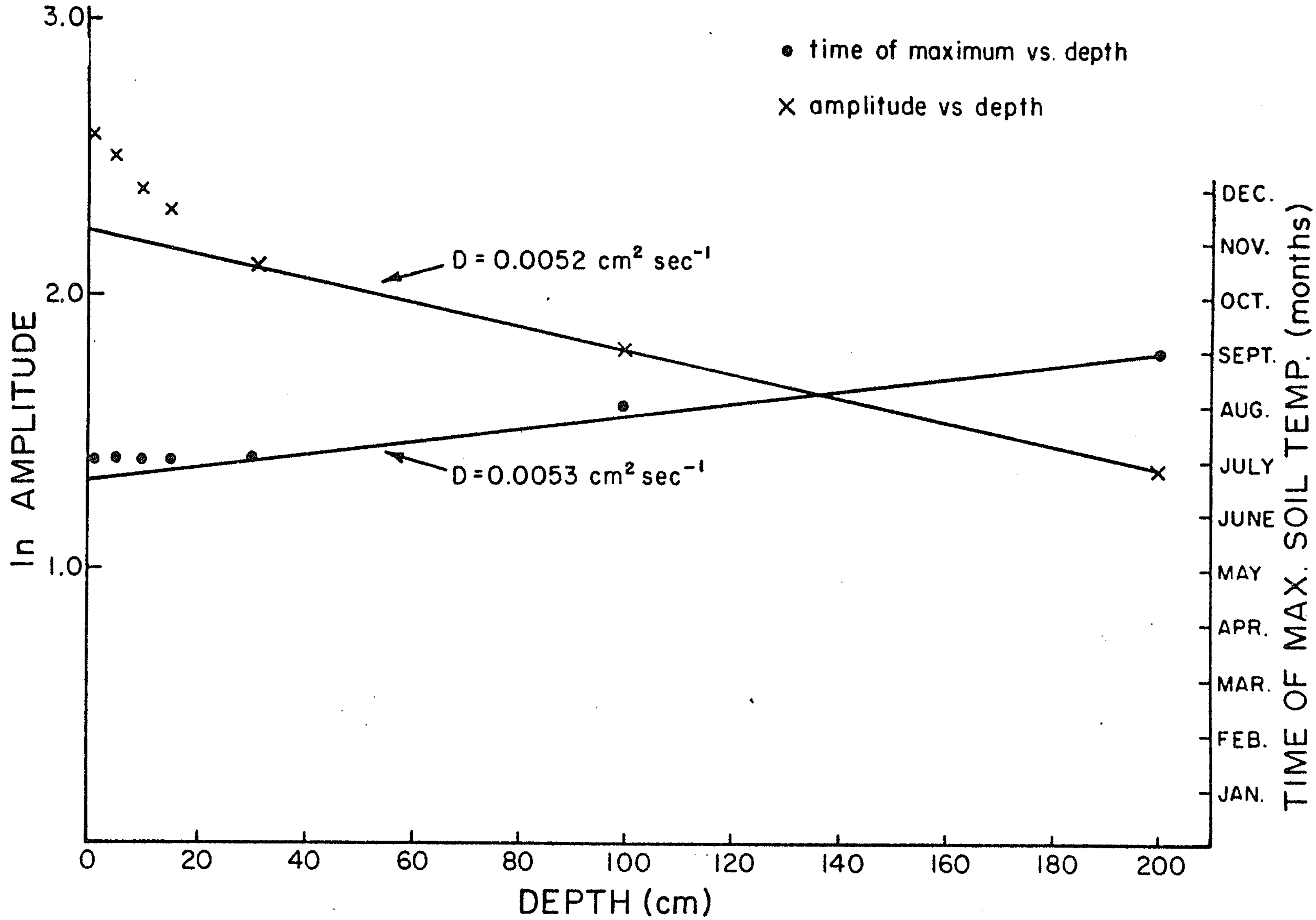

Figure 15. Amplitude of the annual soil temperature change as a function of depth.

diffusivity values are also in reasonable agreement with those found by other investigators for clay soils (Chang, 1958; Carson, 1963).

The failure of the semi-infinite model in the top 20 to 30 cm of the soil is thought to be due to the lack of homogeneity; a more variable water content and a much higher organic matter content was observed for this layer, as compared to layers underneath. Also the upper part of the soil was frozen for a part of the year, and since the thermal properties of frozen and unfrozen soil are quite different (Kersten, 1952), it is not surprising that the thermal behavior of the upper layers cannot be described satisfactorily by average values.

The difference in temperature between the air and the underlying soil is of considerable importance in micrometeorology. The direction and magnitude of the transfer of sensible heat between the two media is to a considerable extent controlled by this parameter. The atmospheric lapse rate near the ground is also strongly influenced by this difference. When the soil is considerably warmer than the air, the layer of air near the ground will be unstable, favoring turbulence and diffusion. When the air is the warmer medium, the air will be stable, with suppressed turbulence and diffusion.

The annual cycle of air-soil temperature difference as based on the average monthly air and soil temperatures for each month in the period under study (from July 1974 to September 1975) is shown in Figure 16. The maximum air-soil difference was found during the winter as a consequence of the insulating effect of the snow cover. The smallest differences were found in spring and fall, the transitional seasons.

An important fact derived from Figure 16 is that the soil temperature at 1 cm depth was colder than the air above it during the months

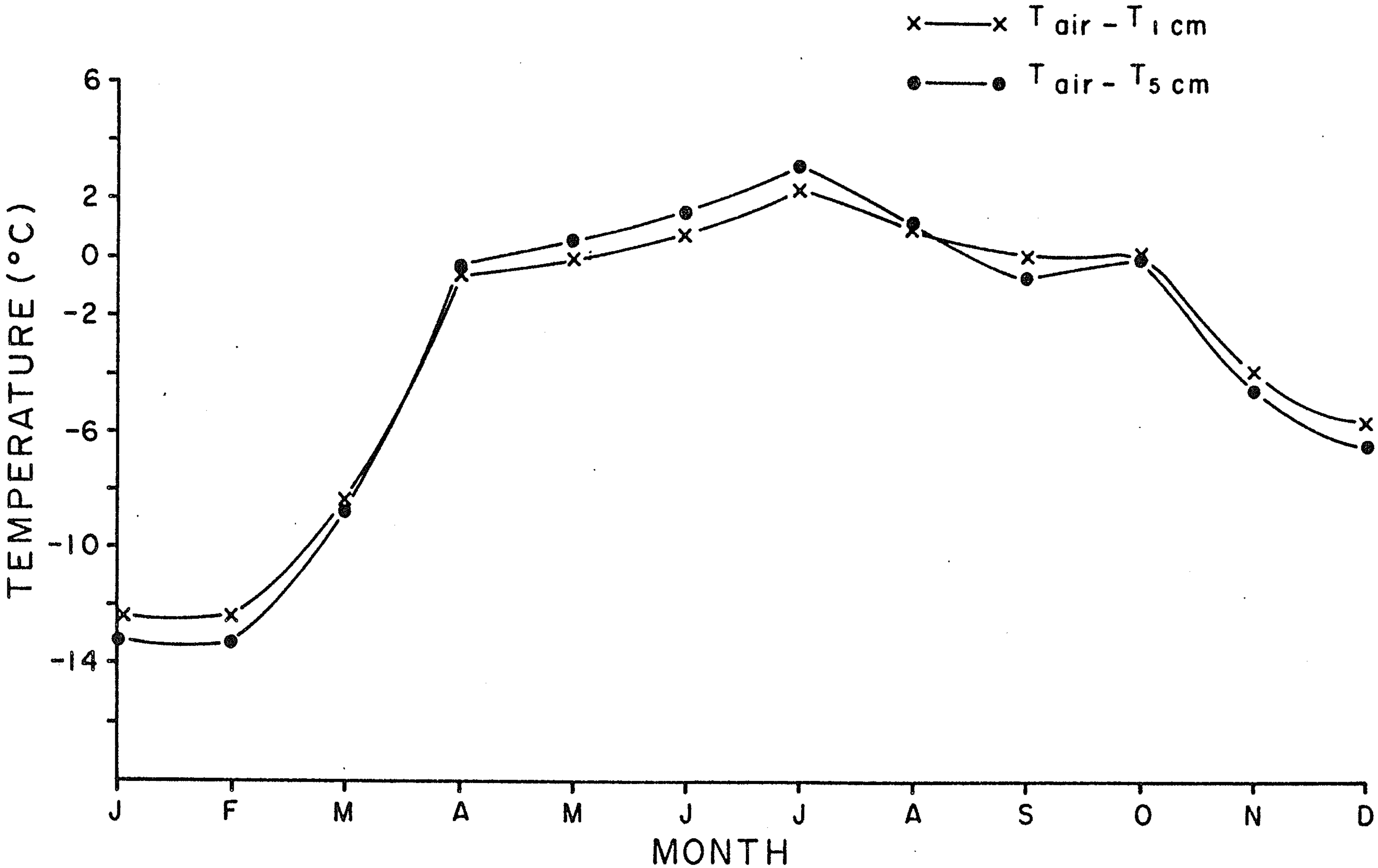

Figure 16. Annual progression of air minus soil temperature differences.

May to October, and thus the soil acted as a heat sink for the atmosphere. During the remainder of the year the soil was a heat source for the atmosphere. It is also interesting to note that a reversal of the heat flux between the 1 and 5 cm depth as indicated by the crossing of the two lines in Figure 16, occurred prior to the reversal of the heat flux between the 1 cm depth and the air above it.

The annual component of the soil heat flux, as measured with the heat flux plates buried at 2 cm depth is shown in Figure 17, along with the measured soil temperatures at the 1 and 5 cm depth. It was to be expected that whenever the measured heat flux reversed the temperature profiles at the 1 and 5 cm depth should cross. This is indicated in Figure 17 by the arrow in March/April and August/September.

The non-symmetrical shape of the soil heat flux wave was very similar to the one presented by Carson and Moses (1963). However the magnitude of the wave was considerably smaller. This was to be expected since the latter authors worked at Argonne (Chicago), which is approximately 10° further south than Pinawa.

There was a noticeable phase shift between the soil temperature in the upper part of the profile and the heat flux wave. During the early spring the energy entering the soil was utilized in thawing out the profile. In May and June, when the soil profile was almost saturated (see Table 12), and therefore had a large heat capacity, large quantities of heat were required to warm the soil. From the middle of the summer till the end of the year, when the soil heat flux decreased, a gradual cooling of the soil profile occurred.

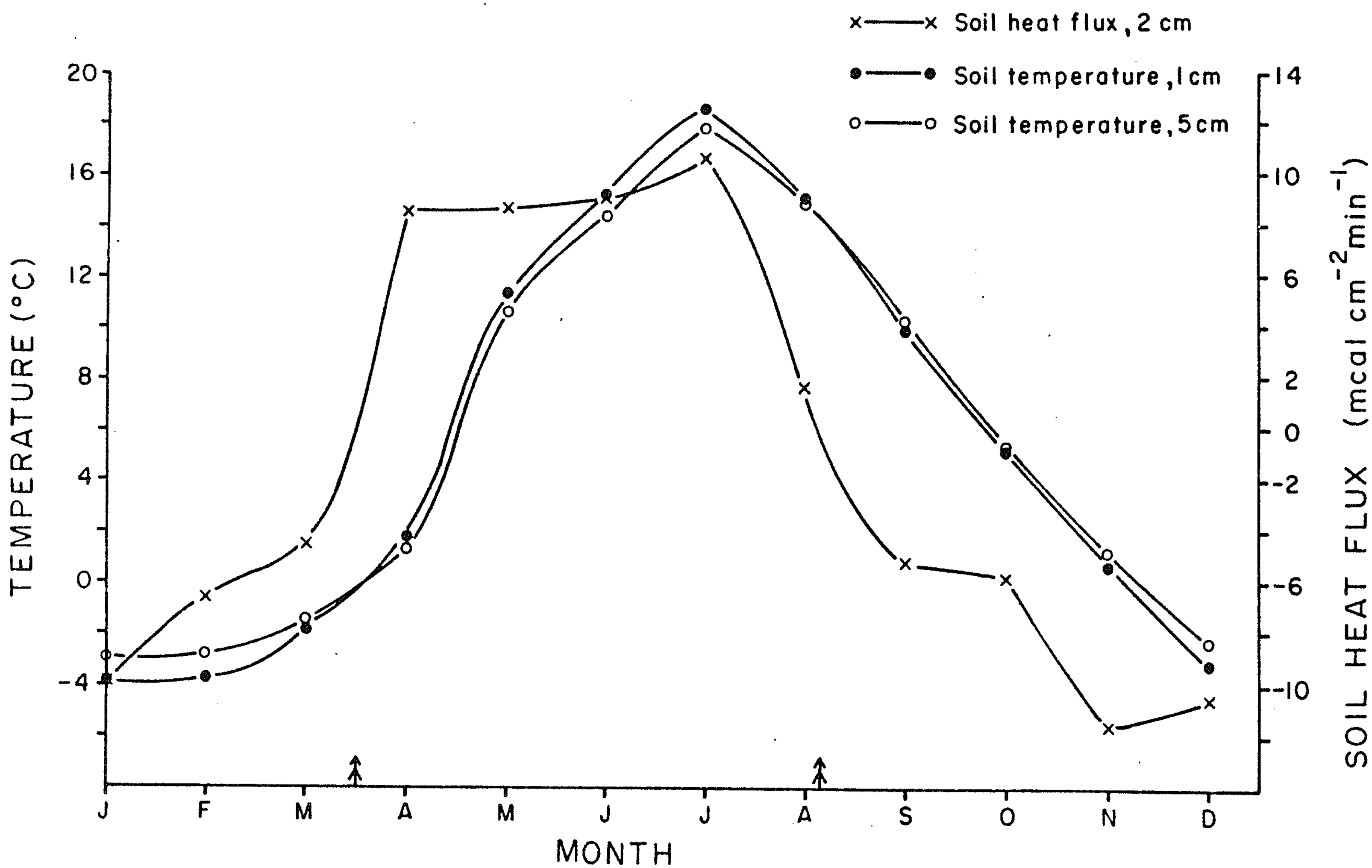

Figure 17. Annual progression of the soil heat flux and soil temperature.

3. Diurnal soil temperature wave and the simple heat conduction model.

The diurnal temperature of the soil varies in a somewhat regular pattern, reflecting the diurnal cycle of solar radiation. Superimposed on this regular cycle are fluctuations of variable duration and amplitude created by changing weather conditions like cloudiness, rain, warm and cold spells, etc. These fluctuations can essentially be removed from the data and the regular cycle isolated and studied by data averaged over a suitable time interval. In this study seven days' hourly soil temperatures were averaged as was described in Chapter III.

In order to obtain an objective description of the variation with depth of the amplitude of the temperature wave and the time of temperature extremes, the averaged soil temperatures at the 1, 5, 10, 20 and 30 cm depth were subjected to a Fourier harmonic analysis. An example of the results of Fourier analysis of soil temperature data at five depths is given in Table 13.

Generally spoken, the accuracy of a Fourier analysis will be higher if more harmonics are taken. The accuracy of the averaged temperature data was approximately 0.1°C, which restricts the number of reliable harmonics. It can be seen from Table 13 that progressively more harmonics can be neglected at the deeper depths. At the 30 cm depth all but the first harmonic can be neglected. The sum of the first three harmonics fitted the measured temperature data reasonably well. An example is given in Figure 18.

As pointed out earlier, the thermal diffusivity of a homogeneous soil can be derived via the constant decrease of the logarithm of amplitude with depth. In Figure 19 the variation of logarithm of amplitude and phase angle, as calculated with the first five harmonics

Table 13. Results of Fourier analysis based on seven days averaged soil temperatures. Period 4 - 8 - 1974 to 10 - 8 - 1974.

Depth cm	Mean temperature °C	A_1 °C	A_2 °C	A_3 °C	A_4 °C	A_5 °C	ϕ_1 rad	ϕ_2 rad	ϕ_3 rad	ϕ_4 rad	ϕ_5 rad
1	22.52	8.42	1.97	0.19	0.07	0.17	4.00	0.73	5.76	3.08	2.76
5	19.91	3.65	0.63	0.05	0.11	0.03	3.36	6.03	0.29	2.81	0.94
10	18.79	1.73	0.21	0.01	0.02	0.02	2.79	5.26	5.21	2.95	3.36
20	17.48	0.34	0.06	0.03	0.02	0.02	1.97	3.16	4.15	3.33	4.92
30	16.42	0.07	0.03	0.04	0.03	0.02	0.56	3.18	4.32	2.38	3.85

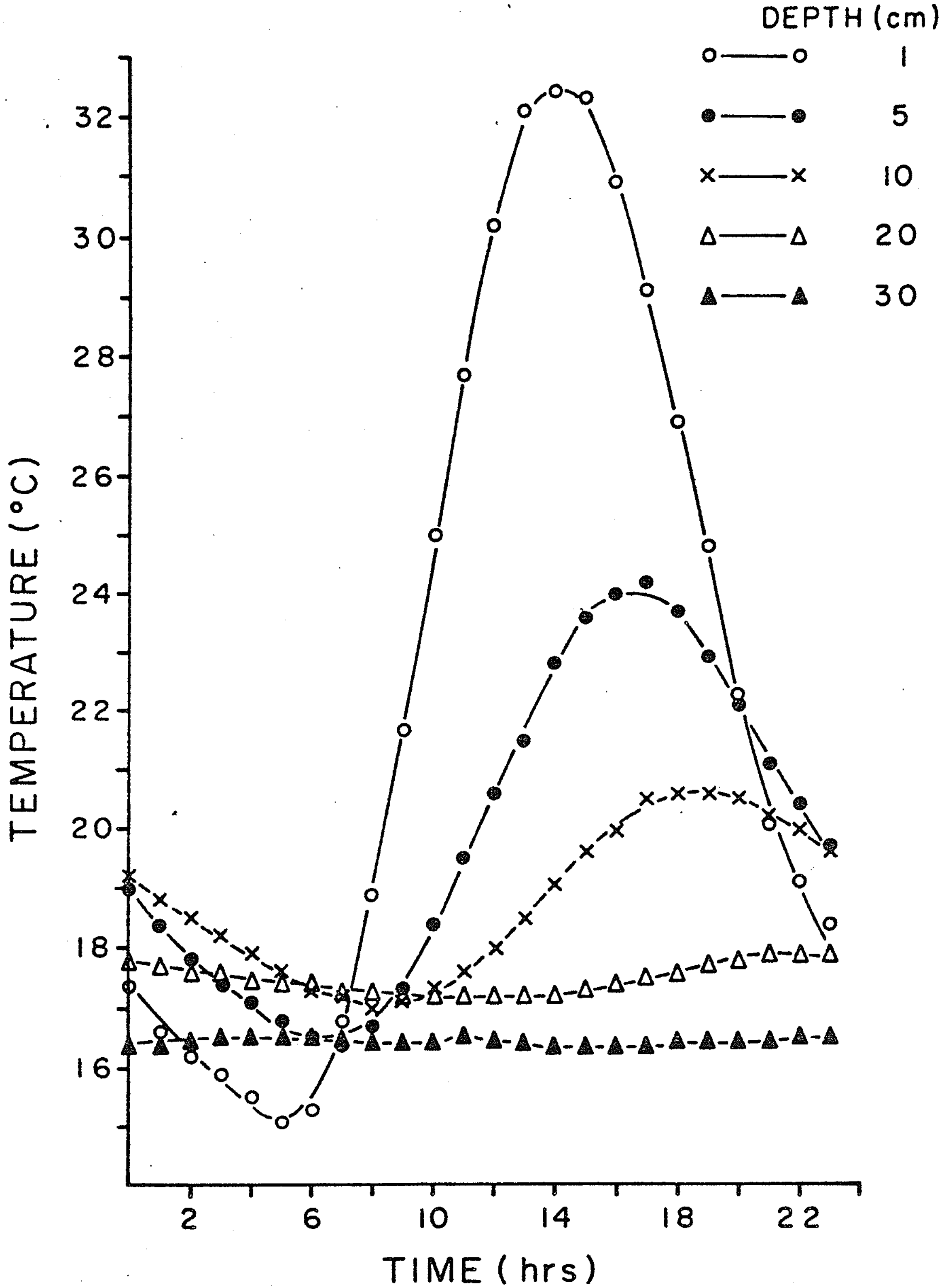

Figure 18. Diurnal variation of the measured soil temperature (symbols) and computed from the first three harmonics in the Fourier expansion.

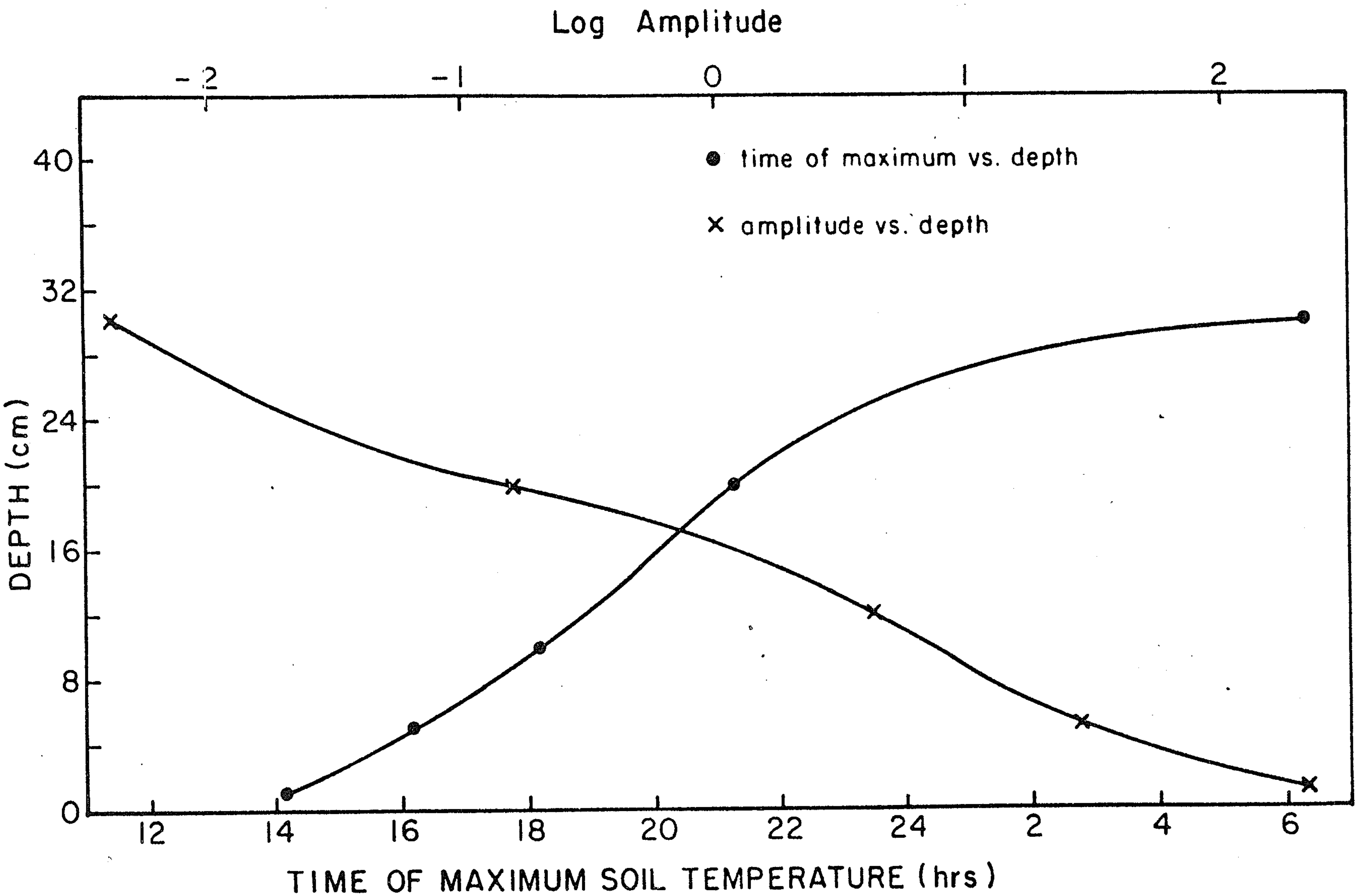

Figure 19. Example of the variation of the amplitude and phase angle of the first five harmonics of the daily soil temperature wave, as obtained by Fourier analysis, with depth.

of the daily soil temperature wave obtained by Fourier analysis, is plotted as a function of depth. It shows that there is a distinct deviation from the above mentioned linear relationship between phase angle and depth. Although a straight line would fit the log amplitude-depth relationship fairly well, the computed diffusivity (0.0014 cm^2 sec^{-1}) was too low to be realistic. The non-uniform water content (varying from 31.1% to 25.8%), the decrease in organic matter content with depth, the assumed nonconvective heat transfer and the assumed 'steady periodic solution' are thought to be responsible for the failure of the model on a daily basis in the upper part of the soil profile. In the lower part of the profile the diurnal temperature wave was dampened to such a degree that no amplitude and phase relationships could be determined.

4. Soil water and temperature simulation model.

The developed mathematical model was programmed to compute potential and actual evapotranspiration, soil water content profiles and soil temperature profiles as a function of time. The computed values were compared to the ones as measured in the field.

The program computation covered the growing season of 1975 (from May 1 to September 30). No attempt was made to simulate the 1974 season because due to initial calibration problems the soil water sensors did not respond to changes in water content.

The computed cumulative potential and actual evapotranspiration are shown in Figure 20. On September 30 the total cumulative potential evapotranspiration was 500 mm, whereas the actual evapotranspiration was 283 mm. Of the latter 38 mm evaporated directly from the soil, while the remaining was removed from the profile by the plant roots.

It was interesting to note that the ratio of the cumulative

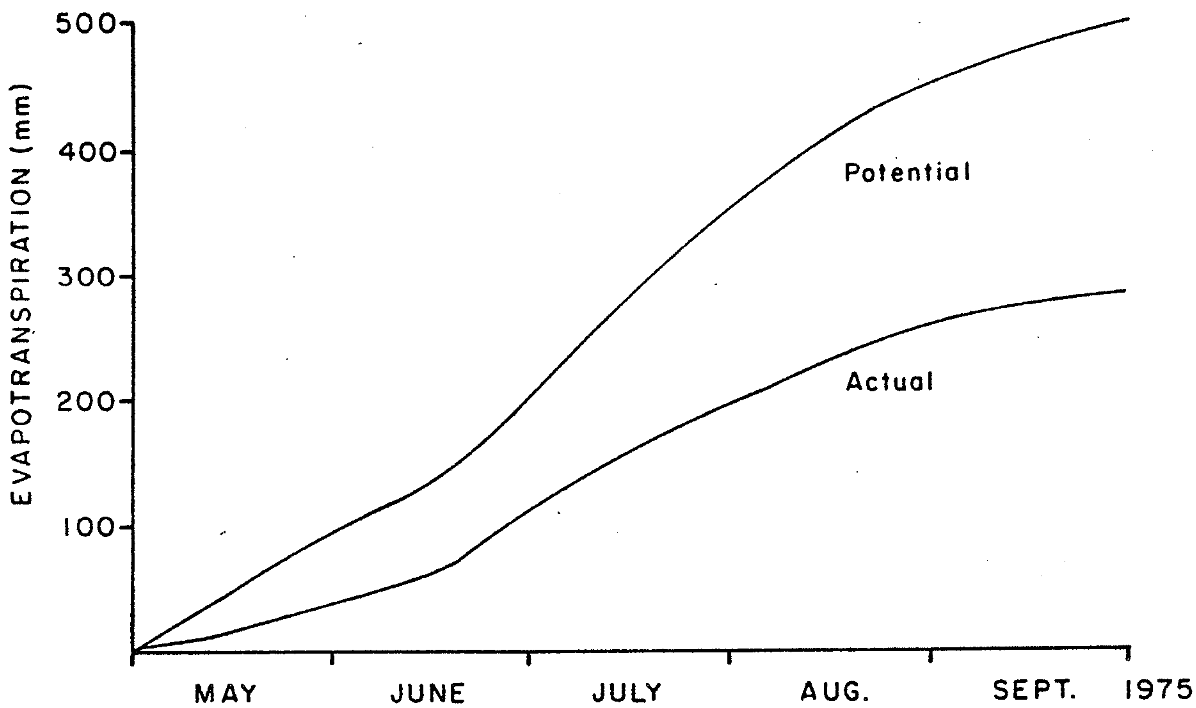

Figure 20. Cumulative potential and actual evapotranspiration over the 1975 growing season.

potential evapotranspiration to the cumulative actual evapotranspiration decreased in May and June, but remained almost constant in July, August and September (Figure 21). The initial large value of the ratio was due to the fact that the soil temperatures were relatively low in May and June, thereby restricting water uptake by the plant roots. However sufficient amounts of water remained available in the upper soil layers to prevent the plants from wilting. When water uptake by the plant roots was not restricted by low temperatures the above mentioned ratio increased slightly with time, indicating that the available soil water became more limiting as time progressed.

The rate of water uptake data (Table 14) indicated that smaller amounts of water were withdrawn by the plant roots from successively deeper soil layers. This must be ascribed to the decreasing rooting density and the decreasing soil temperatures with depth. The only exception was in the surface layer (0-3 cm) where the actual evaporative flux competed strongly with the water demand by the plant roots.

The actual and computed water content profiles for a number of selected days is shown in Figure 22. The soil profile was saturated, except for the upper 20 cm, during the initial part of the growing season. Excellent agreement was found between the computed and the actual measured water content profiles during this period, as is exemplified by the May 15, May 30 and June 16 profiles.

A total of 114 mm rain on June 20, 21 and 22 caused the soil to be completely saturated. During the subsequent week there was a high evaporative demand (calculated potential evapotranspiration was 39 mm from June 23 to June 29) and it was anticipated that the soil water content in at least the upper part of the soil profile would be reduced substantially by June 29. Although the model computations showed this

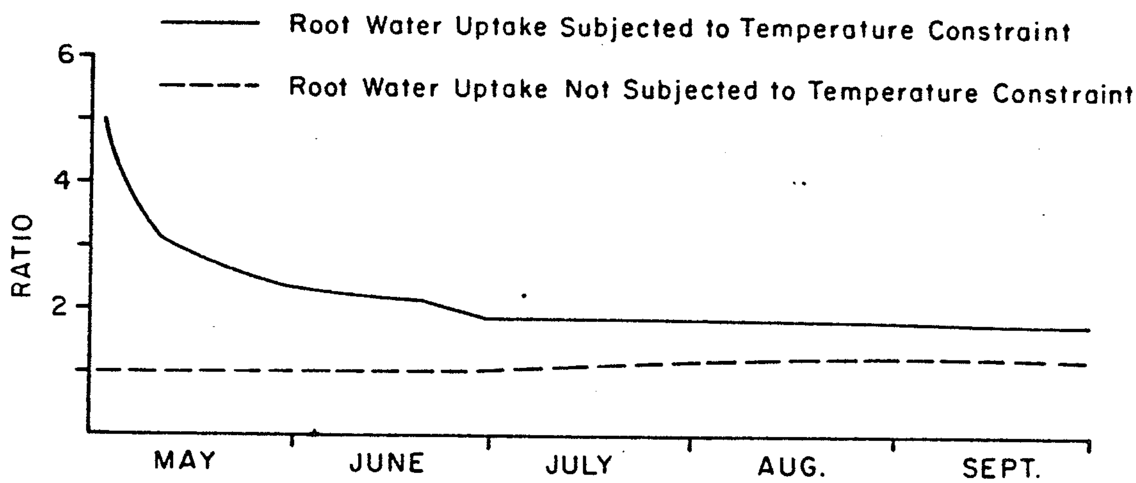

Figure 21. Ratio of cumulative potential evapotranspiration to actual evapotranspiration as a function of time.

Table 14. Daily rate of water uptake by plant roots and daily vapour flux in response to temperature gradients, averaged over the 1975 growing season.

Depth cm	Rate of water uptake by plant roots g cm^{-2} day^{-1}	Vapour flux g cm^{-2} day^{-1}
0		
		2.47×10^{-2}*
1	1.71×10^{-2}	
		3.24×10^{-4}
5	3.10×10^{-2}	
		2.32×10^{-4}
10	2.32×10^{-2}	
		2.29×10^{-4}
15	2.17×10^{-2}	
		1.73×10^{-4}
20	1.98×10^{-2}	
		9.18×10^{-5}
30	1.92×10^{-2}	
		3.47×10^{-5}
50	1.71×10^{-2}	
		1.12×10^{-5}
75	8.77×10^{-3}	
		6.04×10^{-6}
100	3.31×10^{-3}	

*Actual evaporation rate.

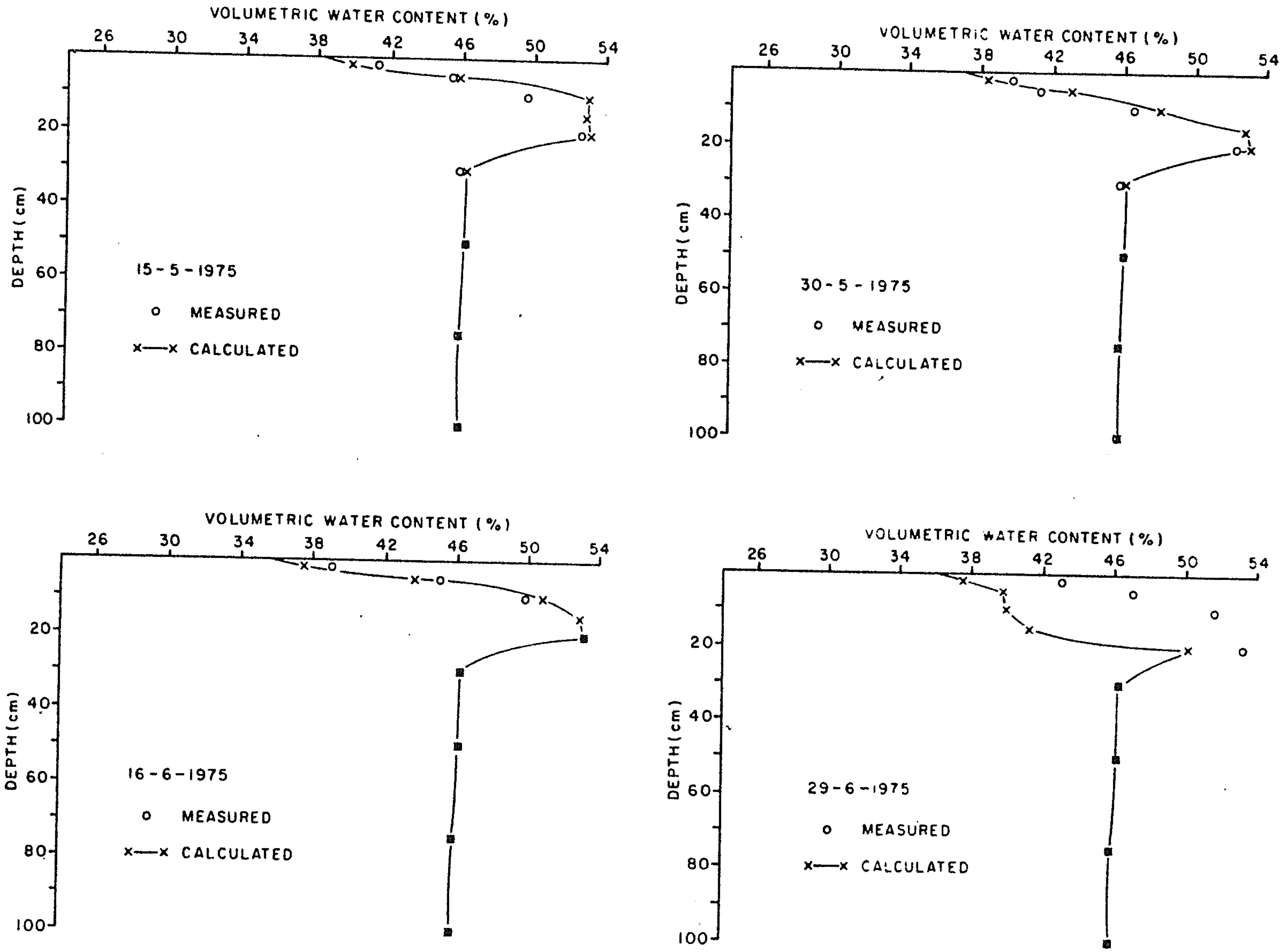

Figure 22. Comparison between measured and calculated water content profiles at indicated dates.

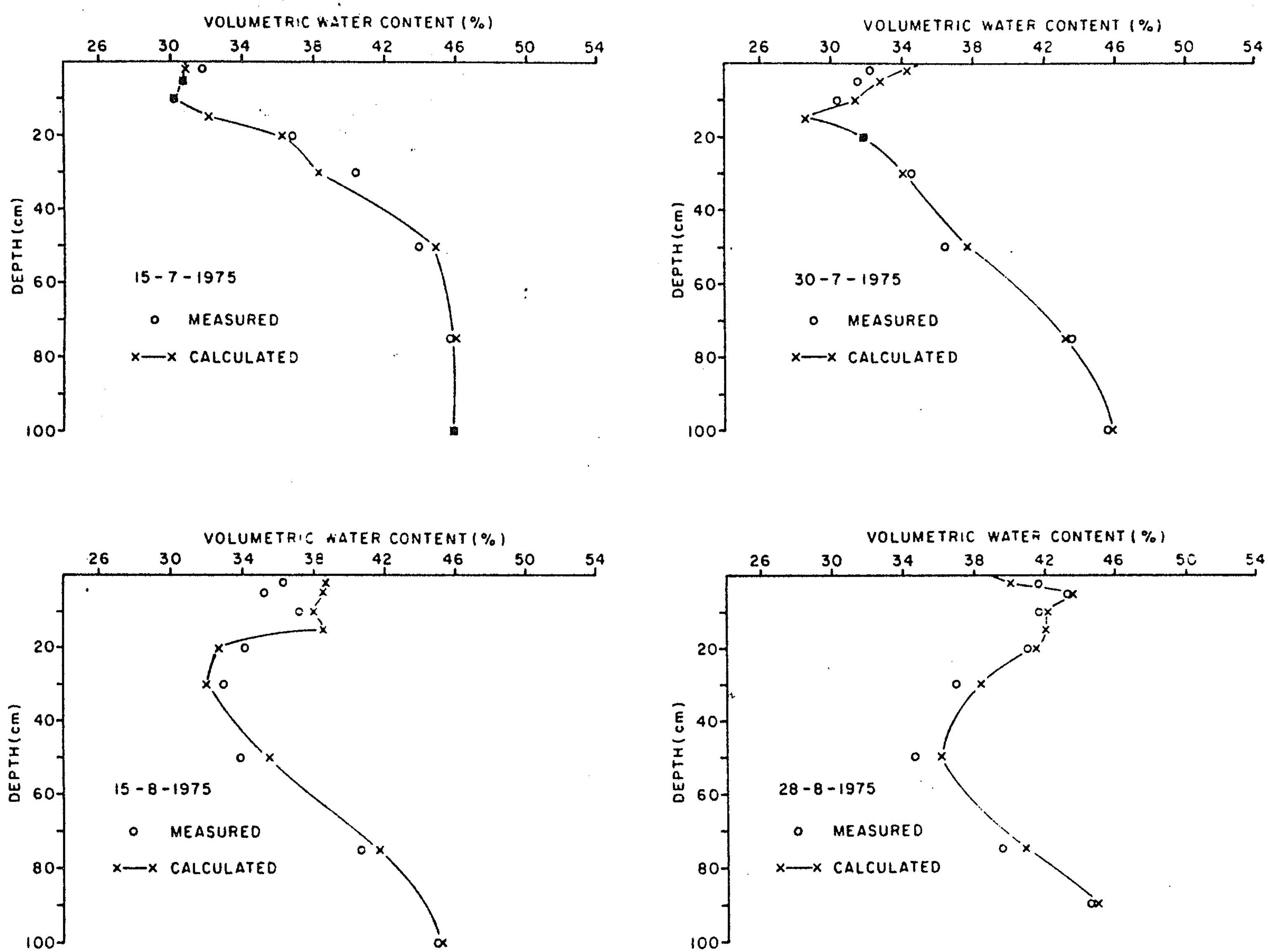

Figure 22 (cont'd.). Comparison between measured and calculated water content profiles at indicated dates.

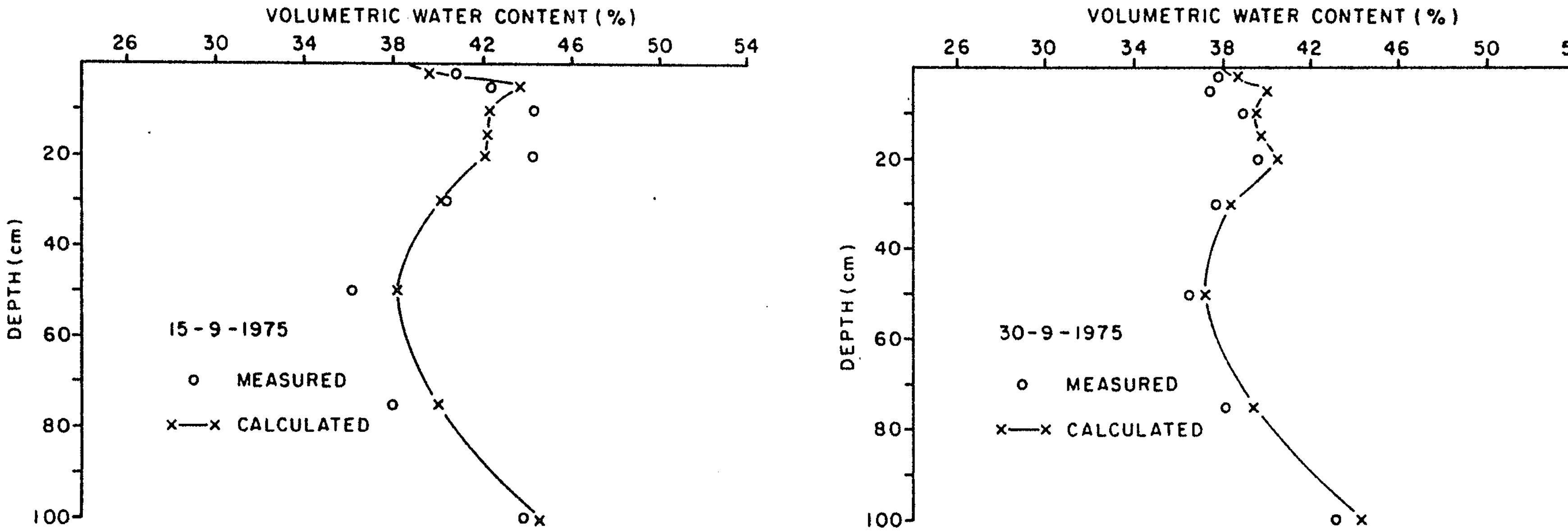

Figure 22 (cont'd.). Comparison between measured and calculated water content profiles at indicated dates.

reduction, the measured soil water content in the entire profile remained unexplainably close to saturation as can be seen in Figure 22 for the June 29th sampling.

The agreement between the computed and observed water content profiles during the remainder of the growing season (July, August and September) was generally fairly good. The small discrepancies between computed and observed profiles can possibly be attributed to the fact that soil water movement due to matric potential gradients was ignored, and that the root distribution was thought to be constant throughout the entire growing season.

The computed daily average soil temperature with respect to time for the entire season at depths 10, 20, 30 and 50 cm agreed well with the measured values (Figures 23a-23d). The greatest difference occurred at the 30 and 50 cm depths, where the model underestimated the temperature values during May and June. A possible explanation is that the relatively warm soil water from the top layers penetrated at a very slow rate deep into the soil profile. However in the model it was assumed that an impermeable layer was present at the 100 cm depth and as a result, during the initial part of the growing season, little or no water could percolate below the 30 cm depth, since the soil was saturated below that depth till the end of June.

An example of the observed and computed diurnal variation in soil temperature is shown in Figure 24. The boundary condition temperature at the 1 cm depth showed rapid changes from one hour to the next; increases or decreases of 1°C per hour were not exceptional.

Although on August 7, 1975 the sky was largely overcast (n/N = 0.26) and less net radiation energy (0.124 ly min^{-1}) reached the surface, the temperatures at the 1 cm depth were higher as compared to

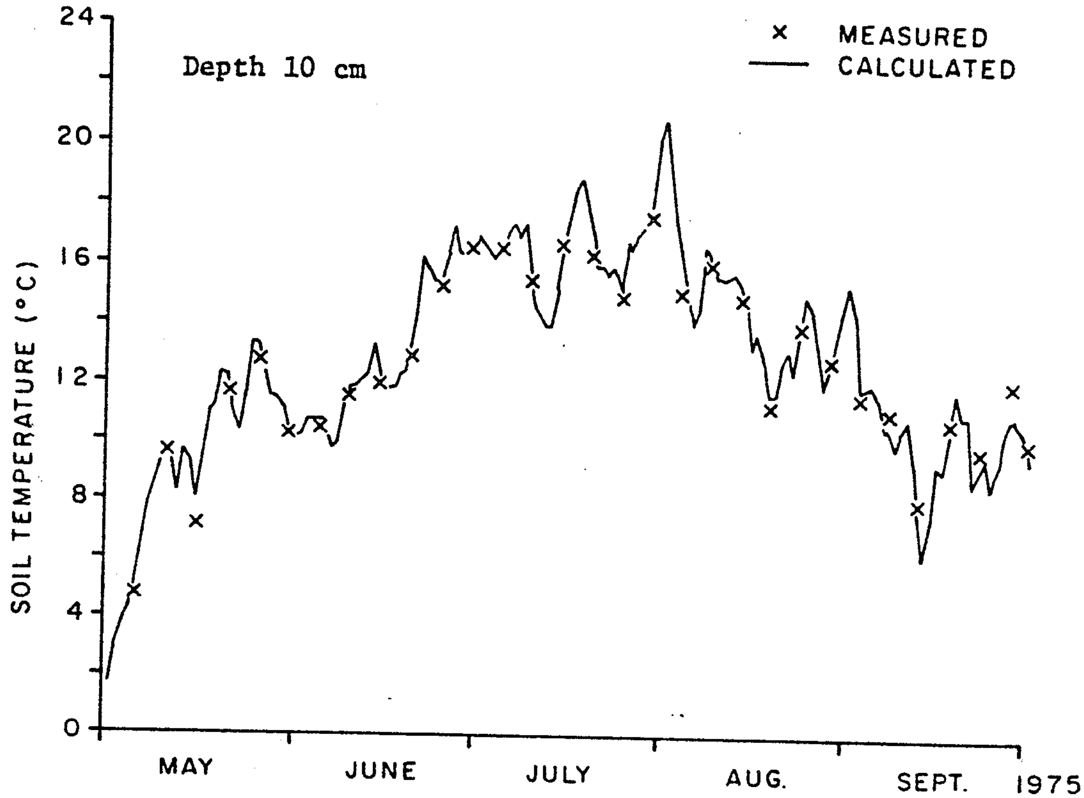

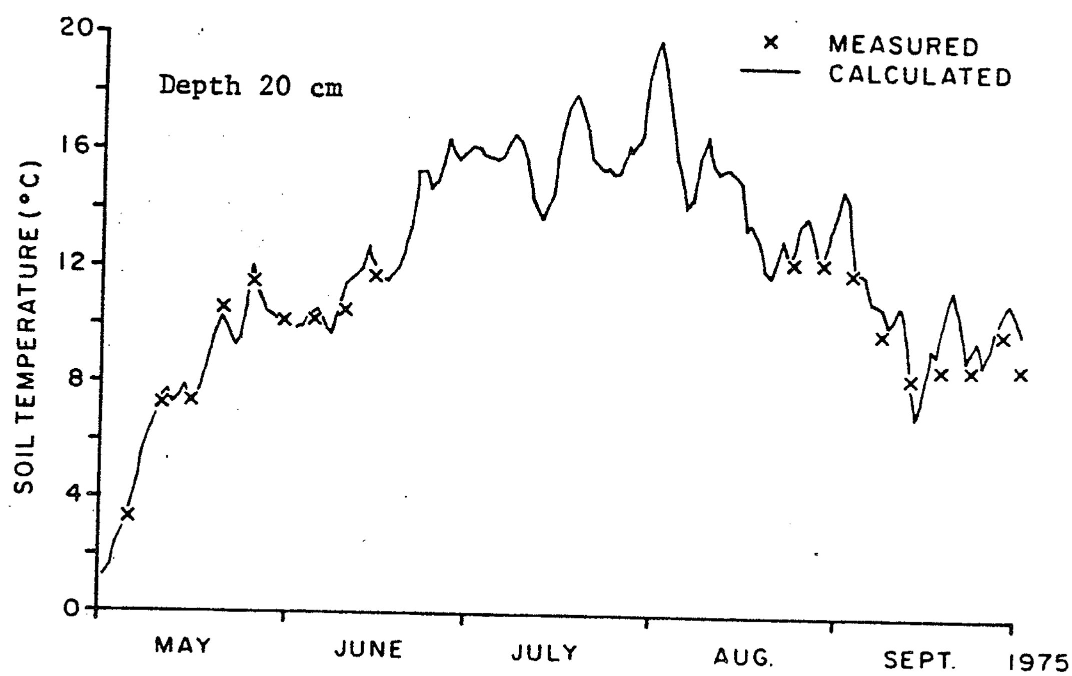

Figure 23. Measured and calculated daily average soil temperatures at indicated depths.

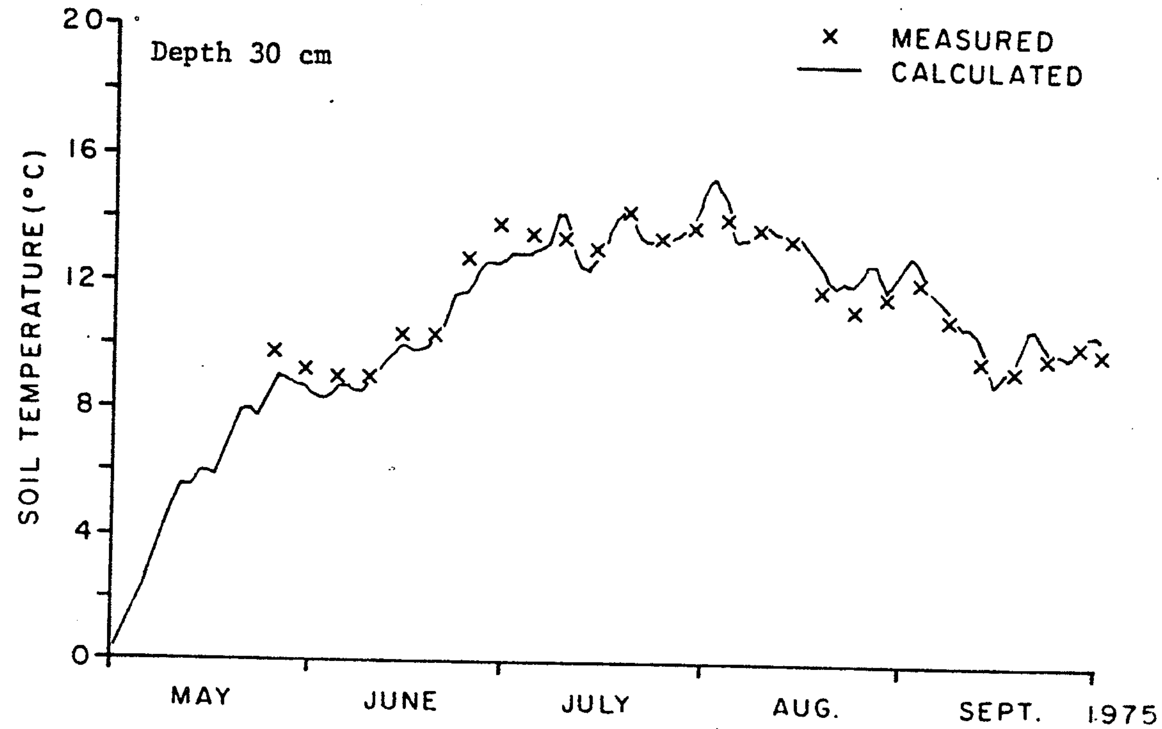

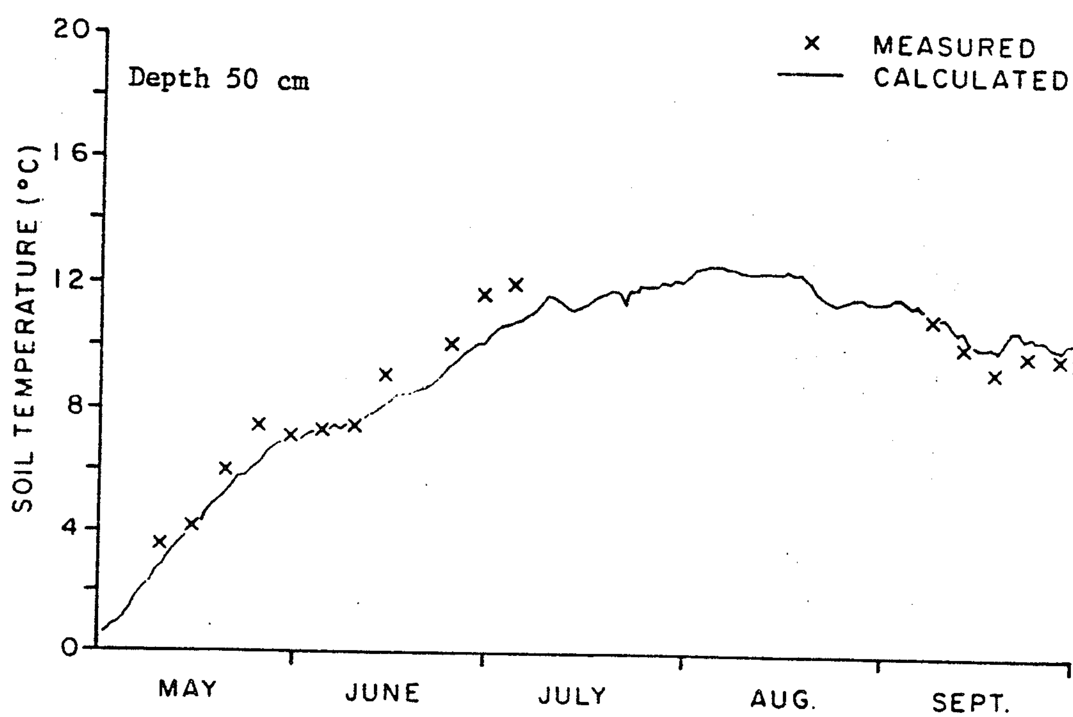

Figure 23 (cont'd.). Measured and calculated daily average soil temperatures at indicated depths.

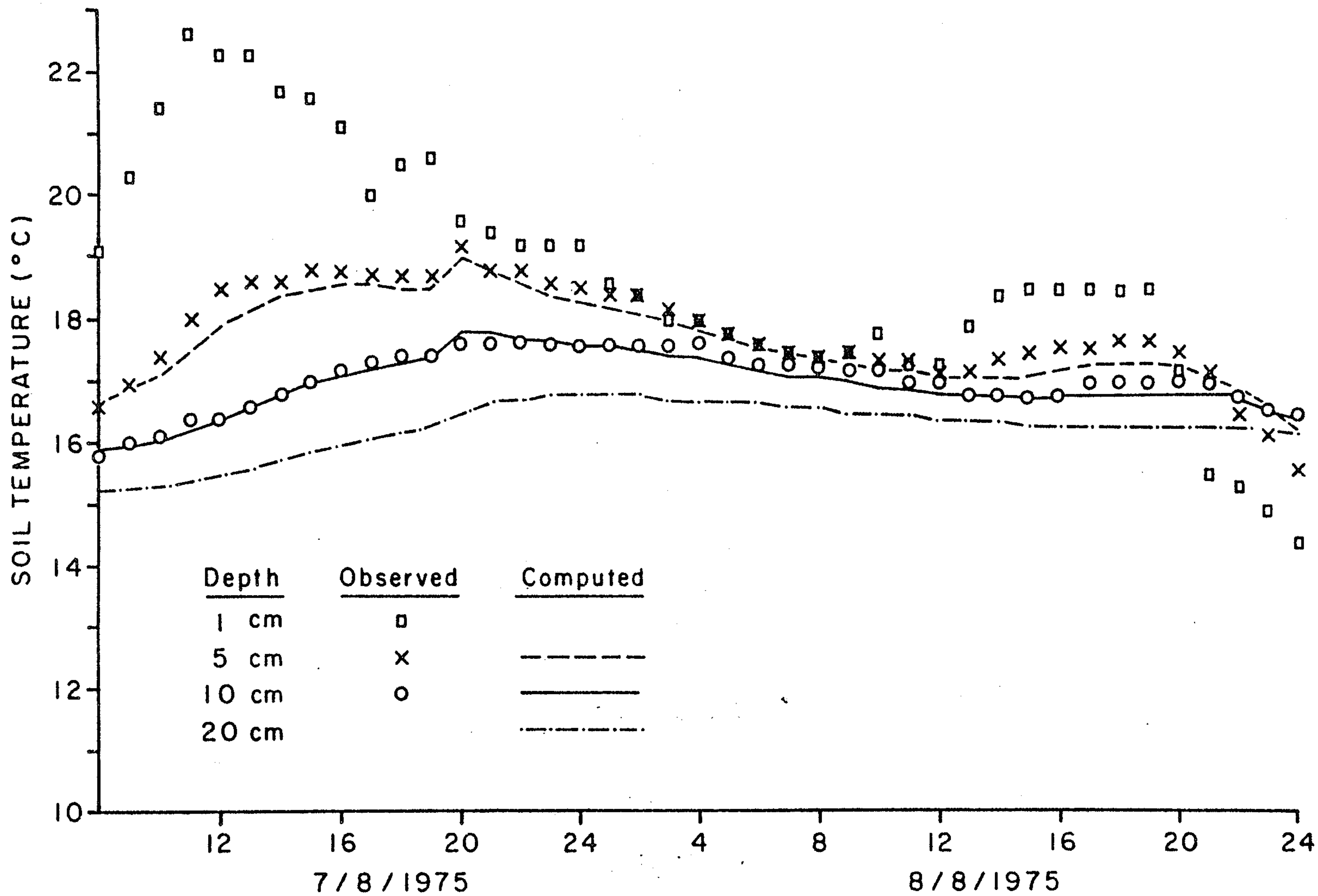

Figure 24. Hourly observed and computed soil temperature variations.

the next day which was sunnier ($n/N = 0.54$) and had larger net radiation flux (0.189 ly min^{-1}). These lower surface temperatures on August 8 were thought to be a direct result of the 25.4 mm rain which fell on August 7 between 6:00 and 8:00 p.m.; increased evaporation from the wetter soil, as postulated by Brooks and Rhoades (1954) and verified experimentally by Wierenga et al. (1970) caused this drop in surface temperatures.

The 20.3 mm rain which fell between 7:00 and 8:00 p.m. on August 7 increased the observed soil temperature at the 5 cm depth by 0.5°C and the observed soil temperature at 10 cm depth by 0.2°C. This compared to a computed increase in soil temperature of 0.5°C and 0.4°C respectively for the above mentioned two depths (see Figure 24). The considerably larger increase in computed soil temperature at the 10 cm depth as compared to the measured one was due to the fact that in the model all water in excess of field capacity was moved instantaneously to a lower zone, which resulted in instantaneous movement of sensible heat in the liquid phase to the lower zone. However in reality a more gradual movement of water and heat occurred, as can be deduced from the temperature curves at the 5 and 10 cm depths after the rainfall. The observed gradual decrease in temperature gradient between the 5 and 10 cm depth indicated that less conductive heat was moving toward the 10 cm depth. However the temperature at the 10 cm depth remained constant for eight hours after the rainfall which was an indication that although less conductive heat moved to this zone, this was compensated by a gradual movement of sensible heat to this zone. It is therefore suggested that the model could be improved by using the Darcy flow equation instead of the field capacity model for water movement.

Figure 24 is an example of predicted diurnal soil temperature variations due to conductive and convective heat transfer. On August 7, 1975, when the total daily precipitation was 25.4 mm, the conductive heat transfer component was approximately 33%, while the convective component was 66% of the total heat transfer. However on most days it was not raining, and therefore the convective heat transfer component was zero. A typical example is presented in Figure 25: there was no rainfall on June 7 and only 0.3 mm on June 8. Consequently there was a negligible influence of convective heat transport upon total heat transfer.

Generally it was found that on days when the precipitation exceeded 10 mm day^{-1}, convective heat transfer formed a significant component (> 25%) of the total heat transfer by conduction, convection and vapour movement. However from May 1 to September 30 there were only 12 days that the daily precipitation exceeded 10 mm, so that the conclusion is reached that, averaged over the entire growing season, convective heat transfer is small compared to conductive heat transfer, but during heavy precipitation and actual water movement in the soil, it forms a much larger component of the total heat transfer.

Under the experimental conditions prevailing in 1975, the temperature gradients in the lower soil layers were less steep than in the upper soil layers. This meant that the saturated vapour pressure gradient, $\partial e^*/\partial z$, for the deeper layers was relatively small and hence thermally induced vapour flow became less important with increasing depth, as is shown in Table 14.

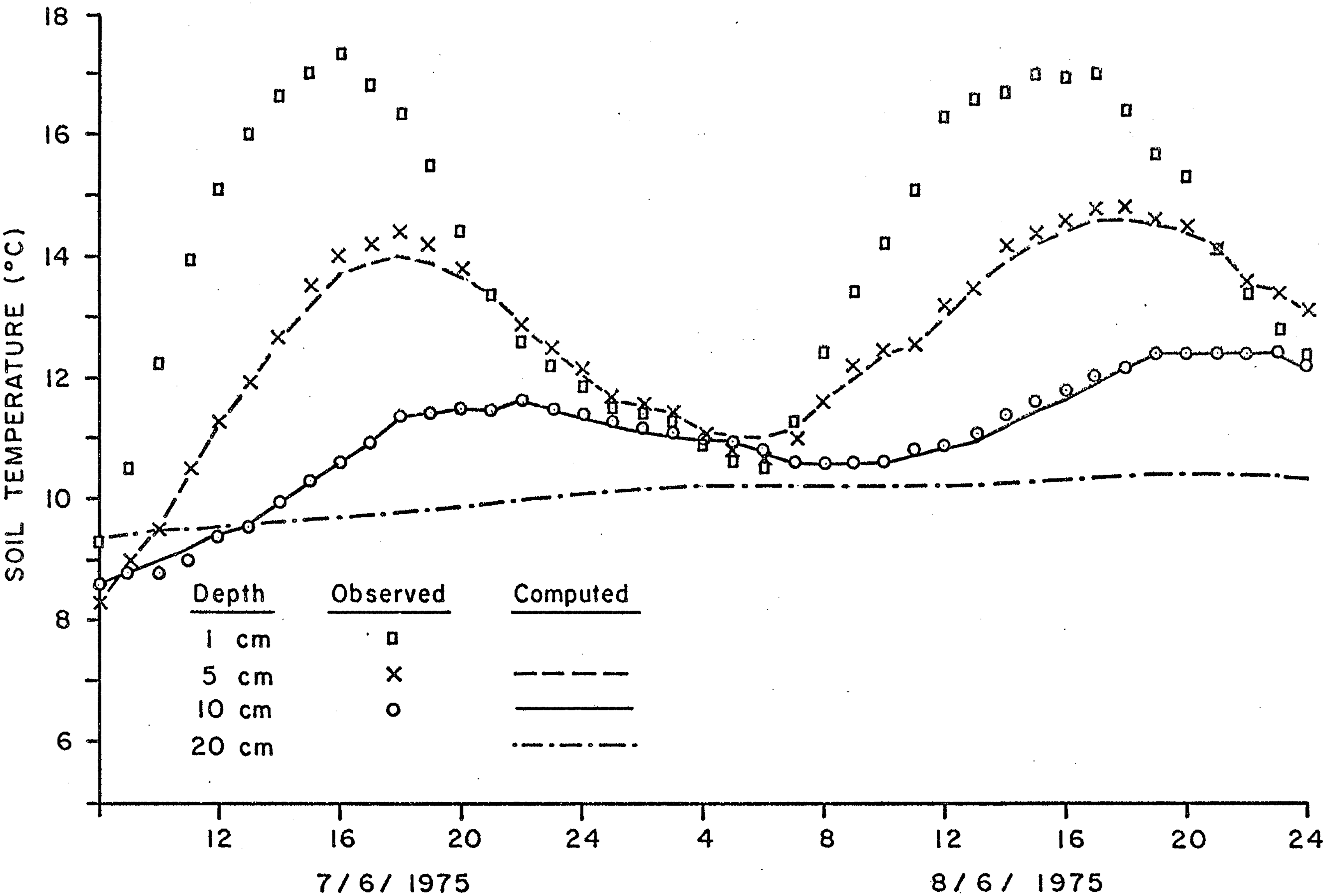

Figure 25. Diurnal observed and computed soil temperature variations.

In the upper part of the soil profile the vapour flow was generally upward (negative) at night and mainly downward (positive) during the day in accordance with the temperature profiles. Between the upper two grid points the daily vapour flux, defined as the sum of the daily upward and downward flux, averaged 3.24×10^{-4} g cm^{-2} day^{-1} over the 1975 growing season. On a few days, when the upper part of the soil profile was relatively dry and a large temperature gradient existed, daily vapour fluxes of approximately 1.0×10^{-3} g cm^{-2} day^{-1} were observed. These values were about one order of magnitude smaller than those reported by Cary (1965) for a steady state laboratory experiment.

The daily vapour flux values reported in Table 14 were approximately two to three orders of magnitude smaller than the rate of water withdrawal by the plant roots. It was therefore not surprising that when a computer run was made without the vapour flow component, the water content profiles were almost identical than when vapour flow was included in the model.

The influence of water vapour movement on soil heat transfer was generally small; only in a few instances when the soil was dry and high temperatures prevailed, the sensible and latent heat flux due to vapour movement, accounted for 5% of the total heat flow. In many cases only 1% of the total heat flow was due to vapour movement, so that the conclusion is reached that, except for very dry conditions in the top layer of the soil, heat flow due to thermally induced vapour movement could be neglected.

V. SUMMARY AND CONCLUSIONS

In order to examine the energy exchange process at the soil-atmosphere interface, the study entailed a review of the radiation and energy balance (Chapter II, A and B). Although empirical and physically based models to predict the net radiation flux are in existence they have not been tested and/or calibrated under the environmental conditions experienced in Manitoba. The energy balance equation has been solved most often for the latent heat flux using either empirical or physically based relationships. A number of publications have dealt with the relationship between the soil heat flux and environmental variables.

A review of soil heat transfer (Chapter II, C) revealed that the simple Fourier heat conduction model has been successfully applied to estimate soil temperatures on an annual basis. In many cases the approach has failed to predict diurnal soil temperature changes; this was ascribed to the non-homogeneous nature of the soil and non-conductive heat transfer mechanisms operating in the upper part of the soil profile. Theories of simultaneous transfer of heat and water were reviewed and it was concluded that their application to field conditions was largely unknown.

Chapter III dealt with the experimental methods, computational procedures and a simultaneous heat and water transfer model development. The experimental methods included the recording of many atmospheric and soil parameters over a period of fifteen months. Most of the data were collected on an hourly basis.

In the section on computational procedures a detailed description of calculating various components of the radiation and energy balance was given. A Fourier analysis of the diurnal soil temperature wave and calculation of the thermal properties of the soil were also discussed.

Since water affects the thermal properties of the soil and might act as an energy transporting medium, it was decided that a model should be developed which considered both heat and water movement. The water model described soil water flow using a bookkeeping approach. Precipitation, root extraction, evaporation and drainage were the main features of the model. The heat transfer model, which used the water model as a foundation, dealt with conductive, convective and latent heat flow. A computer program was written to perform all the calculations necessary for the solution of the equations describing soil water content and soil temperature fields.

In the next chapter (Chapter IV) the results of the field data and the analyses were presented. Very briefly these results may be summarized as follows:

1) The net radiation flux was positive during the summer but negative in the winter because of the large reflectivity of the snow covered ground. The soil heat flux was also positive during the spring and summer and negative during the late summer, fall and winter; it reversed prior to the reversal of the net radiation flux. Large variations from one day to the next were noticed in the diurnal cycle of the net radiation and the soil heat flux.
2) The net radiation flux could be predicted with decreasing accuracy on a monthly, daily and hourly basis using either formulas based on physical considerations or the empirical relationship between net and shortwave radiation flux. It was suggested that the discovered relationships could be used throughout many localities in southern Manitoba.

3) There was generally fairly good agreement between the results of the various potential evapotranspiration calculations and reported Class A pan evaporation measurements. Only the results of the Van Bavel and Penman equations were considerably higher than the reported measured values.
4) A reliable estimate of the thermal diffusivity could be made from the annual soil temperature record. No such estimate could be obtained from the diurnal soil temperature waves, because of the non-homogeneous nature of the upper part of the soil profile.
5) The results of the simultaneous heat and water transport model compared satisfactorily with the actual measured data. Convective heat transfer was only significant during days with heavy rainfall and heat flow due to thermally induced vapour movement could be neglected under the experimental conditions studied.

BIBLIOGRAPHY

Angstrom, A. 1924. Solar and terrestrial radiation. Quart. J. Roy. Meteorol. Soc. 50: 121-125.

Angstrom, A. 1925. The albedo of various surfaces of ground. Geogr. Ann. 7: 323-342.

Arnfield, A.J. 1975. Surface and atmospheric controls on the heating coefficient. Boundary-Layer Meteorol. 8: 109-123.

Baier, W. 1971. Evaluation of latent evaporation estimates and their conversion to potential evaporation. Can. J. Plant Sci. 51: 255-266.

Baier, W. and Robertson, G.W. 1965. Estimation of latent evaporation from simple weather observations. Can. J. Plant Sci. 45: 276-284.

Baier, W. and Robertson, G.W. 1966. A new versatile soil moisture budget. Can. J. Plant Sci. 46: 299-315.

Black, J.N., Bonython, C.W. and Prescott, J.A. 1954. Solar radiation and the duration of sunshine. Quart. J. Roy. Meteorol. Soc. 80: 231-235.

Blake, G.R. and Page, J.B. 1948. Direct measurement of gaseous diffusion in soils. Soil Sci. Soc. Amer. Proc. 13: 37-42.

Bonham, C.D. and Fye, R.E. 1970. Estimation of wintertime soil temperatures. J. Econ. Entomol. 63: 1051-1053.

Bowen, I.S. 1926. The ratio of heat losses by conduction and evaporation from any water surface. Physiol. Rev. 27: 779-787.

Bowers, S.A. and Hanks, R.J. 1965. Reflection of radiant energy from soils. Soil Sci. 100: 130-138.

Brooks, F.A. and Rhoades, D.G. 1954. Daytime partition of irradiation and the evaporation chilling of the ground. Trans. Amer. Geophys. Union 35: 145-152.

Brown, R.W. and Van Haveren, B.P. 1972. Psychrometry in water relations research. Proc. Symp. Thermocouple Psychrometers, Utah State Univ., March 1971. pp. 342.

Brunt, D. 1932. Notes on radiation in the atmosphere. Quart. J. Roy. Meteorol. Soc. 58: 389-420.

Burger, H.C. 1915. Das Leitvermögen verdünnter mischkristallfreier Lösungen. Phys. Zeitschr. 20: 73-76.

Businger, J.A. 1956. Some remarks on Penman's equations for the evapotranspiration. Neth. J. Agr. Sci. 4: 77-80.

Callendar, H.L. 1895. Preliminary results of observations of soil temperatures with electrical resistance thermometers made at the McDonald Physics Building, McGill University. Trans. Roy. Soc. Can., Montreal, 1: 63-74.

Carslaw, H.S. and Jaeger, J.C. 1959. Conduction of heat in solids. Oxford Univ. Press, pp. 509.

Carson, J.E. 1963. Analysis of soil and air temperatures by Fourier techniques. J. Geophys. Res. 68: 2217-2232.

Carson, J.E. and Moses, H. 1963. The annual and diurnal heat-exchange cycles in upper layers of soil. J. Appl. Meteorol. 2: 397-406.

Cartright, K. 1970. Groundwater discharge in the Illinois basin as suggested by temperature anomalies. Water Resources Res. 6: 912-918.

Cary, J.W. 1965. Water flux in moist soil: thermal versus suction gradients. Soil Sci. 100: 168-175.

Cary, J.W. 1966. Soil moisture transport due to thermal gradients: practical aspects. Soil Sci. Soc. Amer. Proc. 30: 428-433.

Cary, J.W. and Taylor, S.A. 1962. Thermally driven liquid and vapor phase transfer of water and energy in soil. Soil Sci. Soc. Amer. Proc. 26: 417-420.

Cassel, D.K., Nielsen, D.R. and Biggar, J.W. 1969. Soil water movement in response to imposed thermal gradients. Soil Sci. Soc. Amer. Proc. 34: 183-189.

Chang, J.H. 1958. Ground temperature. Harvard Univ. Press, Cambridge, Mass., U.S.A. pp. 496.

Christiansen, J.E. 1968. Pan evaporation and evapotranspiration from climatic data. J. Irrig. and Drain., Amer. Soc. Civ. Engr. 94: 243-265.

Christiansen, J.E. and Hargreaves, G.H. 1969. Irrigation requirements from evaporation. Trans. Seventh Congr. Irrig. Drain., Int. Comm. Irrig. Drain., Mexico City, Mexico. pp. 23.569-23.596.

Collins, B.G. and Kyle, T.G. 1966. The spectral variation of the sensitivity of a polyethelene shielded net radiometer. Pure and Appl. Geophys. 63: 231-236.

Cox, L.M. and Boersma, L. 1967. Transpiration as a function of soil temperature and soil water stress. Plant Physiol. 42: 550-556.

Davies, J.A. 1967. A note on the relationship between net radiation and solar radiation. Quart. J. Roy. Meteorol. Soc. 93: 109-115.

Davies, J.A. 1972. Actual, potential and equilibrium evaporation for a bean field in Southern Ontario. Agric. Meteorol. 10: 331-348.

Davies, J.A. and Allen, C.D. 1973. Equilibrium, potential and actual evaporation from cropped surfaces in Southern Ontario. J. Appl. Meteorol. 12: 649-657.

Davies, J.A. and Buttimor, P.H. 1969. Reflection coefficients, heating coefficients and net radiation at Simcoe, Southern Ontario. Agric. Meteorol. 6: 373-386.

Denmead, O.T. and McIlroy, I.C. 1970. Measurements of non-potential evaporation from wheat. Agric. Meteorol. 7: 285-302.

Department of Transport. 1966. Manual of radiation instruments and observations. Meteorological Branch, Department of Transport, Ottawa.

De Vries, D.A. 1950. Some remarks on heat transfer by vapour movement in soils. Fourth Intern. Cong. of Soil Sci. 2: 38-41.

De Vries, D.A. 1952. Het warmtegeleidingsvermogen van de grond. Mededelingen Landbouwhogeshool Wageningen 52: 73.

De Vries, D.A. 1958a. Simultaneous transfer of heat and moisture in porous media. Trans. Amer. Geophys. Union 39: 909-916.

De Vries, D.A. 1958b. The thermal behaviour of soils. Proc. Canberra Symp. Arid Zone Research XI, Climatology and microclimatology: 106-113.

De Vries, D.A. 1966. Thermal properties of soils. _In_ Physics of Plant Environment (Ed. W.R. Van Wÿk) North Holland Publ. Comp. A'dam, 2nd ed.: 210-235.

Driedger, H.L. 1969. An analysis of the relationship between total daily solar radiation receipt and total daily duration of sunshine at Winnipeg, 1950-1967. M.A. Thesis, Univ. of Manitoba. pp. 61.

Driedger, H.L. and Catchpole, A.J.W. 1970. Estimation of solar radiation receipt from sunshine duration at Winnipeg. The Meteorol. Mag. 99: 285-291.

Dyer, A.J. 1967. The turbulent transport of heat and water vapour in an unstable atmosphere. Quart. J. Roy. Meteorol. Soc. 93: 501-508.

Environment Canada, 1974-1975. Monthly record meteorological observations in Canada. Env. Canada, Head Office: 4905 Dufferin St., Downsview, Ont.

Feddes, R.A. and Rÿtema, P.E. 1972. Water withdrawal by plant roots. J. of Hydrol. 17: 33-59.

Fitzpatrick, E.A. and Stern, W.R. 1965. Components of the radiation balance of irrigated plots in a dry monsoonal environment. J. Appl. Meteorol. 4: 649-660.

Fitzpatrick, E.A. and Stern, W.R. 1970. Net radiation estimated from global solar radiation. In Plant response to climatic factors. Proc. Uppsala Symp. 1970: 403-410.

Fluker, B.J. 1958. Soil temperatures. Soil Sci. 86: 35-46.

Fritschen, L.J. 1965. Accuracy of evapotranspiration determinations by the Bowen ratio method. Bull. Int. Ass. Sci. Hydrol. 10: 38-48.

Fritschen, L. 1967. Net and solar radiation relations over irrigated field crops. Agric. Meteorol. 4: 55-62.

Fuchs, M. and Hadas, A. 1972. The heat flux density in a non-homogeneous bare loessial soil. Boundary-Layer Meteorol. 3: 191-200.

Funk, J.P. 1959. Improved polyethelene-shielded net radiometer. J. Sci. Instr. 36: 267-270.

Gardner, W.R. 1960. Dynamic aspects of water availability to plants. Soil Sci. 89: 63-73.

Geiger, R. 1966. The climate near the ground. Harvard Univ. Press, Cambridge, Mass. pp. 611.

Gill, C.B. 1960. The forests of Manitoba. Forest Resources Inventory Report No. 10. Department of Mines and Natural Resources, Winnipeg. pp. 43.

Graham, W.G. and King, K.M. 1961. Short-wave reflection coefficient for a field of maize. Quart. J. Roy. Meteorol. Soc. 87: 425-428.

Hasfurther, V.R. and Burman, R.D. 1974. Soil temperature modeling using air temperature as a driving mechanism. Trans. A.S.A.E. 17: 78-81.

Heldal, B. 1970. Estimating the global radiation at As. Meldinger fra Norges Landbrukshögskole 49, 11: pp. 10.

Ho, P., Schwerdtfeger, P. and Weller, G. 1968. The energy exchange within a vegetation layer. Arch. Met. Geoph. Biokl. Ser. B, 16: 262-271.

Holmes, R.M. and Robertson, G.W. 1963. Application of the relationship between actual and potential evapotranspiration in dry land agriculture. Trans. A.S.A.E. 6: 65-67.

Holmes, J.W. and Watson, C.L. 1967. The water budget of irrigated pasture land near Murray Bridge, South Australia. Agric. Meteorol. 4: 177-188.

Hughes, R. 1965. Climatic factors in relation to growth and survival of pasture plants. J. Brit. Grassland Soc. 20: 263-271.

Idso, S.B. 1968. An analysis of the heating coefficient concept. J. Appl. Meteorol. 7: 716-717.

Idso, S.B. 1974. On the use of equations to estimate atmospheric thermal radiation. Arch. Met. Geoph. Biokl. Ser. B, 22: 287-299.

Idso, S.B., Aase, J.K. and Jackson, R.D. 1975. Net radiation-soil heat flux relations as influenced by soil water content variations. Boundary-Layer Meteorol. 9: 113-122.

Idso, S.B., Baker, D.G. and Blad, B.L. 1969. Relations of radiation fluxes over natural surfaces. Quart. J. Roy. Meteorol. Soc. 95: 244-257.

Idso, S.B. and Jackson, R.D. 1969. Thermal radiation from the atmosphere. J. Geophys. Res. 74: 5397-5403.

Idso, S.B., Jackson, R.D., Reginato, R.J., Kimball, B.A. and Nakayama, F.S. 1975. The dependence of bare soil albedo on soil water content. J. Appl. Meteorol. 14: 109-113.

Impens, I. 1963. Thermohydrodynamische en physiologisch-ecologische aspecten van de potentiële evapotranspiratie uit grasland. Mededel. Landbouwhogeschool Opzoekingssta. Staat Gent 28: 429-485.

Jensen, M.E. 1966. Empirical methods of estimating or predicting evapotranspiration using radiation. Proc. Conf. on Evapotranspiration, A.S.A.E., Chicago. pp. 65.

Jensen, M.E. 1973. Consumptive use of water and irrigation water requirements. Am. Soc. Civil Engn. pp. 215.

Jensen, M.E. and Haise, H.R. 1963. Estimating evapotranspiration from solar radiation. J. Irrig. and Drain., Amer. Soc. Civ. Engn. 89: 15-41.

Jensen, M.E., Robb, D.C.N. and Franzoy, C.E. 1970. Scheduling irrigations using climate-crop-soil data. J. Irrig. and Drain., Amer. Soc. Civ. Engn. 96: 25-28.

Joshua, W.D. and deJong, E. 1973. Soil moisture movement under temperature gradients. Can. J. Soil Sci. 53: 49-57.

Jury, W.A. and Miller, E.E. 1974. Measurement of the transport coefficients for coupled flow of heat and moisture in a medium sand. Soil Sci. Soc. Amer. Proc. 38: 551-557.

Jury, W.A. and Tanner, C.B. 1975. Advection modification of the Priestley and Taylor evapotranspiration formula. Agron. J. 67: 840-842.

Kersten, M.S. 1949. Thermal properties of soils. Minn. Univ. Engn. Exp. Stn. Bul. 28: 228.

Kimball, H.H. 1927. Measurements of solar radiation intensity and determination of its depletion by the atmosphere. Monthl. Weather Rev. 55: 155-169.

King, L.G. and Hanks, R.J. 1973. Irrigation management for control of quality of irrigation return flow. U.S. Env. Protection Agency, Washington. pp. 307.

Kramer, C. 1957. Berekening van de gemiddelde grootte van de verdamping voor de verschillende delen van Nederland volgens de methode van Penman. Mededel. Verhandel. K.N.M.I. 70: 85.

Kreith, F. 1973. Principles of heat transfer. 3rd ed. Intext Educational Publishers, New York. pp. 656.

Krischer, O. and Rohnalter, H. 1940. Wärmeleitung und Dampfdiffusion in feuchten Gütern. Verein Deut. Ing-Forschungsheft 402.

Letey, J. 1968. Movement of water through soil as influenced by osmotic pressure and temperature gradients. Hilgardia 39: 405-418.

Lettau, H.H. 1954. Improved models of thermal diffusion in the soil. Trans. Amer. Geophys. Union 35: 121-132.

Linacre, E.T. 1967. Climate and the evaporation from crops. J. Irrig. and Drain. Div. Amer. Soc. Civ. Engn. 93: 61-79.

Linacre, E.T. 1968. Estimating the net radiation flux. Agric. Meteorol. 5: 49-63.

Makkink, G.F. 1957. Testing the Penman formula by means of lysimeters. J. Inst. Water Engn. 11: 277-288.

Mateer, C.L. 1955. A preliminary estimate of the average insolation in Canada. Can. J. Agric. Sci. 35: 579-594.

McFadden, J.D. and Ragotzkie, R.A. 1967. Climatological significance of albedo in Central Canada. J. Geophys. Res. 72: 1135-1143.

Molz, F.J. and Remson, I. 1970. Extraction term models of soil moisture use by transpiring plants. Water Resources Res. 6: 1346-1356.

Monteith, J.L. 1959. The reflection of shortwave radiation by vegetation. Quart. J. Roy. Meteorol. Soc. 85: 386-392.

Monteith, J.L. 1965. Evaporation and environment. In The State and Movement of Water in Living Organisms. (Ed. G.F. Fogg), Cambridge Univ. Press. pp. 205-234.

Monteith, J.L. and Szeicz, G. 1961. The radiation balance of bare soil and vegetation. Quart. J. Roy Meteorol. Soc. 87: 159-170.

Nielsen, K.F., Halstead, R.L., MacLean, A.J., Bourget, S.J. and Holmes, R.M. 1961. The influence of soil temperature on the growth and mineral composition of corn, bromegrass and potatoes. Soil Sci. Soc. Amer. Proc. 25: 369-372.

Nkemdirim, L.C. 1972a. Relation of radiation fluxes over prairie grass. Arch. Met. Geoph. Biokl., Ser. B, 20: 23-40.

Nkemdirim, L. 1972b. Radiative flux relations over crops. Agric. Meteorol. 11: 229-242.

Norris, D.J. and Funk, J.P. 1961. Radiation observations at Mawson, Antarctica. Aust. J. Appl. Sci. 12: 148-157.

Ogata, G., Richards, L.A. and Gardner, W.R. 1960. Transpiration of alfalfa determined from soil water content changes. Soil Sci. 89: 179-182.

Pasquill, F. 1949. Eddy diffusion of water vapour and heat near the ground. Proc. Roy. Soc. London, Ser. A, 198: 116-140.

Pearce, D.C. and Gold, L.W. 1959. Observations of ground temperature and heat flow at Ottawa, Canada. J. Geophys. Res. 64: 1293-1298.

Pelton, W.L., King, K.M. and Tanner, C.B. 1960. An evaluation of the Thornthwaite method for determining potential evapotranspiration. Agron. J. 52: 387-395.

Pelton, W.L. and Korven, H.C. 1969. Evapotranspiration estimates in a semiarid climate. Can. Agric. Engn. 11: 50-53, 61.

Penman, H.L. 1940. Gas and vapour movements in the soil. J. Agric. Sci. 30: 447-462.

Penman, H.L. 1948. Natural evaporation from open water, bare soil and grass. Proc. Roy. Soc. London, Ser. A, 193: 120-145.

Penner, E. 1962. Thermal conductivity of saturated Leda clay. Geotechnique 12: 168-175.

Penner, E. 1970. Thermal conductivity of frozen soils. Can. J. Earth Sci. 7: 982-987.

Philip, J.R. and de Vries, D.A. 1957. Moisture movement in porous materials under temperature gradients. Trans. Amer. Geophys. Union 38: 222-232.

Piggin, I. and Schwerdtfeger, P. 1973. Variations in the albedo of wheat and barley crops. Arch. Met. Geoph. Biokl., Ser. B, 21: 365-391.

Priestley, C.H.B. and Swinbank, W.C. 1947. Vertical transport of heat by turbulence in the atmosphere. Proc. Roy. Soc. London, Ser. A, 189: 543-561.

Priestley, C.H.B. and Taylor, R.J. 1972. On the assessment of surface heat flux and evaporation using large-scale parameters. Monthl. Weather Rev. 100: 81-92.

Pruitt, W.O. 1964. Cyclic relations between evapotranspiration and radiation. Trans. A.S.A.E. 7: 271-275, 280.

Reimer, A. 1966. The micrometeorology of the Whiteshell Nuclear Research Establishment at Pinawa, Manitoba. Pre-operational survey report. Atomic Energy of Canada Limited report AECL 2620: 37.

Reimer, A. and Desmarais, R. 1973. Micrometeorological energy budget methods and apparent diffusivity for boreal forest and grass sites at Pinawa, Manitoba, Canada. Agric. Meteorol. 11: 419-436.

Rider, N.E. 1957. A note on the physics of soil temperature. Weather 12: 241-246.

Rider, N.E. and Robinson, G.D. 1951. A study of the transfer of heat and water vapour above a surface of short grass. Quart. J. Roy. Meteorol. Soc. 77: 375-401.

Robertson, G.W. and Russelo, D.A. 1968. Astrometeorological estimator. Ag. Met. Tech. Bul. 14, Canada Dept. of Agric. pp. 22.

Rose, C.W. 1968. Water transport in soil with a daily temperature wave. I. Theory and experiment. II. Analysis. Aust. J. Soil Res. 6: 31-44.

Sarson, P.B. 1960. Exceptional sudden changes of earth temperature. Meteorol. Mag. 9: 201-209.

Schneider, P.J. 1955. Conduction heat transfer. Addison Wesley Publ. Comp., Cambridge, Mass. pp. 310.

Scholte Ubing, D.W. 1961. Solar and net radiation, available energy and its influence on evapotranspiration from grass. Neth. J. Agric. Sci. 9: 81-93.

Sellers, W.D. 1965. Physical climatology. The Univ. of Chicago Press, Chicago. pp. 272.

Shaw, R.H. 1956. A comparison of solar radiation and net radiation. Bul. Am. Meteorol. Soc. 37: 205-206.

Shaykewich, C.F. and Warkentin, B.P. 1970. Effect of clay content and aggregate size on availability of soil water to tomato plants. Can. J. Soil Sci. 50: 205-217.

Slatyer, R.O. and McIlroy, I.C. 1961. Practical microclimatology. UNESCO, Paris. pp. 300.

Smith, W.O. 1943. Thermal transfer of moisture in soils. Trans. Amer. Geophys. Union 24: 511-523.

Smith, R.E., Ehrlich, W.A. and Zoltai, S.C. 1967. Soils of the Lac du Bonnet area. Soils Rep. No. 15. Man. Soil Survey. pp. 118.

Smithsonian Meteorological Tables. 1951. Smithsonian Misc. Coll. Vol. 114. Smithsonian Inst., Washington, D.C.

Sorey, M.L. 1971. Measurement of vertical groundwater velocity from temperature profiles in wells. Water Resources Res. 7: 963-970.

Stallman, R.W. 1963. Computation of ground water velocity from temperature data. _In_ Methods of collecting and interpreting ground-water data, compiled by Ray Bentall, U.S. Geol. Surv. Water Supply Paper 1544H: 36-46.

Stallman, R.W. 1965. Steady one-dimensional fluid flow in a semi-infinite porous medium with sinusoidal surface temperature. J. Geophys. Res. 70: 2821-2827.

Stanhill, G. 1970. Some results of helicopter measurements of the albedo of different land surfaces. Solar Energy 13: 59-66.

Stanhill, G., Hofstede, G.H. and Kalma, J.D. 1966. Radiation balance of natural and agricultural vegetation. Quart. J. Roy. Meteorol. Soc. 92: 128-140.

Staple, W.J. 1965. Moisture tension, diffusivity and conductivity of a loam soil during wetting and drying. Can. J. Soil Sci. 45: 78-86.

Stapleton, H.N., Buxton, D.R., Watson, F.L., Nolting, D.J. and Baker, D.N. 1973. Cotton: a computer simulation of cotton growth. Tech. Bul. 206, Agric. Exp. Sta., Univ. of Arizona, Tucson. pp. 124.

Stewart, D.W. and Lemon, E.R. 1969. The energy budget at the earth's surface: a simulation of net photosynthesis of field corn. Microclimate investigations, Interim Report 69-3. E.R. Lemon, Investigations Leader, U.S.D.A. and Cornell Univ., Ithaca, N.Y.

Swinbank, W.C. 1948. Note on the direct measurement of the thermal conductivity of soil. Quart. J. Roy. Meteorol. Soc. 74: 409-410.

Swinbank, W.C. 1955. Eddy transports in the lower atmosphere. C.S.I.R.O. Div. Meteorol. Phys., Tech. Paper 2. pp. 30.

Swinbank, W.C. 1963. Longwave radiation from clear skies. Quart. J. Roy. Meteorol. Soc. 89: 339-348.

Swinbank, W.C. and Dyer, A.J. 1967. An experimental study in micro-meteorology. Quart. J. Roy. Meteorol. Soc. 93: 494-500.

Tanner, C.B. 1960. Energy balance approach to evapotranspiration from crops. Soil Sci. Soc. Amer. Proc. 24: 1-9.

Tanner, C.B. and Fuchs, M. 1968. Evaporation from unsaturated surfaces: a generalized combination method. J. Geophys. Res. 73: 1299-1304.

Tanner, C.B. and Pelton, W.L. 1960. Potential evapotranspiration estimates by the approximate energy balance method of Penman. J. Geophys. Res. 65: 3391-3413.

Taylor, S.A. and Ashcroft, G.L. 1972. Physical Edaphology. The physics of irrigated and nonirrigated soils. Publ. W.H. Freeman and Company, San Francisco. pp. 533.

Taylor, S.A. and Cary, J.W. 1960. Analysis of the simultaneous flow of water and heat or electricity with the thermodynamics of irreversible processes. Trans. 7th Int. Congress Soil Sci. I: 80-90.

Taylor, S.A. and Cary, J.W. 1964. Linear equations for the simultaneous flow of matter and energy in a contineous soil system. Soil Sci. Soc. Amer. Proc. 28: 167-172.

Taylor, S.A. and Cavazza, L. 1954. The movement of soil moisture in response to temperature gradients. Soil Sci. Soc. Amer. Proc. 18: 351-358.

Tetens, O. 1930. Uber einige meteorologische Begriffe. Zeitung Geophys. 6: 297-309.

Thornthwaite, C.W. 1948. An approach toward a rational classification of climate. Geogr. Rev. 38: 55-94.

Turc, L.E. 1961. Estimation of irrigation water requirements, potential evapotranspiration: a simple climatic formula evolved up to date. Ann. Agron. 12: 13-49.

Turner, B.N., Iverson, S.L. and Walley, W.J. 1972. Some aspects of the plant ecology of an old field. Atomic Energy of Canada Limited Report AECL-3955.

Van Bavel, C.H.M. 1966. Potential evaporation: the combination concept and its experimental verification. Water Resources Res. 2: 455-467.

Van Bavel, C.H.M., Stirk, G.B. and Brust, K.J. 1968. Hydraulic properties of a clay loam soil and the field measurement of water uptake by roots. I. Interpretation of water content and pressure profiles. Soil Sci. Soc. Amer. Proc. 32: 310-316.

Van Wÿk, W.R. and De Vries, D.A. 1966. Periodic temperature variations in a homogeneous soil. In Physics of Plant Environment (Ed. W.R. Van Wÿk), North Holland Publ. Comp., A'dam, 2nd ed. pp. 102-143.

Van Wÿk, W.R. and Scholte Ubing, D.W. 1966. Radiation. In Physics of Plant Environment (Ed. W.R. Van Wÿk), North Holland Publ. Comp., A'dam, 2nd ed. pp. 62-101.

Walker, J.M. 1970. Effects of alternating versus constant soil temperatures on maize seedling growth. Soil Sci. Soc. Amer. Proc. 34: 889-892.

Whittaker, E. and Robinson, G. 1958. The calculus of observations. Blackie and Son Ltd., London.

Wierenga, P.J. 1968. An analysis of temperature behavior in irrigated soil profiles. Unpublished Ph.D. Thesis, Univ. of California, Davis, Calif. pp. 152.

Wierenga, P.J., Hagan, R.M. and Gregory, E.J. 1971. Effects of irrigation water temperature on soil temperature. Agron. J. 63: 33-36.

Wierenga, P.J., Hagan, R.M. and Nielsen, D.R. 1970. Soil temperature profiles during infiltration and redistribution of cool and warm irrigation water. Water Resources Res. 6: 230-238.

Wierenga, P.J., Nielsen, D.R. and Hagan, R.M. 1969. Thermal properties of a soil based upon field and laboratory measurements. Soil Sci. Soc. Amer. Proc. 33: 354-360.

Williams, T.F. and Baker, H.M. 1957. Studies of the root development of herbage root investigation. Brit. Grassland Soc. 12: 49-55.

Wilson, R.G. and Rouse, W.R. 1972. Moisture and temperature limits of the equilibrium evapotranspiration model. J. Appl. Meteorol. 11: 436-442.

Woodside, W. and Cliffe, J.B. 1959. Heat and moisture transfers - closed systems. Soil Sci. 87: 75-82.

Woodside, W. and Kuzmak, J.M. 1958. Effect of temperature distribution on moisture flow in porous materials. Trans. Amer. Geophys. Union 39: 676-680.

Yocum, C.S., Allen, L.H. and Lemon, E.R. 1964. Photosynthesis under field conditions. Agron. J. 56: 249-253.

APPENDIX A

List of Symbols Used

LIST OF SYMBOLS USED

The letters K, a, b, c, d, p and q are also used for any given constant. Some of the symbols used in a few consecutive equations falling outside the main line of argument are defined in the text only.

Symbol	Interpretation
A_0, A_1, A_2	Amplitude of the temperature wave respectively at the surface, depth 1 and depth 2.
AE	Actual evaporation rate.
ARU	Actual rate of water uptake by plant roots.
AVH_2O	Fraction of available water.
B	Bowen ratio.
C	Volumetric heat capacity of the bulk soil.
c^a, c^m, c^{om}, c^w, c^v	Specific heat of air, minerals, organic matter, water and water vapour respectively.
D	Thermal diffusivity.
D_a	Molecular diffusion coefficient of water vapour in air.
D_{Tw}, D_{Tv}	Thermal liquid and vapour diffusivity respectively.
$D_{\theta w}$, $D_{\theta v}$	Isothermal liquid and vapour diffusivity respectively.
d	Damping depth.
E	Evaporation rate.
E_a	Aerodynamic term.
E_{pot}	Potential evaporation rate.
e, e^*	Unsaturated and saturated water vapour pressure respectively.
e_a, e_a^*	Unsaturated and saturated water vapour pressure respectively at screen level.
e_o, e_o^*	Unsaturated and saturated water vapour pressure respectively at the soil surface.

Symbol	Interpretation
erf (x)	Tabulated error function ($\text{erf}(x) = \frac{2}{\sqrt{\pi}} \int_o^x e^{-\zeta^2} d\zeta$).
F_1, F_2	Functions expressing evaporation and condensation effects respectively.
f	Function.
G	Soil heat flux.
H	Sensible heat flux.
h	Solar hour angle.
ht	Height of vegetation.
I	Annual heat index.
I_o	Solar constant.
i	Monthly heat index.
K	Hydraulic conductivity.
K_c	Crop coefficient.
Kh, Kv	Eddy transfer coefficients for heat and water vapour respectively.
k	Von Karman's constant.
L	Latent heat of vaporization.
LE	Latent heat flux.
LE_{pot}, LE_{eq}	Potential and equilibrium latent heat flux respectively.
L_{MM}, L_{MT}, L_{TM}, L_{TT}	Phenomenological coefficients.
M	Miscellaneous heat flux.
N	Maximum possible duration of sunshine per day.
n	Actual duration of sunshine per day.
P	Atmospheric pressure.
PE	Potential evaporation rate.
PRU	Potential rate of water uptake by plant roots.
PT	Potential transpiration rate.
Q	Total heat content of the soil.
q^c, q^w, q^v	Conductive, convective and vapour heat flux respectively.

Symbol	Interpretation
R_n, R_s, R_{ln}	Net radiation flux, shortwave radiation flux and effective longwave radiation flux respectively.
R_s^c	Shortwave radiation flux under clear sky conditions.
R_s^{top}	Extra-terrestrial shortwave radiation flux at the top of the atmosphere.
RD	Rooting density.
r	Radius vector of the earth's orbit around the sun.
T	Celsius temperature.
T_k or T^k	Kelvin temperature.
THICKN	Thickness of a soil layer.
t	Time.
u_z	Horizontal windspeed at height z.
V^m, V^w, V^v	Total moisture flux, liquid water flux and water vapour flux respectively.
v	Specific volume of soil water.
Z	Solar zenith angle.
z	Vertical distance from a reference level.
z_o	Roughness length.
α	Reflection coefficient of surface.
β	Heating coefficient.
γ	Psychrometric constant.
Δ	Slope of the saturation vapour pressure curve.
Δt	Time interval.
$\Delta P/\Delta x$	Soil water pressure gradient.
$\Delta T/\Delta x$	Soil temperature gradient.
δ	Solar declination.
ε	Relative molecular weight of water with respect to air.
θ_a, θ_m, θ_{om}, θ_w	Volumetric fractions of air, minerals, organic matter and water respectively.

Symbol	Interpretation
λ	Thermal conductivity of the bulk soil.
λ_a, λ_m, λ_{om}, λ_w	Thermal conductivity of air, minerals, organic matter and water respectively.
ρ_a, ρ_m, ρ_{om}, ρ_w	Density of air, minerals, organic matter and water respectively.
σ	Stefan-Boltzmann constant.
ϕ	Latitude of location.
ϕ_1, ϕ_2	Net radiation and shortwave radiation coefficient respectively.
ϕ_k	Phase angle.
ψ	Capillary potential.
ω	Radial frequency.

APPENDIX B

Monthly Meteorological Summaries

MONTHLY METEOROLOGICAL SUMMARY, JULY 1974

DATE	TEMPERATURE C			PRECIPITATION			WIND-SPEED KM/HR	SUN-SHINE HR
	MAX	MIN	MEAN	RAIN MM	SNOW CM	TOTAL MM	AVE	
5	27.2	17.2	22.2				10.0	10.5
6	32.2	11.1	21.7				3.9	11.5
7	32.2	18.3	25.3	0.5		0.5	5.0	7.5
8	28.3	17.2	22.8				6.2	3.5
9	28.3	17.2	22.8				10.5	11.2
10	30.6	17.2	23.9				10.7	15.0
11	29.4	17.8	23.6	6.4		6.4	14.6	12.3
12	30.6	18.3	24.5				7.4	13.8
13	28.9	16.1	22.5				9.3	13.8
14	23.9	12.8	18.4				11.4	8.8
15	27.2	10.0	18.6				4.7	14.8
16	28.3	11.7	20.0	1.0		1.0	5.6	3.9
17	30.6	13.9	22.3				6.8	14.1
18	31.1	15.6	23.4				4.8	14.0
19	29.4	14.4	21.9				6.6	13.8
20	31.7	14.4	23.1	9.1		9.1	10.0	14.4
21	29.4	19.4	24.4				7.4	14.6
22	27.2	11.7	19.5				5.6	14.9
23	28.9	11.1	20.0	4.6		4.6	5.2	9.1
24	25.0	17.2	21.1	0.5		0.5	12.7	7.4
25	28.9	16.1	22.5	2.5		2.5	8.1	11.1
26	23.3	13.9	18.6				17.8	12.6
27	23.3	12.8	18.1				22.5	12.9
28	17.2	13.9	15.6	10.4		10.4	19.9	2.0
29	19.4	11.1	15.3	0.8		0.8	14.0	6.6
30	21.1	12.2	16.7	0.5		0.5	8.3	5.6
31	23.3	7.8	15.6				5.4	9.3
				TOTAL	TOTAL	TOTAL		TOTAL
MEAN	27.3	14.5	20.9	36.3	0.0	36.3	9.4	289.0
NORMAL WINNIPEG	25.9	13.5	19.7	80.3	0.0	80.3		311.0

MONTHLY METEOROLOGICAL SUMMARY, AUGUST 1974

DATE	TEMPERATURE C MAX	TEMPERATURE C MIN	TEMPERATURE C MEAN	PRECIPITATION MM RAIN	PRECIPITATION CM SNOW	PRECIPITATION MM TOTAL	WIND-SPEED KM/HR AVE	SUN-SHINE HR
1	23.3	14.4	18.9				8.3	6.1
2	20.0	8.3	14.2				10.5	13.3
3	24.4	2.8	13.6				4.4	13.0
4	27.2	13.3	20.3				4.8	10.9
5	28.3	10.0	19.2				2.3	11.6
6	30.6	12.8	21.7				6.8	13.9
7	29.4	15.0	22.2				13.0	13.6
8	28.9	15.0	22.0	T		T	11.2	13.5
9	27.2	15.0	21.1	1.5		1.5	11.5	3.0
10	24.4	13.3	18.9	3.6		3.6	3.5	3.9
11	17.2	14.4	15.8	14.2		14.2	12.8	0.0
12	22.8	12.8	17.8	2.5		2.5	7.3	2.5
13	21.7	13.3	17.5				5.0	3.6
14	19.4	8.9	14.2	7.4		7.4	9.6	0.8
15	20.6	14.4	17.5	1.3		1.3	12.5	7.7
16	23.9	11.7	17.8	1.0		1.0	8.8	11.8
17	21.1	9.4	15.3	1.8		1.8	4.9	11.0
18	21.7	7.2	14.5	0.8		0.8	2.9	7.3
19	23.3	10.6	17.0	13.2		13.2	9.5	10.1
20	15.6	12.2	13.9	11.7		11.7	11.5	0.0
21	13.9	10.0	12.0	11.9		11.9	10.8	0.0
22	13.9	8.9	11.4	0.3		0.3	9.1	1.3
23	16.1	7.2	11.7	0.3		0.3	6.5	3.5
24	20.6	8.9	14.8	3.8		3.8	11.5	5.9
25	26.1	16.1	21.1				12.2	4.7
26	18.3	10.0	14.2				15.0	6.3
27	17.8	8.3	13.1				9.0	8.1
28	13.3	1.1	7.2	17.5		17.5	5.8	0.0
29	16.1	6.7	11.4	15.2		15.2	11.8	9.9
30	12.8	9.4	11.1	5.1		5.1	16.8	3.7
31	12.8	4.4	8.6	1.3		1.3	7.9	6.1
				TOTAL	TOTAL	TOTAL		TOTAL
MEAN	21.1	10.5	15.8	114.4	0.0	114.4	8.9	207.1
NORMAL WINNIPEG	25.0	12.2	18.6	73.7	0.0	73.7		276.0

MONTHLY METEOROLOGICAL SUMMARY, SEPTEMBER 1974

DATE	TEMPERATURE C			PRECIPITATION			WIND-SPEED KM/HR	SUN-SHINE HR
	MAX	MIN	MEAN	RAIN MM	SNOW CM	TOTAL MM	AVE	
1	11.7	1.7	6.7	3.6		3.6	7.5	7.0
2	14.4	1.7	8.1				6.2	9.7
3	18.9	5.0	12.0				4.1	12.2
4	24.4	5.0	14.7				6.7	11.5
5	22.8	8.9	15.9	1.0		1.0	9.3	5.0
6	17.8	11.7	14.8				3.4	1.1
7	17.2	12.2	14.7				10.6	3.5
8	12.2	3.3	7.8				8.1	6.8
9	14.4	5.6	10.0	5.3		5.3	2.4	5.2
10	10.0	5.6	7.8	11.2		11.2	8.5	0.0
11	10.6	6.1	8.4	0.8		0.8	8.6	0.0
12	10.6	-1.1	4.8				5.2	0.0
13	13.3	1.1	7.2				7.1	9.6
14	15.6	7.2	11.4	0.5		0.5	16.8	5.6
15	18.3	-1.1	8.6	3.8		3.8	4.2	4.6
16	18.3	11.7	15.0	10.9		10.9	5.2	3.5
17	14.4	5.6	10.0	13.0		13.0	4.9	7.6
18	17.8	8.9	13.4				9.2	3.9
19	10.0	2.8	6.4	0.5		0.5	5.0	3.3
20	11.1	0.0	5.6	T	T	T	9.5	4.3
21	4.4	-4.4	0.0				6.2	7.3
22	12.8	-4.4	4.2				6.2	7.3
23	17.8	5.0	11.4				7.9	4.0
24	13.3	6.7	10.0	5.6		5.6	11.1	1.6
25	20.6	-1.7	9.5				7.2	4.2
26	26.1	2.2	14.2	0.8		0.8	13.6	7.6
27	6.7	2.2	4.5				8.9	3.6
28	11.7	-5.6	3.1				4.2	3.0
29	6.1	2.2	4.2	7.9	0.8	8.7	14.0	0.0
30	3.3	-2.2	0.6		3.8	3.8	5.6	0.4
MEAN	14.2	3.4	8.8	TOTAL 64.9	TOTAL 4.6	TOTAL 69.5	7.6	TOTAL 143.4
NORMAL WINNIPEG	18.4	6.6	12.5	52.6	0.3	52.9		183.0

MONTHLY METEOROLOGICAL SUMMARY, OCTOBER 1974

DATE	TEMPERATURE C MAX	MIN	MEAN	PRECIPITATION MM RAIN	CM SNOW	MM TOTAL	WIND-SPEED KM/HR AVE	SUN-SHINE HR
1	3.3	-3.9	-0.3				4.6	2.4
2	10.6	-4.4	3.1				16.3	8.9
3	16.1	5.6	10.9	T		T	8.5	5.1
4	7.2	0.6	3.9				11.1	0.7
5	7.8	-0.6	3.6		2.5	2.5	7.7	6.3
6	1.7	-2.2	-0.3		0.5	0.5	8.8	0.0
7	5.6	-4.4	0.6				10.0	0.0
8	7.8	3.3	5.6				7.0	0.1
9	22.2	2.8	12.5				6.3	9.0
10	21.7	3.3	12.5				5.9	8.7
11	7.8	4.4	6.1				8.5	0.6
12	10.6	-5.6	2.5				6.6	8.4
13	12.2	3.3	7.8				12.1	1.6
14	2.2	0.6	1.4	0.3	3.0	3.3	12.8	0.0
15	3.3	-1.1	1.1	2.3	0.5	2.8	5.7	0.0
16	14.4	-1.1	6.7	0.5		0.5	13.8	4.4
17	2.2	-1.7	0.3	T	T	T	4.4	0.2
18	5.6	-1.1	2.3				4.4	3.0
19	7.2	-2.2	2.5				3.7	9.3
20	12.2	-2.8	4.7				14.3	9.0
21	14.4	3.9	9.2				11.9	9.1
22	8.9	-0.6	4.2				9.2	8.3
23	14.4	-0.6	6.9				8.6	9.1
24	12.2	4.4	8.3				14.9	7.8
25	13.9	-3.3	5.3				3.6	8.2
26	19.4	0.0	9.7				5.4	9.4
27	19.4	0.6	10.0				4.0	8.4
28	15.6	0.0	7.8				1.9	5.8
29	13.3	0.0	6.7				3.8	4.0
30	12.2	7.2	9.7	0.3		0.3	1.9	0.0
31	5.0	-0.6	2.2				9.3	0.0
MEAN	10.7	0.1	5.4	TOTAL 3.4	TOTAL 6.5	TOTAL 9.9	8.0	TOTAL 147.8
NORMAL WINNIPEG	11.9	1.1	6.5	29.2	5.6	34.8		158.0

MONTHLY METEOROLOGICAL SUMMARY, NOVEMBER 1974

DATE	TEMPERATURE C			PRECIPITATION			WIND-SPEED KM/HR	SUN-SHINE HR
				MM	CM	MM		
	MAX	MIN	MEAN	RAIN	SNOW	TOTAL	AVE	
1	2.2	-3.3	-0.6	3.6		3.6	11.4	2.6
2	0.6	-2.2	-0.8		0.8	0.8	7.9	0.0
3	-2.2	-3.9	-3.1		2.8	2.8	7.4	0.0
4	1.1	-3.9	-1.4				2.5	0.0
5	1.1	-2.8	-0.9				7.7	2.4
6	8.9	-2.2	3.4				8.4	7.8
7	11.1	0.6	5.9				4.6	3.6
8	11.7	2.2	7.0				11.1	1.1
9	6.7	0.0	3.4				9.0	8.7
10	5.6	-6.7	-0.6				8.9	4.9
11	2.8	-6.1	-1.7		T	T	12.3	2.1
12	-3.9	-6.1	-5.0		T	T	12.9	0.2
13	-4.4	-7.2	-5.8		4.1	4.1	15.2	0.4
14	-2.2	-7.2	-4.7		0.8	0.8	18.0	0.9
15	-1.7	-11.7	-6.7				2.6	7.3
16	1.7	-6.1	-2.2				6.6	6.2
17	3.3	-3.3	0.0				10.9	6.4
18	0.6	-12.2	-5.8	0.3	0.3	0.6	4.7	5.8
19	-1.1	-2.2	-1.7		4.3	4.3	10.3	0.0
20	-3.9	-8.3	-6.1				7.9	3.0
21	-1.1	-6.7	-3.9	T			15.3	0.0
22	0.0	-2.8	-1.4	T	T	T	9.7	6.8
23	-5.0	-7.2	-6.1				5.6	2.0
24	-6.7	-15.6	-11.2		T	T	6.1	0.0
25	-3.9	-18.9	-11.4		T	T	14.1	0.0
26	-0.6	-6.1	-3.4		1.8	1.8	9.7	0.0
27	-6.1	-8.3	-7.2		0.5	0.5	11.1	0.0
28	-6.1	-7.2	-6.7		0.5	0.5	9.5	5.3
29	-5.6	-10.0	-7.8		T	T	2.7	4.3
30	-7.2	-17.8	-12.5				3.3	7.6
				TOTAL	TOTAL	TOTAL		TOTAL
MEAN	-0.1	-6.4	-3.3	3.9	15.9	19.8	8.9	89.4
NORMAL WINNIPEG	-0.5	-8.3	-4.4	7.1	21.3	28.4		81.0

MONTHLY METEOROLOGICAL SUMMARY, DECEMBER 1974

DATE	TEMPERATURE C MAX	TEMPERATURE C MIN	TEMPERATURE C MEAN	PRECIPITATION MM RAIN	PRECIPITATION CM SNOW	PRECIPITATION MM TOTAL	WIND-SPEED KM/HR AVE	SUN-SHINE HR
1	-1.1	-13.9	-7.5		T	T	8.9	7.6
2	-5.0	-8.9	-7.0		T	T	5.9	0.8
3	-5.0	-12.8	-8.9		T	T	10.7	0.0
4	-3.9	-6.7	-5.3				3.8	0.0
5	-2.8	-5.0	-3.9				8.5	0.0
6	0.0	-5.0	-2.5				3.9	5.0
7	-15.0	-16.7	-15.9				14.7	2.6
8	-8.3	-22.2	-15.3				10.9	6.1
9	1.7	-12.2	-5.3				12.9	0.4
10	2.2	-6.7	-2.3		0.3	0.3	5.2	7.1
11	-6.7	-9.4	-8.1		T	T	6.6	0.0
12	-10.6	-20.6	-15.6				2.1	7.2
13	-6.1	-20.6	-13.4				0.2	3.9
14	-3.3	-13.3	-8.3		0.5	0.5	2.5	0.0
15	-3.3	-4.4	-3.9		1.5	1.5	3.4	0.0
16	-9.4	-11.1	-10.3		T	T	10.1	0.0
17	-10.0	-20.6	-15.3		0.8	0.8	2.5	5.9
18	-8.3	-17.2	-12.8		2.3	2.3	6.2	0.0
19	-7.8	-13.9	-10.9		T	T	1.8	0.0
20	-8.3	-11.7	-10.0		0.3	0.3	1.3	1.1
21	-9.4	-16.1	-12.8				5.3	0.0
22	-7.2	-12.8	-10.0		3.0	3.0	15.4	0.0
23	-7.2	-8.3	-7.8		T	T	11.3	0.0
24	-7.8	-17.8	-12.8				2.9	5.3
25	-6.1	-16.1	-11.1				9.5	7.3
26	1.7	-10.6	-4.5				8.8	3.7
27	3.3	-10.6	-3.7				10.3	3.0
28	1.7	-6.1	-2.2				10.6	1.4
29	-6.1	-15.0	-10.6				3.9	7.5
30	-2.2	-12.8	-7.5				6.8	7.3
31	-4.4	-9.4	-6.9				7.6	2.8
MEAN	-5.0	-12.5	-8.8	TOTAL 0.0	TOTAL 8.7	TOTAL 8.7	6.9	TOTAL 86.0
NORMAL WINNIPEG	-9.2	-18.2	-13.7	0.8	23.9	24.7		86.0

MONTHLY METEOROLOGICAL SUMMARY, JANUARY 1975

DATE	TEMPERATURE C MAX	MIN	MEAN	PRECIPITATION RAIN MM	SNOW CM	TOTAL MM	WIND-SPEED KM/HR AVE	SUN-SHINE HR
1	-5.0	-19.4	-12.2				7.9	7.5
2	-1.7	-8.9	-5.3		0.5	0.5	12.1	5.0
3	-7.8	-9.4	-8.6		0.3	0.3	8.8	0.0
4	-6.7	-10.0	-8.4				2.5	0.4
5	-7.8	-10.0	-8.9		0.3	0.3	3.0	0.0
6	-6.7	-12.8	-9.8		T	T	3.2	0.0
7	-4.4	-7.8	-6.1		T	T	4.8	0.0
8	-5.6	-7.2	-6.4		0.3	0.3	5.6	0.0
9	-2.8	-8.9	-5.9		4.8	4.8	10.3	0.0
10	-1.7	-3.9	-2.8		4.6	4.6	8.8	0.0
11	-21.1	-23.9	-22.5		5.6	5.6	32.8	0.0
12	-23.3	-24.4	-23.9				19.7	4.3
13	-18.9	-33.9	-26.4		0.3	0.3	4.4	7.7
14	-15.0	-23.9	-19.5		1.0	1.0	7.9	4.9
15	-16.7	-26.1	-21.4		0.5	0.5	4.5	3.4
16	-18.3	-38.3	-28.3		1.0	1.0	4.6	3.4
17	-3.9	-21.1	-12.5		1.0	1.0	9.9	3.8
18	-19.4	-21.1	-20.3		T	T	14.4	2.5
19	-23.3	-33.9	-28.6		2.8	2.8	9.9	5.5
20	-6.1	-22.2	-14.2		1.0	1.0	11.1	0.2
21	-18.9	-30.6	-24.8		0.5	0.5	9.1	8.0
22	-11.7	-32.2	-22.0		T	T	10.3	1.7
23	-4.4	-21.1	-12.8		3.3	3.3	3.7	0.0
24	-3.9	-8.9	-6.4		13.0	13.0	11.4	0.0
25	-10.0	-12.8	-11.4		0.8	0.8	10.1	0.0
26	-16.1	-23.9	-20.0				4.5	4.7
27	-15.6	-27.8	-21.7		T	T	3.4	8.2
28	-12.2	-24.4	-18.3				3.9	5.1
29	-18.9	-24.4	-21.7				5.4	7.6
30	-16.7	-36.1	-26.4				1.6	6.9
31	-15.6	-30.6	-23.1				2.8	7.4
				TOTAL	TOTAL	TOTAL		TOTAL
MEAN	-11.6	-20.6	-16.1	0.0	41.6	41.6	8.1	98.2
NORMAL WINNIPEG	-13.4	-23.2	-18.3	0.3	24.9	25.2		112.0

MONTHLY METEOROLOGICAL SUMMARY, FEBRUARY 1975

DATE	TEMPERATURE C			PRECIPITATION			WIND-SPEED KM/HR	SUN-SHINE HR
				MM	CM	MM		
	MAX	MIN	MEAN	RAIN	SNOW	TOTAL	AVE	
1	-16.7	-34.4	-25.6				0.9	7.9
2	-12.8	-27.2	-20.0				2.0	7.9
3	-3.9	-21.1	-12.5		2.8	2.8	9.4	0.0
4	-15.0	-16.1	-15.6		T	T	12.0	0.0
5	-16.7	-28.3	-22.5		0.3	0.3	6.9	7.7
6	-15.6	-21.7	-18.7		0.5	0.5	10.1	4.7
7	-20.0	-25.0	-22.5				11.2	8.1
8	-25.0	-33.3	-29.2				8.1	8.6
9	-17.8	-35.0	-26.4				5.0	0.0
10	-15.0	-32.8	-23.9		1.5	1.5	3.2	1.1
11	-13.9	-22.8	-18.4		2.3	2.3	6.7	1.8
12	-23.3	-30.6	-27.0				8.9	9.0
13	-15.6	-37.2	-26.4		2.8	2.8	1.2	1.0
14	-12.2	-19.4	-15.8		0.5	0.5	1.3	0.0
15	-10.6	-18.3	-14.5				1.9	0.0
16	-6.7	-23.3	-15.0		0.3	0.3	8.4	9.3
17	-3.9	-15.6	-9.8			2.8	2.7	0.5
18	-1.7	-27.2	-14.5				2.6	9.2
19	1.7	-17.8	-8.1				6.2	2.1
20	5.6	-13.3	-3.9				8.3	9.3
21	5.0	-6.7	-0.9		4.3	4.3	9.6	6.3
22	-6.1	-9.4	-7.8				13.7	3.8
23	-2.2	-26.7	-14.5				2.4	8.0
24	4.4	-12.8	-4.2		2.3	2.3	14.1	5.1
25	-4.4	-7.8	-6.1		T	T	25.4	2.4
26	-7.8	-13.9	-10.9		T	T	12.6	4.4
27	-8.3	-26.1	-17.2				4.8	7.3
28	-11.7	-27.2	-19.5		2.3	2.3	6.6	10.0
MEAN	-9.6	-22.5	-16.1	TOTAL 0.0	TOTAL 22.7	TOTAL 22.7	7.4	TOTAL 135.5
NORMAL WINNIPEG	-10.4	-21.1	-15.8	0.8	19.8	20.6		139.0

MONTHLY METEOROLOGICAL SUMMARY, MARCH 1975

DATE	TEMPERATURE C			PRECIPITATION			WIND-SPEED KM/HR	SUN-SHINE HR
	MAX	MIN	MEAN	MM RAIN	CM SNOW	MM TOTAL	AVE	
1	-10.0	-18.9	-14.5	0.3		0.3	11.5	0.0
2	-11.7	-17.8	-14.8				4.3	8.1
3	-7.2	-27.8	-17.5				1.3	8.0
4	-6.7	-16.7	-11.7		1.3	1.3	6.9	0.0
5	-1.7	-8.9	-5.3		0.3	0.3	4.3	6.6
6	-4.4	-12.8	-8.6		0.3	0.3	3.2	6.6
7	-8.3	-14.4	-11.4				8.2	9.6
8	-11.1	-28.3	-19.7				2.9	9.4
9	-11.1	-32.8	-22.0				4.5	9.5
10	-10.0	-29.4	-19.7				2.3	8.2
11	-5.0	-23.9	-14.5		0.8	0.8	8.5	3.1
12	-11.7	-16.7	-14.2				12.0	8.4
13	-2.8	-25.6	-14.2				11.3	9.4
14	1.1	-13.3	-6.1		0.8	0.8	5.2	9.5
15	4.4	-9.4	-2.5				6.6	8.9
16	7.8	-9.4	-0.8				13.3	7.4
17	3.9	1.1	2.5	4.3	T	4.3	15.0	0.0
18	3.3	0.0	1.7				7.7	4.2
19	2.2	-7.8	-2.8				8.3	3.3
20	3.3	-10.0	-3.4	1.5	T	1.5	8.0	0.8
21	1.1	-3.9	-1.4	0.3	1.5	1.8	14.5	0.0
22	-2.8	-9.4	-6.1				12.4	3.9
23	-5.0	-15.6	-10.3				18.9	8.3
24	-7.8	-15.6	-11.7				22.5	6.0
25	-6.7	-18.3	-12.5				9.1	9.2
26	-4.4	-17.2	-10.8		9.7	9.7	14.7	0.3
27	-2.8	-7.2	-5.0		10.4	10.4	14.2	0.0
28	-1.7	-5.6	-3.7		6.9	6.9	12.9	0.0
29	-13.9	-17.8	-15.9				16.3	5.2
30	-13.9	-26.1	-20.0				5.5	10.4
31	-11.7	-30.0	-20.9				6.0	9.9
				TOTAL	TOTAL	TOTAL		TOTAL
MEAN	-4.7	-15.8	-10.2	6.4	32.0	38.4	9.4	174.2
NORMAL WINNIPEG	-2.9	-13.3	-8.1	6.1	21.1	27.2		170.0

MONTHLY METEOROLOGICAL SUMMARY, APRIL 1975

DATE	TEMPERATURE C MAX	MIN	MEAN	PRECIPITATION MM RAIN	CM SNOW	MM TOTAL	WIND-SPEED KM/HR AVE	SUN-SHINE HR
1	-7.8	-26.1	-17.0				5.2	10.5
2	-5.0	-27.8	-16.4				3.2	10.8
3	-3.9	-27.8	-15.9				3.2	10.4
4	-1.1	-19.4	-10.3				9.0	7.4
5	2.2	-7.8	-2.8				20.1	4.8
6	2.8	-3.3	-0.3	T	T	T	16.2	1.6
7	6.7	-1.1	2.8				18.0	2.3
8	7.8	-2.8	2.5				18.9	7.2
9	8.3	-3.9	2.2				6.2	10.5
10	8.3	-9.4	0.5				3.4	11.8
11	9.4	-9.4	0.0				1.9	9.3
12	10.0	-4.4	2.8				2.8	12.4
13	12.2	-5.6	3.3	T	T	T	3.3	11.7
14	11.1	0.0	5.6	5.1		5.1	2.5	3.7
15	6.7	1.7	4.2	6.1		6.1	0.3	0.2
16	8.3	1.7	5.0	1.5		1.5	2.3	0.7
17	5.6	2.2	3.9	1.8		1.8	6.2	0.0
18	3.3	0.0	1.7	4.6	4.6	9.2	11.3	0.0
19	-0.6	-3.3	-2.0				15.8	0.0
20	5.0	-2.2	1.4	0.8		0.8	3.1	7.4
21	11.1	-2.2	4.5				8.9	10.1
22	14.4	-0.6	6.9				8.7	4.6
23	14.4	-1.1	6.7				4.5	8.2
24	12.8	-1.1	5.9				7.3	4.8
25	15.0	3.9	9.5				10.2	9.0
26	8.3	3.3	5.8	3.3			15.0	0.0
27	11.1	3.9	7.5	0.5			19.7	0.3
28	15.0	6.7	10.9				23.2	1.9
29	11.7	2.2	7.0	0.5	0.3	0.8	18.2	11.3
30	4.4	-0.6	1.9	2.0	0.3	2.3	8.9	0.0
				TOTAL	TOTAL	TOTAL		TOTAL
MEAN	6.9	-4.5	1.2	26.2	5.2	31.4	9.2	172.9
NORMAL WINNIPEG	8.6	-1.9	3.4	25.4	11.9	37.3		209.0

MONTHLY METEOROLOGICAL SUMMARY, MAY 1975

DATE	TEMPERATURE C			PRECIPITATION MM	CM	MM	WIND-SPEED KM/HR	SUN-SHINE HR
	MAX	MIN	MEAN	RAIN	SNOW	TOTAL	AVE	
1	5.0	0.0	2.5	1.5	T	1.5	6.4	0.0
2	9.4	1.7	5.6	2.5		2.5	6.4	2.3
3	11.1	1.7	6.4	0.5		0.5	3.5	4.4
4	13.3	-1.7	5.8				5.2	2.0
5	15.6	-1.1	7.3				10.8	12.0
6	20.0	3.9	12.0				15.5	13.5
7	20.6	6.7	13.7				14.8	12.1
8	21.7	2.8	12.3				5.3	12.0
9	23.9	1.1	12.5				3.8	12.3
10	23.3	2.2	12.8				7.6	9.2
11	14.4	2.8	8.6				7.9	14.2
12	21.7	-3.3	9.2				7.1	12.5
13	24.4	9.4	16.9	13.5		13.5	7.6	6.2
14	10.0	2.8	6.4	0.5		0.5	12.5	4.9
15	20.0	-1.7	9.2				3.9	11.5
16	24.4	5.6	15.0	1.8		1.8	12.4	6.9
17	18.9	7.8	13.4	4.8		4.8	9.3	5.2
18	22.2	7.8	15.0	2.5		2.5	8.7	12.1
19	24.4	10.6	17.5	T		T	9.1	10.3
20	15.6	11.1	13.4	0.5		0.5	11.4	0.3
21	10.6	4.4	7.5	T		T	11.9	6.9
22	16.7	3.3	10.0	2.8		2.8	6.3	7.3
23	21.1	10.6	15.9	27.2		27.2	10.2	0.4
24	23.3	12.2	17.8				10.7	11.1
25	20.0	14.4	17.2				9.3	9.9
26	16.1	8.3	12.2	0.5		0.5	10.7	13.1
27	18.9	6.1	12.5	6.4		6.4	5.4	4.7
28	20.0	2.2	11.1	0.5		0.5	3.8	10.1
29	13.9	3.3	8.6	0.3		0.3	9.9	7.3
30	12.2	5.0	8.6	3.6		3.6	8.9	2.2
31	15.6	3.3	9.5	0.8		0.8	7.1	7.8
MEAN	17.7	4.6	11.2	TOTAL 70.2	TOTAL 0.0	TOTAL 70.2	8.5	TOTAL 244.7
NORMAL WINNIPEG	17.1	4.1	10.6	54.6	2.5	57.1		246.0

MONTHLY METEOROLOGICAL SUMMARY, JUNF 1975

DATE	TEMPERATURE C MAX	MIN	MEAN	PRECIPITATION MM RAIN	CM SNOW	MM TOTAL	WIND-SPEED KM/HR AVE	SUN-SHINE HR
1	16.7	1.1	8.9				7.4	7.1
2	19.4	2.8	11.1	T		T	6.9	7.3
3	15.6	7.8	11.7				10.1	9.3
4	16.1	6.1	11.1	14.2		14.2	9.1	0.1
5	10.6	8.3	9.5	0.8		0.8	21.7	0.8
6	13.3	6.1	9.7	0.3		0.3	8.3	2.0
7	20.0	0.0	10.0				2.4	11.6
8	22.2	8.3	15.3	0.3		0.3	4.8	4.8
9	16.1	10.6	13.4	12.4		12.4	6.3	0.0
10	17.2	11.1	14.2	33.5		33.5	5.4	0.3
11	20.0	7.8	13.9				2.5	5.0
12	24.4	8.3	16.4				4.4	13.0
13	20.0	12.2	16.1				9.0	6.3
14	17.2	5.6	11.4				6.8	7.6
15	19.4	2.8	11.1				3.3	12.7
16	21.1	4.4	12.8				3.7	13.9
17	21.1	6.7	13.9				5.2	15.1
18	23.9	5.6	14.8				2.4	11.6
19	24.4	11.1	17.8	3.0		3.0	11.8	4.6
20	28.9	15.6	22.3	25.4		25.4	15.0	8.4
21	26.7	16.1	21.4	15.0		15.0	6.7	8.4
22	17.2	15.6	16.4	73.4		73.4	11.5	0.0
23	25.0	12.2	18.6				5.5	14.0
24	28.9	11.1	20.0	1.0		1.0	5.9	11.3
25	30.0	17.8	23.9				15.6	14.2
26	28.3	20.6	24.5	4.3		4.3	16.0	9.7
27	27.8	12.8	20.3				10.0	15.4
28	27.2	16.7	22.0	2.0		2.0	12.8	5.5
29	27.2	16.7	22.0	6.9		6.9	5.4	7.6
30	26.7	17.2	22.0				5.6	6.7
				TOTAL	TOTAL	TOTAL		TOTAL
MEAN	21.8	10.0	15.9	192.5	0.0	192.5	8.0	234.3
NORMAL WINNIPEG	22.7	10.3	16.5	80.3	0.0	80.3		259.0

MONTHLY METEOROLOGICAL SUMMARY, JULY 1975

DATE	TEMPERATURE C			PRECIPITATION			WIND-SPEED KM/HR	SUN-SHINE HR
	MAX	MIN	MEAN	MM RAIN	CM SNOW	MM TOTAL	AVE	
1	27.2	12.8	20.0				2.1	11.1
2	27.8	13.9	20.9				4.5	14.5
3	28.9	12.2	20.6				3.1	13.9
4	30.6	13.3	22.0				1.4	15.0
5	29.4	16.1	22.8				7.5	13.0
6	27.2	17.2	22.2	0.3		0.3	5.4	11.6
7	26.7	13.9	20.3				10.3	11.8
8	20.0	11.1	15.6				13.7	6.4
9	17.8	8.9	13.4				13.5	14.1
10	20.6	8.9	14.8				11.1	13.8
11	18.9	10.0	14.5				7.5	14.1
12	27.8	8.9	18.4	1.0		1.0	5.1	4.3
13	29.4	14.4	21.9				2.4	8.4
14	31.7	18.9	25.3				3.8	13.4
15	32.8	18.3	25.6	0.5		0.5	5.6	13.9
16	33.9	18.3	26.1	1.8		1.8	4.2	6.3
17	30.0	20.6	25.3	1.8		1.8	5.2	8.3
18	25.6	16.1	20.9	2.0		2.0	7.3	8.4
19	22.2	15.0	18.6	6.1		6.1	12.9	8.3
20	21.1	10.6	15.9	3.0		3.0	6.7	4.2
21	25.6	15.6	20.6				9.7	14.4
22	22.2	10.6	16.4	0.5		0.5	1.6	2.2
23	22.8	16.1	19.5	8.9		8.9	8.8	6.0
24	23.3	13.3	18.3				9.2	11.7
25	28.3	14.4	21.4	0.8		0.8	9.9	13.4
26	25.6	17.8	21.7				17.4	11.5
27	26.7	14.4	20.6				8.8	14.5
28	32.8	15.0	23.9				10.2	10.0
29	33.3	18.9	26.1				5.2	11.4
30	35.0	22.2	28.6				13.6	13.9
31	29.4	23.3	26.4	3.3		3.3	8.4	4.9
MEAN	26.9	14.9	20.9	TOTAL 30.0	TOTAL 0.0	TOTAL 30.0	7.6	TOTAL 328.7
NORMAL WINNIPEG	25.9	13.5	19.7	80.3	0.0	80.3		311.0

MONTHLY METEOROLOGICAL SUMMARY, AUGUST 1975

DATE	TEMPERATURE C			PRECIPITATION			WIND-SPEED KM/HR	SUN-SHINE HR
	MAX	MIN	MEAN	MM RAIN	CM SNOW	MM TOTAL	AVE	
1	24.4	20.6	22.5				6.1	0.6
2	20.0	13.3	16.7				10.0	4.9
3	23.9	8.9	16.4	4.8		4.8	8.8	3.6
4	20.0	8.3	14.2	1.3		1.3	4.9	9.5
5	22.2	6.1	14.2				4.7	13.4
6	25.0	8.9	17.0	T		T	13.1	13.8
7	26.1	18.9	22.5	25.4		25.4	8.9	3.9
8	22.1	17.2	19.7	1.0		1.0	15.3	8.0
9	22.8	11.1	17.0	2.5		2.5	10.3	10.8
10	23.3	12.8	18.1	8.4		8.4	7.8	12.0
11	24.4	12.8	18.6	0.8		0.8	2.7	11.8
12	22.8	13.9	18.4	0.5		0.5	10.3	9.5
13	22.8	12.2	17.5	3.3		3.3	11.9	12.2
14	16.1	13.9	15.0	0.3		0.3	2.9	1.6
15	21.1	2.8	12.0	1.3		1.3	5.0	12.1
16	16.7	7.2	12.0	1.5		1.5	15.0	10.1
17	16.7	8.3	12.5				10.7	9.9
18	18.3	1.7	10.0				2.2	7.0
19	19.4	3.9	11.7				4.4	6.3
20	18.9	8.9	13.9	17.0		17.0	7.9	2.9
21	17.2	12.2	14.7	0.3		0.3	6.2	0.4
22	20.6	5.6	13.1	21.6		21.6	9.9	5.0
23	28.3	15.0	21.7				8.4	6.9
24	26.7	16.1	21.4	1.0		1.0	9.1	6.7
25	17.8	11.1	14.5	5.6		5.6	14.8	4.2
26	15.6	9.4	12.5	2.0		2.0	8.8	2.3
27	14.4	6.1	10.3	T		T	6.7	2.2
28	23.9	10.6	17.3				12.3	8.9
29	19.4	13.3	16.4				13.1	4.2
30	24.4	15.0	19.7				12.1	9.3
31	23.9	16.1	20.0				6.5	4.7
				TOTAL	TOTAL	TOTAL		TOTAL
MEAN	21.3	11.0	16.2	110.3	0.0	110.3	8.7	218.7
NORMAL WINNIPEG	25.0	12.2	18.6	73.7	0.0	73.7		276.0

MONTHLY METEOROLOGICAL SUMMARY, SEPTEMBER 1975

DATE	TEMPERATURE C			PRECIPITATION			WIND-SPEED KM/HR	SUN-SHINE HR
				MM	CM	MM		
	MAX	MIN	MEAN	RAIN	SNOW	TOTAL	AVE	
1	15.6	11.7	13.7				11.8	6.9
2	16.1	2.8	9.5	4.6		4.6	11.4	4.0
3	16.7	8.3	12.5				12.8	5.3
4	20.0	6.7	13.4	T		T	8.0	7.4
5	14.4	7.8	11.1	6.1		6.1	6.2	0.9
6	11.7	4.4	8.1	27.2		27.2	7.6	0.0
7	14.4	8.9	11.7				8.7	4.7
8	16.7	0.0	8.4				6.7	10.5
9	20.0	8.3	14.2	0.3		0.3	9.4	8.4
10	15.0	8.3	11.7	0.8		0.8	11.2	0.0
11	7.8	3.3	5.6	5.3	0.3	5.6	11.4	2.2
12	7.2	1.1	4.2	0.3	T	0.3	9.8	0.1
13	11.1	-5.0	3.1				6.7	7.6
14	26.1	3.9	15.0				8.5	10.0
15	12.2	6.1	9.2				7.6	9.2
16	17.8	2.2	10.0	T		T	8.6	10.0
17	22.2	11.7	17.0	1.0		1.0	18.9	8.8
18	17.2	12.2	14.7	8.6		8.6	12.2	0.0
19	13.3	5.6	9.5	2.5		2.5	9.6	0.4
20	6.1	5.0	5.6	0.5		0.5	14.1	0.6
21	14.4	0.6	7.5	0.3		0.3	9.2	3.8
22	17.8	5.0	11.4				8.1	2.9
23	13.9	3.9	8.9				7.2	8.6
24	18.9	-0.6	9.2				8.2	9.6
25	22.2	6.1	14.2				12.6	9.4
26	22.8	6.1	14.5				10.9	9.2
27	22.8	5.1	14.0				4.2	8.7
28	15.0	7.8	11.4				3.0	1.0
29	16.1	4.4	10.3	1.5		1.5	7.8	1.1
30	7.8	1.7	4.8	1.0		1.0	17.0	4.4
MEAN	15.8	5.1	10.4	TOTAL 60.0	TOTAL 0.3	TOTAL 60.3	9.6	TOTAL 155.7
NORMAL WINNIPEG	18.4	6.6	12.5	52.6	0.3	52.9		183.0

APPENDIX C

Program Documentation for Soil Water and Temperature Simulation Model

```
CC     HEAT AND WATER TRANSFER MODEL
       COMMON/EVAPDY/WIND(155),TMAX(155),TMIN(155),RH(155),RNM(155),
      1PLATE(155),SUNS(155),DAYL(155),RSTOP(155),NDAY(155),RS00(155),
      1TRANS,ROOTD(10),TDENS,DAILYT(10),JT
       COMMON/FIELDC/WFLUX(10),SINK(10),      PPT(3720),TIM,SINKT,ACCDR
       COMMON/SURALL/PWP(10),FC(10),THICKN(10),TMTOT,TRANSN(10),M,XW(10),
      1XWN(10),LA,P(10),PET,PE,AE,AT
       COMMON/BASIC/AW(10)          ,BD(10),XMIN(10),XSIO2(10),XORG(10),XSOL(
      110),COND(10),CONST(10)
       COMMON/VAP/VFLUX(10),TC(10),DFLZ(10)
       COMMON/PRIN/ACCPET,ACCPE,ACCPT,ACCAET,ACCAE,ACCAT
       COMMON/PRIND/DVFLUX(10),DWFLUX(10),DELT,DNADD(10),ZDCOND(10),ZDCON
      1V(10),ZDVAP(10),ZDVLU(10),UPV(10),DOV(10),DSINK(10),ACSINK(10),ACW
      1ATR(10),ACVAPR(10),ACUPV(10),ACDOV(10),DCOND(10),DCONV(10),DVAP(10
      1)
       INTEGER IPPT(24),TMTOT,TIM,IDD(155),DFLT
       REAL W(10),T(10),TCN(10),LHEAT,NVFLUX(10),NCOND(10)
       REAL C(10),Z(10),WSAT(10),ORG(10),SIO2(10),NCONT(10)
       REAL DNCOND(10),DNCONV(10),DNVAP(10),DNVFLU(10),CO(10)
       ACCUM=0.0
       ACCDR=0.0
       PET=0.0
       PF=0.0
       TRANS=0.0
       AE=0.0
       AT=0.0
       ACCPET=0.0
       ACCPF=0.0
       ACCPT=0.0
       ACCAET=0.0
       ACCAE=0.0
       ACCAT=0.0
 C  READ NUMBER OF NODES AND DELTA TIME.
       READ (5,801) M,DELT
       WRITE (6,801) M,DELT
 801   FORMAT (1X,I2,1X,I3)
       JT=3600/DELT
       READ (5,811)   (THICKN(I),I=1,9)
       WRITE(6,811)   (THICKN(I),I=1,9)
 811   FORMAT (9(1X,F4.1))
       READ (5,810)   (ROOTD(I),I=1,9),TDENS
       WRITE(6,810)   (ROOTD(I),I=1,9),TDENS
 810   FORMAT (5X,10(1X,F4.2))
       DO 1  J=1,M
       READ (5,800) Z(J),BD(J),WSAT(J),PWP(J),ORG(J),SIO2(J),CONST(J),FC(
      1J)
       WRITE(6,800) Z(J),BD(J),WSAT(J),PWP(J),ORG(J),SIO2(J),CONST(J),FC(
      1J)
 800   FORMAT (12X,F5.1,1X,F4.2,1X,F5.3,5(1X,F6.4))
 C  CALCULATE VOLUME FRACTIONS.
       PWP(J)=BD(J)*PWP(J)
       P(J)=BD(J)*WSAT(J)
       FC(J)=BD(J)*FC(J)
       RATIO=(ORG(J)/1.3)/((1.0-ORG(J))/2.65)
       XSOL(J)=(1.0-P(J))-XORG(J)
       XORG(J)=(RATIO/(1.0+RATIO))*(1.0-P(J))
       XSIO2(J)=SIO2(J)*XSOL(J)
       XMIN(J)=XSOL(J)-XSIO2(J)
       DAILYT(J)=0.0
       DWFLUX(J)=0.0
       DVFLUX(J)=0.0
       UPV(J)=0.0
       DOV(J)=0.0
       ZDCOND(J)=0.0
       ZDCONV(J)=0.0
       ZDVAP(J)=0.0
       ZDVLU(J)=0.0
       DNADD(J)=0.0
       DSINK(J)=0.0
       ACSINK(J)=0.0
       ACWATR(J)=0.0
       ACVAPR(J)=0.0
       ACUPV(J)=0.0
       ACDOV(J)=0.0
       DCOND(J)=0.0
       DCONV(J)=0.0
       DVAP(J)=0.0
 1     CONTINUE
 C  READ FISCHER AND PORTER PRECIPITATION DATA.
       L=0
 11    READ (5,804) IDP,(IPPT(I),I=1,24)
       WRITE (6,500) IDP,(IPPT(I),I=1,24)
 804   FORMAT (I2,5X,24I1)
 500   FORMAT ('0',2X,I3,24(1X,I4))
       IF(IDP.EQ.99) GOTO 9
       DO 10  I=1,24
       PPT(L+I)=(IPPT(I)/10.0)*(2.540/3600.0)
 10    CONTINUE
       L=L+24
       GOTO 11
 C  READ INITIAL WATER CONTENT PROFILE.
 9     READ (5,805) IDW,(W(I),I=1,8)
 805   FORMAT (I2,11X,8(4X,F4.1))
       WRITE (6,501) IDW,(W(I),I=1,9)
 501   FORMAT ('0',2X,I3,9(4X,F6.2))
       DO 13  J=1,6
       W(10-J)=W(9-J)
 13    CONTINUE
       W(4)=(W(3)+W(5))/2.0
       WRITE (6,661) IDW,(W(I),I=1,10)
 661   FORMAT (2X,I3,10(4X,F6.2))
 C  READ THE DAILY DATA.
       L=1
 15    READ (5,806) IDD(L),TMAX(L),TMIN(L),SUNS(L),WIND(L),DAYL(L),RSTOP(
      1L),RNM(L),PLATE(L),NDAY(L),RS00(L),RH(L)
 806   FORMAT (I2,4X,2F4.1,F3.1,F4.2,4X,F3.1,F5.1,F6.5,F5.2,I3,3X   ,F4.1,
      1F4.1)
       RS00(L)=RSTOP(L)*(0.251+0.616*(SUNS(L)/DAYL(L)))
       A1=0.50187-0.0020752*NDAY(L)+0.00000483*(NDAY(L)*NDAY(L))
       B1=0.35526+0.0032518*NDAY(L)-0.00000796*(NDAY(L)*NDAY(L))
       RSURDC=RS00(L)*(A1+B1*(SUNS(L)/DAYL(L)))
       RSURDC=RSURDC/1440.0
       RLNLI=0.00032*(1.0+4.0*(SUNS(L)/DAYL(L)))*(100.0-((TMAX(L)+TMIN(L)
      1)/2.0))
       IF(IDD(L).EQ.99) GOTO 14
       L=L+1
```

```
      GOTO 15
14    II=M-1
      DO 16  I=1,II
      DELZ(I)=Z(I+1)-Z(I)
16    CONTINUE
      LA=0
      L=1
C  INITIAL TEMPERATURE PROFILE.
      READ (5,807) IDTT,IM,IY,TIM,(T(I),I=1,M)
807   FORMAT (4I2,17X,9(1X,F4.1))
      WRITE (6,503) IDTT,IM,IY,TIM,(T(I),I=1,M)
503   FORMAT ('0',2X,4I3,9(2X,F6.2))
      STORE1=T(1)
      STORE2=T(M)
      LA=LA+1
      IF(LA.NE.1) GOTO 17
      DO 18  J=1,M
      TC(J)=T(J)
      XW(J)=(W(J)/100.0)*BD(J)
18    CONTINUE
      CALL DAILY(L)
      LA=LA-24
17    READ (5,807) IDTT,IM,IY,TIM,(T(I),I=1,M)
      IF(IDTT.EQ.99) STOP
      IF(TIM.EQ.0) L=L+1
      IF(TIM.EQ.0) CALL DAILY (L)
C  LOOP THRU THE HOUR AND DEPTH.
      DO 19  I=1,JT
      TMTOT=TMTOT+DELT
      CALL VAPOR
      CALL DIFF
      CALL WATER
      ACCUM=ACCUM+SINKT
      NVFLUX(1)=WFLUX(1)-VFLUX(2)
      DO 20  J=2,II
C  NET CONDUCTIVE HEAT FLUX.
      NCOND(J)=(COND(J)/DELZ(J-1))*(TC(J-1)-TC(J))-(COND(J+1)/DELZ(J))*(
     1TC(J)-TC(J+1))
C  NET CONVECTIVE HEAT FLUX IN LIQUID PHASE.
      DNCONV(J)=((WFLUX(J)/DELT)*(TC(J-1)+273.0))-((WFLUX(J+1)/DELT)*(TC
     1(J)+273.0))
C  NET CONVECTIVE HEAT FLUX IN VAPOUR PHASE.
      DNVAP(J)=(VFLUX(J)*((0.45*(TC(J-1)+273.0))+597.0))-(VFLUX(J+1)*((
     10.45*(TC(J)+273.0))+597.0))
C  VOLUMETRIC HEAT CAPACITY.
      CO(J)=0.46*XSOL(J)+0.6*XORG(J)+XW(J)
      C(J)=0.46*XSOL(J)+0.6*XORG(J)+XWN(J)
C  HEAT BALANCE EQUATION.
      TCN(J)=((DELT/THICKN(J))*(NCOND(J)+DNCONV(J)+DNVAP(J))+(CO(J)*TC(J
     1)))/C(J)
C  ADD COMPONENTS.
101   ZDCOND(J)=ZDCOND(J)+NCOND(J)
      ZDCONV(J)=ZDCONV(J)+DNCONV(J)
      ZDVAP(J)=ZDVAP(J)+DNVAP(J)
      DNADD(J)=DNADD(J)+ NCOND(J)+DNCONV(J)+DNVAP(J)
      DVFLUX(J)=DVFLUX(J)+VFLUX(J)*DELT
      DCOND(J)=DCOND(J)+(COND(J)/DELZ(J-1))*(TC(J-1)-TC(J))
      DCONV(J)=DCONV(J)+(WFLUX(J)/DELT)*TC(J-1)
      DVAP(J)=DVAP(J)+VFLUX(J)*(0.45*(TC(J-1)+273.0)+597.0)
      IF(VFLUX(J).GT.0.0) GOTO 50
      UPV(J)=UPV(J)+VFLUX(J)*DELT
      GOTO 20
50    DOV(J)=DOV(J)+VFLUX(J)*DELT
20    CONTINUE
      TCN(1)=TC(1)+(T(1)-STORE1)/JT
      TCN(M)=TC(M)+(T(M)-STORE2)/JT
      DO 21  J=1,M
      TC(J)=TCN(J)
      XW(J)=XWN(J)
      DAILYT(J)=DAILYT(J)+TCN(J)
21    CONTINUE
19    CONTINUE
      STORE1=TC(1)
      STORE2=TC(M)
      IF(IDTT.EQ.30) GOTO 23
      IF(TIM.LE.14.OR.TIM.GE.16) GOTO 22
23    WRITE (6,900) IDTT,IM,IY,TIM
      WRITE (6,901) (T(I),I=1,M)
      WRITE (6,902) (TCN(I),I=1,M)
      WRITE (6,903) (XWN(I),I=1,M)
900   FORMAT ('-',1X,4I4)
901   FORMAT ('0',4X,'TMEAS',9(7X,F5.1))
902   FORMAT ('0',4X,'TCN  ',9(7X,F5.1))
903   FORMAT ('0',4X,'XWN  ',9(6X,F6.4))
22    ACCUM=0.0
      GOTO 17
      END
```

```
      SUBROUTINE WATER
      COMMON/FIELDC/WFLUX(10),SINK(10),      PPT(3720),TIM,SINKT,ACCOR
      COMMON/SUBALL/PWP(10),FC(10),THICKN(10),TMTOT,TRANSN(10),M,XW(10),
     1XWN(10),LA,P(10),PET,PE,AE,AT
      COMMON/VAP/VFLUX(10),TC(10),DFLZ(10)
      COMMON/PRIND/DVFLUX(10),DWFLUX(10),DELT,DNADD(10),ZDCOND(10),ZDCON
     1V(10),ZDVAP(10),ZDVLU(10),UPV(10),DOV(10),DSINK(10),ACSINK(10),ACW
     1ATR(10),ACVAPR(10),ACUPV(10),ACDOV(10),DCOND(10),DCONV(10),DVAP(10
     1)
      INTEGER TMTOT,TIM,DELT
      DO 1  J=1,M
      WFLUX(J)=0.0
      SINK(J)=0.0
1     CONTINUE
      DO 11  J=2,M
      IF(VFLUX(J).EQ.0.0) GOTO 11
      IF(VFLUX(J).GT.0.0) GOTO 12
C   VAPOUR FLUX IS NEGATIVE,I.E. UPWARD
      XW(J-1)=((THICKN(J-1)*XW(J-1))+(VFLUX(J)*DELT))/THICKN(J-1)
      GOTO 11
C   VAPOUR FLUX IS POSITIVE, I.E. DOWNWARD.
12    XW(J)=((THICKN(J)*XW(J))+(VFLUX(J)*DELT))/THICKN(J)
11    CONTINUE
      SINKT=0.0
      RAIN     =DELT*PPT(LA+TIM-1)
      IF(TIM.LE.8.OR.TIM.GT.20) GOTO 2
C   CALCULATE ROOT UPTAKE AND EVAPORATION DURING DAYLIGHT HOURS.
      TNORM=(TMTOT-32400.0)/7200.0-2.75
      DO 4  J=1,M
      AVH20=(XW(J)-PWP(J))/(FC(J)-PWP(J))
      IF(AVH20.GT.0.793) AVH20=0.793
      IF(AVH20.LT.0.0) AVH20=0.0
      RTEMP=EXP(-((TC(J)-20.0)*(TC(J)-20.0))/100.0)
      IF(RTEMP.LT.0.03916) RTEMP=0.0
      SINK(J)=-EXP(-TNORM*TNORM/2.0)*1.0/60.0*TRANSN(J)*(0.10*EXP(3.00*A
     1VH20))*RTEMP
      IF(J.EQ.1) WFLUX(J)=-EXP(-TNORM*TNORM/2.0)*1.0/60.0*(0.10*EXP(3.00
     1*AVH20))*PE
      IF(J.EQ.1) AE=AE+WFLUX(J)
      SINKT=SINKT+SINK(J)
      AT=AT+SINK(J)
      DSINK(J)=DSINK(J)+SINK(J)
4     CONTINUE
2     J=1
      IF(RAIN.GT.0.0) AE=AE-WFLUX(1)
      IF(RAIN.GT.0.0) WFLUX(1)=RAIN
6     XWN(J)=((THICKN(J)*XW(J))+WFLUX(J)+SINK(J))/THICKN(J)
      IF(XWN(J).LT.FC(J)) GOTO 3
      WFLUX(J+1)=(XWN(J)-FC(J))*THICKN(J)
      XWN(J)=FC(J)
      J=J+1
      IF(J.EQ.M) GOTO 5
      GOTO 6
3     JPLUS1=J+1
      DO 7  I=JPLUS1,M
      XWN(I)=((THICKN(I)*XW(I))+SINK(I))/THICKN(I)
7     CONTINUE
C   APPLY FC MODEL BETWEEN FC AND SATN. AFTR PLANT UPTAKE.
      N=M
20    IF(XWN(N).GE.P(N)) GOTO 21
      IF(XWN(N-1).GT.FC(N-1)) GOTO 22
24    N=N-1
      IF(N.EQ.1) GOTO 23
      GOTO 20
21    WFLUX(N)=0.0
      GOTO 24
22    WFLUX(N)=  (XWN(N-1)-FC(N-1))*THICKN(N-1)
      XWN(N-1)=FC(N-1)
      XWN(N)=(THICKN(N)*XWN(N)+WFLUX(N))/THICKN(N)
      IF(XWN(N).GT.P(N)) GOTO 25
      GOTO 24
25    RFLUX=(P(N)-XWN(N))*THICKN(N)
      XWN(N)=P(N)
      WFLUX(N)=WFLUX(N)+RFLUX
      IF(WFLUX(N).LT.0.0) WFLUX(N)=0.0
      XWN(N-1)=((THICKN(N-1)*XWN(N-1))-RFLUX)/THICKN(N-1)
      GOTO 24
5     XWN(J)=((THICKN(J)*XW(J))+WFLUX(J)+SINK(J))/THICKN(J)
8     IF(XWN(J).GT.P(J)) GOTO 9
      GOTO 23
9     RFLUX=(P(J)-XWN(J))*THICKN(J)
      XWN(J)=P(J)
      WFLUX(J)=WFLUX(J)+RFLUX
      IF(WFLUX(J).LT.0.0) WFLUX(J)=0.0
      XWN(J-1)=((THICKN(J-1)*XWN(J-1))-RFLUX)/THICKN(J-1)
      J=J-1
      IF(J.NE.1) GOTO 8
      IF(XWN(J).GT.P(J)) GOTO 10
      GOTO 23
10    DRAIN=(XWN(J)-P(J))*THICKN(J)
      XWN(J)=P(J)
      ACCOR=ACCOR+DRAIN
      WRITE (6,600) DRAIN,ACCOR
600   FORMAT ('0',4X,'SOIL IS SUPER SATURATED.',6X,'RUNOFF     ',F7.4,6X,'
     1ACCUMULATED RUNOFF     ',F8.4)
23    DO 26  J=2,M
      DWFLUX(J)=DWFLUX(J)+WFLUX(J)
26    CONTINUE
      RETURN
      END
```

```
      SUBROUTINE DAILY (L)
      COMMON/EVAPDY/WIND(155),TMAX(155),TMIN(155),RH(155),RNM(155),
     1PLATE(155),SUNS(155),DAYL(155),RSTOP(155),NDAY(155),RS00(155),
     1TRANS,ROOTD(10),TDENS,DAILYT(10),JT
      COMMON/SUBALL/PWP(10),FC(10),THICKN(10),TMTOT,TRANSN(10),M,XW(10),
     1XWN(10),LA,P(10),PET,PE,AE,AT
      COMMON/PRIN/ACCPET,ACCPE,ACCPT,ACCAET,ACCAE,ACCAT
      COMMON/PRIND/DVFLUX(10),DWFLUX(10),DELT,DNADD(10),ZDCOND(10),ZDCON
     1V(10),ZDVAP(10),ZDVLU(10),UPV(10),DOV(10),DSINK(10),ACSINK(10),ACW
     1ATR(10),ACVAPR(10),ACUPV(10),ACDOV(10),DCOND(10),DCONV(10),DVAP(10
     1)
      INTEGER  TMTOT,DELT
      REAL LH
      LA=LA+24
      TMTOT=0
      AET=AE+AT
      ACCPET=ACCPET+PET
      ACCPE=ACCPE+PE
      ACCPT=ACCPT+TRANS
      ACCAET=ACCAET+AET
      ACCAE=ACCAE+AE
      ACCAT=ACCAT+AT
      DO 3  J=1,M
      ACSINK(J)=ACSINK(J)+DSINK(J)
      ACWATR(J)=ACWATR(J)+DWFLUX(J)
      ACVAPR(J)=ACVAPR(J)+DVFLUX(J)
      ACUPV(J)=ACUPV(J)+UPV(J)
      ACDOV(J)=ACDOV(J)+DOV(J)
3     CONTINUE
      WRITE (6,902) PET,PE,TRANS,AET,AE,AT
902   FORMAT ('0',4X,'   PET ',F9.3,5X,'   PE   ',F9.3,5X,'   PT   ',F9.3,
     15X,'   AET ',F9.3,5X,'   AE ',F9.3,5X,'   AT   ',F9.3)
      WRITE (6,903) ACCPET,ACCPE,ACCPT,ACCAET,ACCAE,ACCAT
903   FORMAT ('0',4X,'ACCPET ',F9.3,5X,'ACCPE   ',F9.3,5X,'ACCPT   ',F9.3,
     15X,'ACCAET ',F9.3,5X,'ACCAE ' ,F9.3,5X,'ACCAT   ',F9.3)
      WRITE (6,905) (DWFLUX(J),J=2,M)
      WRITE(6,904) (DVFLUX(J),J=2,M)
      WRITE (6,804)  (UPV(J),J=2,M)
      WRITE (6,804)  (DOV(J),J=2,M)
      WRITE(6,805)  (ACWATR(J),J=2,M)
      WRITE (6,806)  (ACVAPR(J),J=2,M)
      WRITE (6,807)  (ACUPV (J),J=2,M)
      WRITE (6,808)  (ACDOV(J),J=2,M)
      WRITE (6,809)  (ACSINK(J),J=1,M)
      WRITE (6,810)  (DCOND(J),J=2,M)
      WRITE(6,811)  (DCONV(J),J=2,M)
      WRITE (6,812)  (DVAP(J) ,J=2,M)
804   FORMAT (18X,8(3X,E9.2))
904   FORMAT ('0',3X,'DVFLUX',8X,8(4X,F8.5))
905   FORMAT ('0',3X,'DWFLUX',8X,8(4X,F8.5))
805   FORMAT ('0',3X,'ACWATR',8X,8(4X,F8.5))
806   FORMAT ('0',3X,'ACVAPR',8X,8(4X,F8.5))
807   FORMAT ('0',3X,'ACUPV ',8X,8(4X,F8.5))
808   FORMAT ('0',3X,'ACDOV ',8X,8(4X,F8.5))
809   FORMAT ('0',4X,'ACSINK',3X,9(4X,F8.5))
810   FORMAT ('0',4X,'DCOND',8X,8(4X,F8.5))
811   FORMAT ('0',4X,'DCONV',8X,8(4X,F8.5))
812   FORMAT ('0',4X,'DVAP ',8X,8(4X,F8.5))
      AE=0.0
      AT=0.0
      Z0=4.5857
      WND=WIND(L)*1.253
      TM=(TMAX(L)+TMIN(L))/2.0
      LH=597.67-0.58*TM
      S=(25028.0/((TM+237.3)*(TM+237.3)))*EXP((17.27*TM)/(TM+237.3))
      C=236.3643/(0.622*LH)
      VPS=6.107*EXP((17.27*TM)/(TM+237.3))
      VP=(RH(L)*VPS)/100.0
      HV=(0.0127*WND*24.0*(VPS-VP))/(ALOG(200.0/70))**2.0
      PET=(((S/C)*((RNM(L)-PLATE(L)/1000.0)*1440.0)+LH*HV)/(S/C+1.))/LH
      TFMAX=(TMAX(L)*9.0/5.0)+32.0
      TFRAN=((TMAX(L)-TMIN(L))*9.0/5.0)
      WM=WND/1.61
      CONST2=-78.68+0.897*TFMAX+0.34*TFRAN+0.00166*RSTOP(L)+0.118*WM*24.
      PET=(CONST2+0.0613*RS00(L))*0.0094
      IF(PET.LT.0.0) PET=0.0001
      TRANS=0.9*PET
      PE=PET-TRANS
      ADD=0.0
      DO 1  I=1,M
      TRANSN(I)=(ROOTD(I)/TDENS)*TRANS*THICKN(I)
      ADD=ADD+TRANSN(I)
      DAILYT(I)=DAILYT(I)/(JT*24)
      CONTINUE
      DUMMY=ADD/TRANS
      WRITE (6,901) (DAILYT(I),I=1,M)
901   FORMAT ('-',4X,'TMEAN',9(7X,F5.1)//)
      DO 2  I=1,M
      TRANSN(I)=TRANSN(I)/DUMMY
      DAILYT(I)=0.0
      DWFLUX(I)=0.0
      DVFLUX(I)=0.0
      UPV(I)=0.0
      DOV(I)=0.0
      ZDCOND(I)=0.0
      ZDCONV(I)=0.0
      ZDVAP(I)=0.0
      ZDVLU(I)=0.0
      DNADD(I)=0.0
      DSINK(I)=0.0
      DCOND(I)=0.0
      DCONV(I)=0.0
      DVAP(I)=0.0
2     CONTINUE
      RETURN
      END
```

```
      SUBROUTINE  DIFF
      COMMON/BASIC/AW(10)       ,BD(10),XMIN(10),XSIO2(10),XORG(10),XSOL(
     110),COND(10),CONST(10)
      COMMON/SUBALL/PWP(10),FC(10),THICKN(10),TMTOT,TRANSN(10),M,XW(10),
     1XWN(10),LA,P(10),PET,PE,AE,AT
      INTEGER TMTOT
      REAL KSIO2,KMIN,KORG,KAIR,CON(10)
      CAIR=0.238
      KSIO2=0.2594
      KMIN=0.5130
      KORG=1.2915
      DO 103  J=1,M
      IF(XW(J).GE.P(J)) GOTO 100
      IF(XW(J).GE.PWP(J)) GOTO 101
C  SOIL IS BETWEEN PWP AND DRY.
      XAIR=P(J)-XW(J)
      CONAIR=0.0615+(XW(J)/PWP(J))*(CAIR-0.0615)
      GA=0.013+(XW(J)/PWP(J))*(CONST(J)-0.013)
      GOTO 102
C   SOIL IS BETWEEN SATURATION AND PWP.
101   XAIR=P(J)-XW(J)
      CONAIR=0.0615+CAIR
      GA=0.333-(XAIR/P(J))*0.298
      GOTO 102
C  SOIL IS SATURATED.
100   XAIR=0.0
      CONAIR=0.0615
      GA=0.333
C   CALCULATE THERMAL CONDUCTIVITY .
102   GC=1.0-2.0*GA
      KAIR=0.333*((2.0/(1.0-0.957*GA))+(1.0/(1.0-0.957*GC)))
      CON (J)=0.001*((XW(J)*1.42+KSIO2*XSIO2(J)*20.4+KMIN*XMIN(J)*7.0
     1+KORG*XORG(J)*0.6+KAIR*XAIR*CONAIR)/(XW(J)+KSIO2*XSIO2(J)
     1+KMIN*XMIN(J)+KORG*XORG(J)+KAIR*XAIR))
103   CONTINUE
      DO 104  J=2,M
      COND(J)=SQRT(CON(J-1)*CON(J))
104   CONTINUE
      RETURN
      END
```